HRVATSKO DRUŠTVO
ZA STROJARSKE TEHNOLOGIJE

CROATIAN SOCIETY
FOR MECHANICAL TECHNOLOGIES

In association with:

University of Split
Faculty of Electrical Engineering,
Mechanical Engineering and
Naval Architecture

Slovak Academy of Science
Institute of Materials and
Machine Mechanics

Croatian Society for
Materials and Tribology

Dublin Institute
of Technology

Rogante Engineering
Office

ISSN 1847-7917

2nd International Conference

MTSM 2011

CONFERENCE PROCEEDINGS

General sponsors:
City of Split
Split - Dalmatia County
Ministry of Science, Education and Sports Republic of Croatia

September, 29th - 30th,2011.
Split - Republic of Croatia

ZBORNIK RADOVA

CONFERENCE PROCEEDINGS

STROJARSKE TEHNOLOGIJE I KONSTRUKCIJSKI MATERIJALI

MECHANICAL TECHNOLOGIES AND STRUCTURAL MATERIALS

Split

Hrvatska / Croatia

29. rujan / September 2011.

ORGANIZATOR / ORGANIZED BY:

HRVATSKO DRUŠTVO ZA STROJARSKE TEHNOLOGIJE, Hrvatska

CROATIAN SOCIETY FOR MECHANICAL TECHNOLOGIES, Croatia

SURGANIZATORI / CO-ORGANIZERS:

SVEUČILIŠTE U SPLITU
FAKULTET ELEKTROTEHNIKE, STROJARSTVA I BRODOGRADNJE

HRVATSKO DRUŠTVO ZA MATERIJALE I TRIBOLOGIJU

DUBLIN INSTITUTE OF TECHNOLOGY

SLOVAK ACADEMY OF SCIENCE INSTITUTE OF MATERIALS AND MACHINE MECHANICS

ROGANTE ENGINEERING OFFICE

SPONZORI / SPONSORS:

GRAD SPLIT

SPLITSKO-DALMATINSKA ŽUPANIJA

MINISTARSTVO ZNANOSTI, OBRAZOVANJA I ŠPORTA

IZDAVAČ / PUBLISHER:

HRVATSKO DRUŠTVO ZA STROJARSKE TEHNOLOGIJE, Hrvatska

CROATIAN SOCIETY FOR MECHANICAL TECHNOLOGIES, Croatia

c/o FESB, Ruđera Boškovića 32, 21000 SPLIT

tel.: +385 21 305 910; fax.: +385 21 463 877

e-mail: info@strojarska-tehnologija.hr

http://www.strojarska-tehnologija.hr

UREDNIK / EDITOR:

dr.sc. Dražen Živković

ISSN 1847-7917

NAKLADA / ISSUE: 70

ORGANIZACIJSKI ODBOR
ORGANIZING COMMITEE:

- Zvonko MRDULJAŠ (Split) - Predsjednik
- Igor GABRIĆ (Split) - Dopredsjednik

- Ante ALUJEVIĆ (Split)
- Ante BAROVIĆ (Split)
- Dražen DELIĆ (Split)
- Nikola GJELDUM (Split)
- Krešimir GRILEC (Zagreb)
- Dario ILJKIĆ (Rijeka)
- Sonja JOZIĆ (Split)
- Neven KUZMANIĆ (Split)
- Branimir LELA (Split)
- Petar LJUMOVIĆ (Split)
- Gojko MARIĆ (Zagreb)
- Slaven ŠITIĆ (Split)

PROGRAMSKI I RECENZENTSKI ODBOR
PROGRAMME AND REVIEW COMMITEE:

- Dražen ŽIVKOVIĆ (Split) - Predsjednik
- Dražen BAJIĆ (Split) - Dopredsjednik

- Boris ANZULOVIĆ (Split)
- Goran CUKOR (Rijeka)
- Vinko IVUŠIĆ (Zagreb)
- Jaroslav JERZ (Bratislava)
- David KENNEDY (Dublin)
- John LAWLOR (Dublin)
- Kai MERTINS (Berlin)
- Zoran PANDILOV (Skopje)
- Mladen PERANIĆ (Rijeka)
- Massimo ROGANTE (CM – It.)
- Zdravko SCHAUPERL (Zagreb)
- Wilfried SIHN (Wien)
- František SIMANČIK (Bratislava)
- Božo SMOLJAN (Rijeka)
- Ivica VEŽA (Split)

SADRŽAJ

A History of the Use of Passively Safe Street Furniture to EN 12767 in the UK

Author David MILNE,

Editor of "Designing Safer Roadsides, a Handbook for Highway Engineers"

UK

d.milne@homecall.co.uk

Keywords

Passive safety
Lattix
Highways
Roads
EN12767
Crash testing
Road safety
Signposts
Lighting columns
ASI
THIV

Ključne riječi

Pasivna sigurnost
Lattix
Autoputevi
Ceste
EN12767
"Crash test"
Cestovna sigurnost
Nosači znakova
Rasvjetni stupovi
ASI
THIV

Review article

This article describes how and why the UK has adopted passively safe street furniture.
Figure 1 demonstrates how dangerous street furniture can be. Such accidents are distressingly common.

Figure 1. A car sliced in two when hitting a large steel signpost
Slika 1. Automobil prepolovljen uslijed udara u veliki čelični stup za prometni znak

Passively safe street furniture to the *European Standard EN12767 Passively safe support structures for roadside equipment* [1] can eliminate most deaths and serious injuries in this sort of accident. Passively safety was a Scandinavian development in the 1980's and 1990's. Norway developed aluminium Lattix signposts and passively safe lighting columns in steel and aluminium were a parallel Scandinavian development. Finland in particular pioneered the national use of passively safe lighting columns (see *Finra Engineering News 9E* [2])

European *Standard EN12767* was first published in 2000 and is a test protocol to evaluate product safety performance in crash tests. Test items are impacted by a 950kg car and the vehicle behaviour and measured accelerations evaluated against safe limiting values in the standard. EN12767 products are unlikely to cause severe injuries to vehicle occupants in real life crashes.

Lattix passively safe signposts were first installed on a new UK trunk road scheme in 2002. This was the first major use of a passively safe product in the UK. An internal UK standard *TA89 Use of Passively Safe Signposts Lighting Columns and Traffic signal Posts To BSEN 12767* [3] was published in 2004 and updated in 2005 to give positive guidance on how and where to use passively safe street furniture on UK trunk roads and greatly encouraged the use of passively safe products. The UK is a now a major market for EN12767 products.

Povijest korištenja pasivne sigurnosne cestovne opreme prema EN12767 u Ujedinjenom Kraljevstvu

Pregledni članak

Članak opisuje kako je i zašto je Ujedinjeno Kraljevstvo usvojilo pasivnu sigurnosnu cestovnu opremu.

Slika 1 prikazuje koliko opasana može biti cestovna oprema. Ovakve nezgode su zabrinjavajuće česte.
Cestovna oprema s pasivnom sigurnošću, prema Europskom Standardu EN 12767 „Passively safe support structures for roadside equipment", može eliminirati većinu smrtnih slučajeva i ozbiljnih ozljeda kod ovakvih vrsta nezgoda. Pasivna sigurnost je skandinavsko postignuće iz 80-tih i 90-tih godina prošlog stoljeća. Norveška je razvila „Lattix" aluminijske nosive konstrukcije za prometne znakove, dok su rasvjetni stupovi od čelika i aluminija s pasivnom sigurnosti razvijali u svim skandinavskim zemljama. Finska je posebno prednjačila u uporabi rasvjetnih stupova s pasivnom sigurnosti na nacionalnoj razini (pogledati Finra Engineering News 9E).
Europski Standard EN 12767 prvi put je objavljen u 2000. godini i predstavlja testni protokol za procjenu sigurnosnih svojstava proizvoda pri crash-testovima. Testni uzorci su udareni vozilom mase 950 kg, te su ponašanje vozila i promjena ubrzanja uspoređeni s graničnim standardnim vrijednostima. Proizvodi izrađeni prema EN 12767 u pravilu ne izazivaju teške ozljede putnika u vozilu kod stvarnih prometnih nezgodama.
Lattix nosive konstrukcije za prometne znakove s pasivnom sigurnosti prvi put su postavljene na novoj mreži glavnih cesta u Ujedinjenom Kraljevstvu 2002. godine. To je bila prva velika primjena proizvoda s pasivnom sigurnosti u Ujedinjenom Kraljevstvu. Interni standard Ujedinjenog Kraljevstva TA89 „Uporaba stupova za prometne znakove, rasvjetnih stupova i stupova za semafore s pasivnom sigurnosti prema BSEN 12767 ", objavljen je 2004. godine i dopunjen 2005. godine. Svrha norme je davanje pozitivnih smjernica kako i gdje koristiti cestovnu opremu s pasivnom sigurnosti na glavnim cestama u Ujedinjenom Kraljevstvu. To je uvelike potaklo upotrebu proizvoda s pasivnom sigurnosti. Ujedinjeno Kraljevstvo je danas glavno tržište za EN 12767 proizvode.

Symbols

ASI Acceleration severity index, m^2s^{-2}
THIV Theoretical Head Impact Velocity, ms^{-1}

1. Introduction

Figure 2. First major use of Lattix signposts on a new UK trunk road scheme in 2002 (the A43 Silverstone Bypass in 2002)

Slika 2. Prva značajnija upotreba Lattix nosača znakova na novoj mreži glavnih cesta u UK 2002. (A43 zaobilaznica Silverstone-a u 2002.)

Passively safe street furniture (primarily signposts, lighting columns and traffic lights poles) deform, yield or shear when hit by a car which greatly reduces the accelerations and damage to the car and the consequent forces and risk of physical injury to the vehicle's occupants.

EN12767 describes the crash test methodology. Cars weighing 950 kg are crashed into the test item at high speed (100 kph or 70 kph) and low speed (35 kph). The measured accelerations and vehicle behaviour are used to calculate the EN12767 classification.

EN12767 products have excellent safety records in the UK, Finland, Norway and Denmark. About 12,000 Lattix signposts have been installed on UK roads since 2002 mainly on the national trunk road network. 140 have been hit by vehicles and replaced without any deaths or serious injuries.

The increasing demand for passively safe street products has attracted many suppliers from across Europe who compete for sales and this is driving down costs.

EN 12767 products have proved remarkably safe in real life crashes on UK roads.

2. EN 12767 Test Requirements

A brief outline of the EN 12767 test procedures and classifications is given below

EN 12767 testing must be carried by an accredited testing organisation and the results assessed by a notified body.

Products will also need to conform to the relevant product standard e.g. *EN 40 Lighting Columns* [4] for

lighting columns and *EN 12899-1; 2001 Fixed, vertical road traffic signs* [5] for road signs.

Figure 3. A steel signpost in a 100 kph EN 12767 test. This testing contract by TRL in the UK established a safe upper size limit of 89 mm diameter and 3.2 mm wall thickness for a steel signpost.

Slika 3. Test čeličnog stupa prema normi EN 12767 pri brzini od 100 km/h. Ovaj test proveden od strane TRL, u UK uspostavio je gornju sigurnosnu granicu od 89 mm promjera i 3.2 mm debljine stjenke za čelične stupove.

In an EN 12767 test evaluations:

a) 950 kg cars are crashed into the test item in two separate tests, the high speed test (usually 100 kph) and the low speed test (always 35kph). Vehicle speed, direction and impact position are carefully controlled. The chosen vehicle's crash characteristics must lie within specified limits. Crash test procedures, methodology and safety evaluation closely follow the *EN 1317 Road Restraint Systems* protocols for crash barrier tests. Test cars are instrumented with accelerometers in 3 dimensions to log accelerations during the impact
b) The vehicle must behave safely in the crash with no dangerous intrusion into the vehicle
c) Measured vehicle accelerations are used to calculate values of ASI (Accident Severity Index with limits reflecting maximum safe accelerations for the human body) and THIV (Theoretical Head Impact Velocity with velocity limits reflecting the safe velocity for an "unrestrained human head" to hit the inside of the vehicle). Measured ASI and THIV values determine the safety level. There are 4 safety levels in EN 12767 but the UK considers all of these levels to be acceptable.
d) Speed loss in the high speed impact is used to classify the item either as NE (no energy), LE (low energy), or HE (High Energy) where:
    - NE products only marginally slow the vehicle over the course of the impact.
    - LE products significantly slow the vehicles
    - HE products greatly slow or totally stop a vehicle relatively gently over several metres as the metal deforms to absorb the energy of the vehicle.
e) The classification NE, LE or HE reflects how much of the vehicle's kinetic energy is absorbed by the product in the high speed test. Signposts are typically NE products which usually break away barely slowing the vehicle. Lighting columns may accord to NE LE or HE classifications. HE lighting columns may be favoured for town use because they greatly slow or stop the vehicle thus reducing the chance of a vehicle careering on and hitting a pedestrian in a secondary impact.
f) Products if they pass the two tests are classified to EN12767. The label shown in Figure 4 for a Varley and Gulliver Hi-Mast signpost gives a classification 100:NE:2 which means:
    - The product was successfully crash tested at 100 kph (and at the mandatory 35kph test)
    - Minimal velocity was lost in the 100kph impact resulting in NE classification
    - Safety level was 2 (but any of the 4 safety levels are acceptable in the UK)

Figure 4. Varley and Gulliver Signpost Label on a passively safe signpost showing the EN12767 classification.

Figure 4. Oznaka Varley / Gulliver za sigurnosni stup testiran i odobren prema EN12767 normi.

3. History of Passive Safety in the UK

In 2002 the main contractor for A34 Silverstone bypass trunk road scheme asked the Highways Agency for permission to use the Norwegian Lattix passively safe signposts (supplied in the UK by Signpost Solutions) for the 30 large signs on the scheme so he could omit the usual lengths of safety barrier in front of the signs. This

was the first major use of a passively safe product in the UK and set a precedent for the UK road construction industry which was actively adopted by contractors on other schemes.

In 2004 the UK government published *TA89/04 Use of Passively Safe Signposts* to give guidance on the use of passively safe signposts for use on the trunk road network. The document was published to avoid the need for approvals on a scheme by scheme basis and also to encourage the use of passively safe street furniture. The document legitimised the use of passively safe street furniture but steel posts protected by barrier remained a permitted alternative.

UK employs crash barriers on the national trunk road network to prevent direct impacts with roadside hazards including large signposts, bridge piers and tall embankments. Large signs would typically be protected by 37.5m lengths of crash barrier. Since *TA89/04 Use of Passively Safe Signposts* was published most large new signs on the UK trunk road network employ passively safe signposts with no barrier provision.

The advantages are:

- Passively safe signposts are usually cheaper than structural steel signposts safeguarded by barrier
- Contract period is reduced as barriers are the last item to be installed on a new road scheme
- Less visual clutter
- Damaged passively safe signposts can often be easily replaced on an undamaged foundation with minimal traffic disruption
- Lack of barrier speeds erection of new signs on existing trunk roads and reduces traffic disruption on the busy network

The Highways Agency before publishing TA89/04:

- Discussed the Lattix safety record with the Norwegian government and were suitably reassured
- Carried out EN 12767 tests to determine the maximum size for a circular hollow section steel post. The answer was the surprisingly small size of 89 mm diameter and 3.2 mm wall thickness.

In 2005 *TA89/05 Use of Passively Safe Signposts, Lighting Columns and Traffic Light Posts to EN 12767* was published. This extended the rules for passive safety to cover to lighting columns and traffic signal posts on trunk roads.

EN 12767 was updated in 2007. The British version EN 12767 now contained a national annex giving national recommendations for the use of passively safe street furniture and in particular where to use what class of EN 12767 product. TA89/05 was withdrawn at this time.

In 2010 a new free document available on the internet was published by UK Roads *Passive Safety UK Guidelines for Specification and Use of Passively Safe Street Furniture on the UK Road Network.* This document provides comprehensive advice on the use of passively safe street furniture.

4. Use of passively safe products in the UK

On trunk roads, passively safe signposts and lighting columns are almost universally used for new large signs and new lighting columns where the speed limit is over 50 mph or over (unless barriers are needed for other reasons).

For non-trunk roads and in cities progress has been slower. Barrier is rarely specified on these roads. The more progressive highway authorities are however now starting to use passively safe signposts and lighting columns on their faster and busier roads but money is short.

Figure 5. Hi-Mast passively safe signposts by Varley and Gulliver

Slika 5. Veliki sigurnosni stupovi tvrtke Varley and Gulliver

Initially passively safe products were Scandinavian. Passively safe products have now been developed in the UK and are even now exported.

EN 12767 products available in the UK include:

- 5 suppliers of passively safe signposts (materials include glass fibre/resin composites, carbon fibre/resin composites, and aluminium)
- 5 suppliers for passively safe lighting columns (materials include steel folded plate construction,

glass fibre resin composites and extruded aluminium)
- Several bollard suppliers (typically plastic)
- Several suppliers for traffic light poles in (materials are aluminium and glass fibre composites)
- Aluminium signposts have also been used to mount roadside cameras
- Passively safe EN 12767 roadside phones

Figure 6. A passively safe emergency roadside phone

Slika 6. Pasivno siguran nosač telefona za hitnost

5. Safety Record

In 2002 the only passively safe product being actively marketed was the Lattix aluminium lattice mast marketed by Signpost Solutions. Lattix today is still the only signpost strong enough for very large signs. Signpost Solutions have sold about 12000 Lattix posts. About 180 of these posts have been hit by vehicles (and replaced free of charge by Signpost Solutions in exchange for an account of the accident). Nobody has been seriously injured in any of these accidents. Most of these signposts will have been specified because they were significantly cheaper than structural steel signposts when hoarded by barrier.

Figure 7. Accident with a Lattix signpost. The driver was unhurt and is standing near the car.

Slika 7. Prometna nezgoda s Lattix nosačem putokaza. Vozač je neozlijeđen i stoji pokraj vozila.

There has been only been one single severe injury accident with an EN 12767 product when a car hit two resin/glass fibre composite signposts supporting a large sign in a side impact.

In comparison in 2009 alone 46 people were killed and 269 were seriously injured in single vehicle accidents with safety barrier alone on UK roads in 2009. Deaths and serious injuries from hitting roadside furniture in Britain in 2009 in single vehicle accidents are listed in Table 1.

Table 1. Single Vehicle Accidents (extracted from Road Casualties Great Britain 2009 [7])

Tablica 1. Prometna nezgoda s jednim vozilom (podaci uzeti od "Road Casualties Great Britain 2009 [7]")

Single Vehicle Accidents in Great Britain 2009		
Object hit	**Fatal**	**Serious**
Road sign or traffic signal	**35**	**234**
Lamp post	**41**	**293**
Telegraph pole or electricity pole	**14**	**104**
Tree	**175**	**791**
Crash barrier	**46**	**269**

Figure 8. The car hit a Sahko Jokinen Kapu HE lighting column in a sideways impact. The driver was unhurt.

Slika 8. Automobil je bočno udario u "Sahko Jokinen Kapu HE" rasvjetni stup. Vozač je ostao neozlijeđen.

Figure 9. The HE Kapu lighting column hit by the car above progressively deformed during the impact

Slika 9. "HE Kapu" rasvjetni stup udaren vozilom s gornje slike progresivno se deformirao za vrijeme trajanja sudara

The Table 1 casualty figures could be greatly reduced if passively safe street furniture use was universal and trees close to the carriageway were felled. Many of these serious accidents occur on rural non-trunk A roads.

6. Recommendations for the Use of Passively Safe Street Furniture

Highway authorities should consider creating forgiving roadsides that are safer for vehicles leaving the road at speed. Suitable actions are:

- Creating a clear zone next to the carriageway free of trees, larger road signs, lighting columns and utility poles. A suggested minimum width of 4.5m if at all possible should be provided.
- Limiting the size of steel signposts in the clear zone. Circular hollow section posts for signs in the clear zone should not exceed the EN 12767 limits of 102 mm in diameter and 3.2 mm wall thickness.
- Using passively safe signposts and lighting columns to EN 12767within the clear zone
- To visit countries who use passively safe products to see how they are used and to discuss policies and experiences with the highway authorities
- Specifying passively safe signposts on a new rural road scheme could give a chance to evaluate the benefits
- Consult the *Passive Safety UK Guidelines for Specification and Use of Passively Safe Street Furniture on the UK Road Network* [] for appropriate advice
- Read *Designing Safer Roadsides A Handbook for Highway Engineers* [9] This book contains in depth advice on passively safe products and their use with authors from several countries.

REFERENCES

[1] EN12767 Passively safe support structures for roadside equipment

[2] Finra Engineering News 9E
This document gives Finland's national policy for use of passively safe lighting columns in Finland and can be read on:
http://alk.tiehallinto.fi/thohje/fen9e.pdf

[3] TA89/05 Use of Passively Safe Signposts Lighting Columns and Traffic signal Posts To BSEN 12767
This document was withdrawn in 2008 but can be read on:
http://www.signfix.co.uk/pdfdata/advicenote-ta8905.pdf

[4] EN 40 Lighting Columns Parts 1 to 7
Describes the requirements for lighting columns in all materials.

[5] EN 12899-1; 2001 Fixed, vertical road traffic signs
This document gives the requirements for road signs and their design including the loading and structural strength requirements for sign supports

[6] BS EN 1317 Road restraint systems Parts 1 to 8
Describes requirements for different barriers, crash cushions, terminals and transitions

[7] Passive Safety UK Guidelines for Specification and Use of Passively Safe Street Furniture on the UK Road Network.
This document can be can be viewed at:
http://www.ukroads.org/webfiles/Guidelines%20Print%20ready.pdf

[8] Road Casualties Great Britain 2009.
A comprehensive breakdown of all the road casualties in Britain can be viewed at:
http://www.dft.gov.uk/pgr/statistics/datatablespublications/accidents/casualtiesgbar/rrcgb2009
The casualties for single vehicle accidents with roadside objects are given in Table 20

[9] *Designing Safer Roadsides A Handbook for Highway Engineers*
This book is the best source of advice on all issues relating to passive safety. It can be purchased from d.milne@homecall.co.uk for £10.00 pls p&p

Testing of safety barriers according to EN 1317-2

***Boris ADUM*[1)], *Željko LEKŠIĆ*[1)]**
1) Dalekovod d.d.
Dalekovod jsc
Marijana Čavića 4, 10 000 Zagreb, **Croatia**
boris.adum@dalekovod.hr
zeljko.leksic@dalekovod.hr

Keywords
safety barriers
containment level
crash test
accidents
safety barrier regulations

Ključne riječi
zaštitna ograda
nivo zadržavanja
ispitivanja sudara
nesreće
propisi za zaštitne ograde

Professional article
A road restraint system is any device installed on the road and has a purpose to reduce the consequences of roadside collisions or uncontrolled vehicles that are leaving the carriageway. The intention of the EU and member countries is to continuously reduce the number of road accident victims in the European Union. Road accidents are the main cause of death in the group of people under 45. Although safety barriers do not eliminate almost any of the accident causes and do not reduce the probability of an accident occurring they can significantly reduce the consequences of accidents. There has an improvement in overall safety over the last 30 years but the situation is still socially unacceptable and difficult to justify to the citizen. Because of everything mentioned we are witnessing a continuous upgrade in the requirements of safety barriers levels. The EU and individual countries are trying to reduce the number of road accident victims and also the great cost associated with accidents. In order to further decrease the number of fatalities more attention should be given to installing suitable class barriers according and passive safety support structures in urban areas and state roads, particularly targeting the so called particularly hazardous places (so called "black spots"). This could lead to a significant reduction of road accidents fatalities.

Stručni rad
Zaštitna cestovna oprema je bilo koji dio opreme za ceste montiran u svrhu smanjenja posljedica sudara ili nekontroliranog gibanja vozila koje napušta kolnik. Namjera je EU i država članica da kontinuirano smanjuje broj žrtava prometnih nezgoda u EU. Prometne nezgode su glavni uzrok smrti ljudi do 45 godina starosti. Iako zaštitne ograde ne eliminiraju gotovo niti jedan od uzroka prometnih nesreća mogu značajno smanjiti njihove posljedice. Iako općenito postoji poboljšanje sigurnosti prometa na cestama u zadnjih 30 godina situacija je još uvijek neprihvatljiva i teško objašnjiva građanima. Zbog svega spomenutog svjedoci smo kontinuiranog povećanja zahtjeva vezanih uz nivoe zadržavanja zaštitnih ograda. EU i države članice nastoje smanjiti broj žrtava prometnih nesreća i troškove vezano uz nesreće. U cilju daljnjeg smanjenja broja poginulih na cestama posebnu više pažnje trebalo bi posvetiti ugradnji odgovarajućih sigurnosnih ograda i nosača opreme za ceste s pasivnom sigurnošću na cestama u naseljima i državnim cestama posebno imajući u vidu tzv. „crne točke". Na taj način moguće je značajno smanjiti broj poginulih u prometnim nesrećama.

1. Introduction

A road restraint system is any device installed on the road and has a purpose to reduce the consequences of roadside collisions or uncontrolled vehicles that are leaving the carriageway. In general the road restraint systems can be divided in:

- Safety barriers (shoulder, median, bridge)
- Crash cushions
- Terminals of safety barriers
- Transitions of safety barriers
- Pedestrian restraint systems
- Motorcycle road restraint systems

The intention of the EU and member countries is to continuously reduce the number of road accident victims in the European Union. Each year in the European Union more than 35 000 people die as a cause of road accidents and more than 1 500 000 persons were injured [9]. Road accidents are the main cause of death in the group of people under 45 [1]. There is a large number accident causes, according to [1] main accident causes are: excessive and improper speed, consumption of alcohol and drugs or fatigue, failure to wear a seat belt or crash helmet, lack of sufficient protection provided by vehicles, high-risk accident sites (black spots), non-compliance with driving and rest times by professional drivers, poor visibility of other users or an insufficient field of vision for the driver.

Although safety barriers do not eliminate almost any of the accident causes and do not reduce the probability of an accident occurring they can significantly reduce the consequences of accidents.

Symbols/Oznake

ASI	- Acceleration severity index, m^2s^{-2} - Indeks intenziteta ubrzanja	*D*	- Dynamic deflection, m - Dinamički progib
HGV	- Heavy goods vehicle - Teško teretno vozilo	*W*	- Working width, m - Radna širina
THIV	- Theoretical Head Impact Velocity, ms^{-1} - Teoretska brzina udara glave	*VI*	- Vehicle intrusion - Prodor vozila
VCDI	- Vehicle Cockpit Deformation Index - Indeks deformacije putničkog prostora		

Subscripts/Indeksi

m	- Measured value - Mjerena vrijednost
N	- Normalized value - Normirana vrijednost

2. Testing of safety barriers

2.1. Vehicle impact tests and containment levels

The standard EN 1317-2 [3] defines the performance classes impact test acceptance criteria and test methods for safety barriers. There are several impact tests defined by the standard, for each test a different combination of vehicle type, mass, impact speed and angle is defined.

Table 1. Vehicle impact tests
Tablica 1. Ispitivanja sudara

Test/ Ispiti-vanje	Impact speed/ Brzina u udara [km/h]	Impact angle/ Kut udara [°]	Vehicle mass/ Masa vozila [kg]	Type of vehicle/ Vrsta vozila
TB11	100	20	900	Car
TB21	80	8	1300	Car
TB22	80	15	1300	Car
TB31	80	20	1500	Car
TB32	110	20	1500	Car
TB41	70	8	10000	Rigid HGV
TB42	70	15	10000	Rigid HGV
TB51	70	20	13000	Bus
TB61	80	20	16000	Rigid HGV
TB71	65	20	30000	Rigid HGV
TB81	65	20	38000	Articulated HGV

A containment level of a barrier is a description of the standard of protection offered to vehicles by a safety barrier. Barriers that have a different containment level have a different strength and can contain different amounts of kinetic energy.
The different containment levels defined in EN 1317–2 are shown in Table 2.
The low angle containment levels are intended for temporary barriers, but temporary barriers can be tested for higher containment levels also. In general a barrier that satisfies a given containment level is considered fulfilling the requirements of a lower level with the following exceptions: N1 and N2 do not include T3, H levels do not include L levels or the N2 level.

Table 2. Containment levels
Tablica 2. Nivoi zadržavanja

Containment levels/ Nivo zadržavanja				Acceptance test/ Potrebna ispitivanja
Low angle containment/ Zadržavanje kod malog kuta udara	T1			TB 21
	T2			TB 22
		T3		TB 41 & TB 21
Normal containment/ Normalni nivo	N1			TB 31
	N2			TB 31 & TB 11
Higher containment/ Viši nivo		H1		TB 42 & TB 11
			L1	TB 42 & TB 32 & TB 11
		H2		TB 51 & TB 11
			L2	TB 51 & TB 32 & TB 11
		H3		TB 61 & TB 11
			L3	TB 61 & TB 32 & TB 11
Very high containment/ Vrlo visoki nivo		H4a		TB 71 & TB 11
		H4b		TB 81 & TB 11
			L4a	TB 71 & TB 32 & TB 11
			L4b	TB 81 & TB 32 & TB 11

2.2. Performance evaluation and acceptance criteria

The standard defines different criteria for the performance evaluation of the safety barriers.

Qualitative criteria:

- There must be no ejection of parts
- The vehicle most not roll over and it must be contained
- VCDI – Vehicle Cockpit Deformation Index
- Exit trajectory must comply with the exit box criterion

Quantitative criteria:

- ASI: Acceleration Severity Index
- THIV: Theoretical Head Impact Velocity (m/s)
- Working width of the barrier (m)

The impact severity is assessed through indices ASI and THIV, the lower they are the greater is the safety of car occupant. The design of safety barriers, specially for higher levels of containment, is a balance of strength and elasticity/deformability to achieve both the desired small vehicle occupant safety and the desired vehicle and barrier behavior when a impact of a HGV or a Bus occurs.

The deformation of the safety barrier is characterized by: dynamic deflection, working width and vehicle intrusion (Figure 1).

Table 3. Impact severity levels
Tablica 3. Nivoi intenziteta udara

Impact severity level/ Nivo intenziteta udara	Index values/ Vrijednost indeksa		
A	ASI ≤ 1,0	and	THIV ≤ 33 km/h
B	ASI ≤ 1,4		
C	ASI ≤ 1,9		

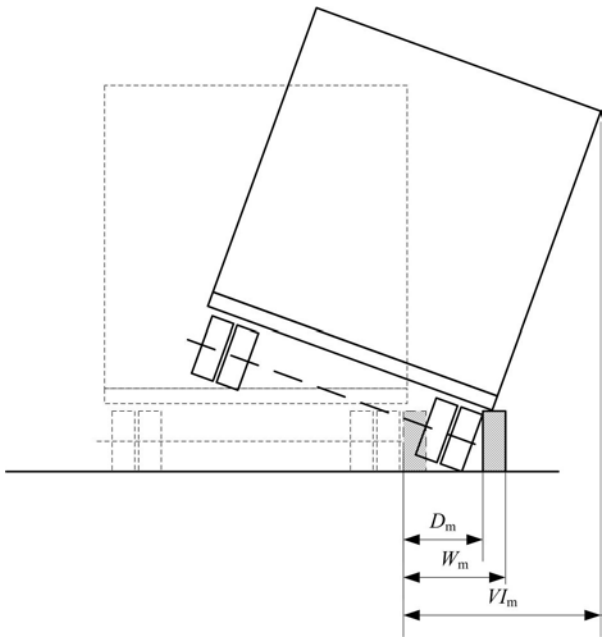

Figure 1. Dynamic deflection, working width and vehicle intrusion [m]
Slika 1. Dinamički progib, radna širina i prodor vozila [m]

The so normalized working width levels are classified in 8 classes, while the vehicle intrusion level is classified in 9 classes. For both of the barrier properties a level less that level 1 (the level with the smallest width) may be specified if required. The dynamic deflection, working width and vehicle intrusion serve to determine the installation conditions for the barrier and the distances that need to be provided in front of obstacles.

Table 4. Levels of normalized working width
Tablica 4. Nivoi normirane radne širine

Classes of normalized working width levels/ Klase normirane radne širine	Levels of normalized working width/ Nivoi normirane radne širine m
*W*1	$W_N \leq 0,6$
*W*2	$W_N \leq 0,8$
*W*3	$W_N \leq 1,0$
*W*4	$W_N \leq 1,3$
*W*5	$W_N \leq 1,7$
*W*6	$W_N \leq 2,1$
*W*7	$W_N \leq 2,5$
*W*8	$W_N \leq 3,5$

Table 5. Levels of normalized vehicle intrusion
Tablica 5. Nivoi normiranog prodora vozila

Classes of normalized working width levels/ Klase normirane radne širine	Levels of normalized vehicle intrusion / Nivoi normiranog prodora vozila m
*VI*1	$VI_N \leq 0,6$
*VI*2	$VI_N \leq 0,8$
*VI*3	$VI_N \leq 1,0$
*VI*4	$VI_N \leq 1,3$
*VI*5	$VI_N \leq 1,7$
*VI*6	$VI_N \leq 2,1$
*VI*7	$VI_N \leq 2,5$
*VI*8	$VI_N \leq 3,5$
*VI*9	$VI_N > 3,5$

The vehicle cockpit deformation index was introduced to standardize the description of the vehicle interior deformation. The index designates the location and the extent of the cockpit deformation. It consist of two alphabetic characters plus seven numeric characters in the following form: XXabcdefg

The first two alphanumeric characters (Figure 2) indicate the location of deformation, while the remaining seven numeric (Figure 3) characters indicate the percentage of reduction of seven interior dimensions

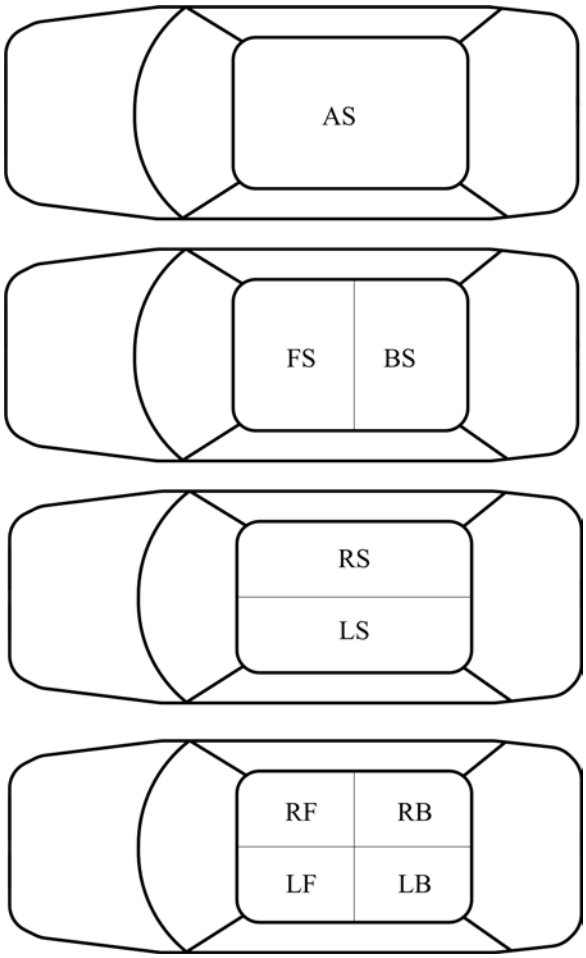

Figure 2. Location of cockpit deformation

Slika 2. Mjesto deformacije putničkog prostora

The meaning of the VCDI characters is: AS – all seats, FS – front seats, LF – left front, etc.

The dimensions of the interior (Figure 3) have the following meaning:

- a Minimum distance between the dashboard and the top rear seat
- b Minimum distance between the roof and the floor panel
- c Minimum distance between rear seat and the motor panel
- d Minimum distance between the lower dashboard and the floor panel
- e Minimum interior width between the right and lefot lower edges of windows
- f Minimum distance between the lower edge of right window and the upper edge of the left window
- g Minimum distance between the lower edge of left window and the upper edge of the right window

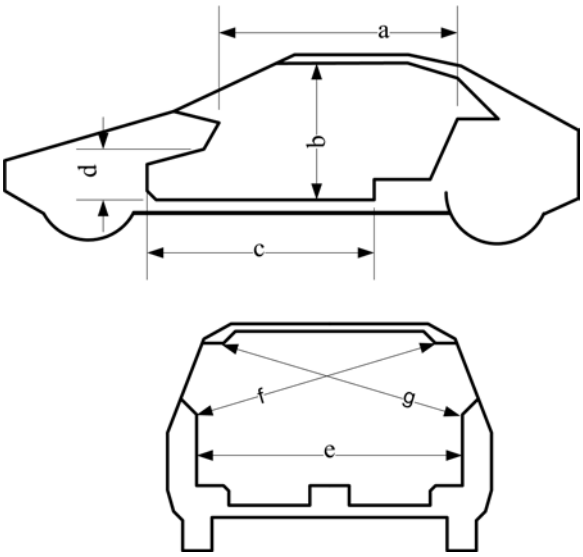

Figure 3. Interior dimensions

Slika 3. Dimenzije putničkog prostora

An important part of the safety barrier test is the vehicle behavior. For example only one of the vehicle wheels is allowed to pass completely over or under the barrier, and the vehicle must not roll over. One of the parameters of the vehicle behavior is the so called exit box criterion (Figure 4), where the wheel track is not allowed to cross the line parallel to the initial traffic face of the system at a distance A plus the width of the vehicle plus 16% of the vehicle length within a distance from point P defined by the standard.

3. Changes in the new edition of the standard

The latest 2010 edition of the EN 1317-2 standard, compared to the 1998 edition, brings the some significant changes, some of them are:

- New "High containment" and "Very High Containment" classes *L*1, *L*2, *L*3, *L*4a and *L*4b have been added. Compared to the *H*1, *H*2, *H*3, *H*4a and *H*4b classes, besides the TB 11 900 kg passenger car test they include also a TB 32 1500 kg passenger car test.
- When assessing the severity of the impact the requirement for the Post Impact Head Deceleration (PHD) has been canceled
- There is an introduction of barriers families (product families)
- The installation of the barrier for the test is described in more detail
- Regarding the deformation of the restraint system a new definition of the Vehicle Intrusion has been added
- There are more detailed criteria for the barrier and vehicle behavior

It is important to say that modifications included in the 2010 edition are not changes of test criteria, in the sence of EN 317-5:2007+A1:2008, ZA.3.

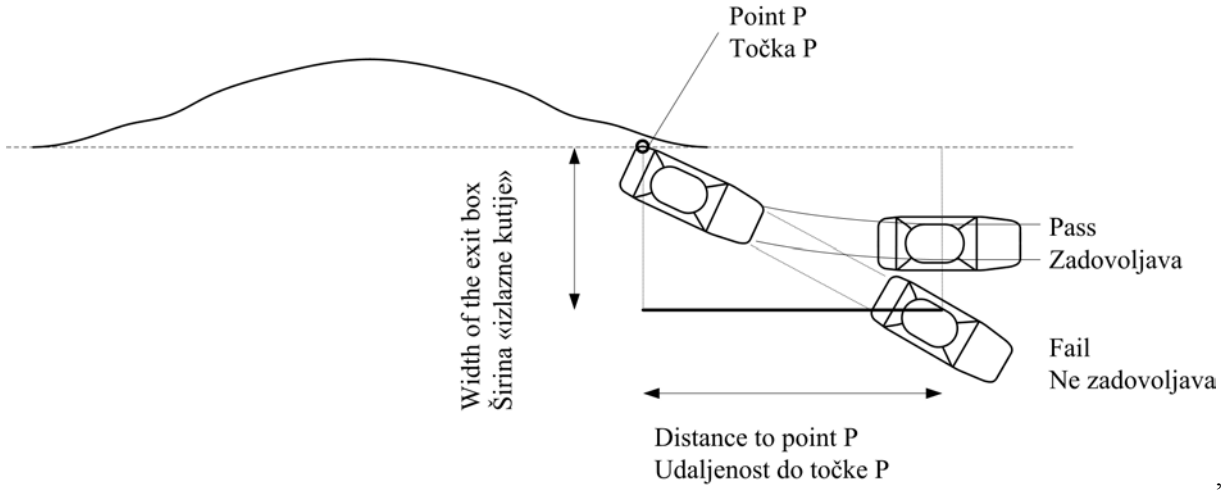

Figure 4. "Exit box" criterion

Slika 4. Kriterij "izlazne kutije"

4. Conclusion

Road safety directly affects all of the Europe's inhabitants. Although there has an improvement in overall safety (Figure 5) the situation is still socially unacceptable and difficult to justify to the citizen.

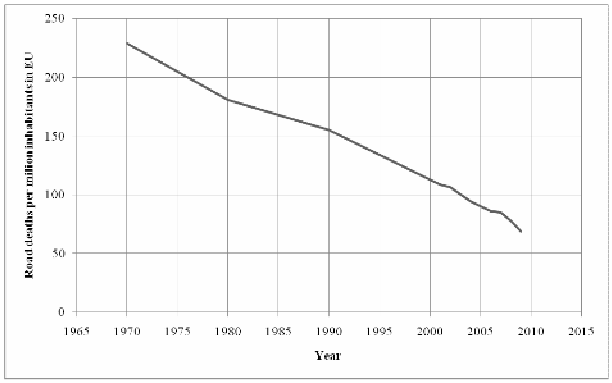

Figure 5. Number of people killed per million inhabitants in road accidents in EU, trend 1970-2009 [1], [10]

Slika 5. Broj poginulih u prometnim na million stanovnika nesrećama u EU, trend za razdoblje 1970-2000

Only in the last decade in the EU the number of fatalities has decreased 36% [10], while in Croatia in the same period there is no obvious trend or improvement (Figure 6).

Most of the road accidents both in EU and in Croatia occur in urban environments, 69% in the EU and 80,4% in Croatia [8], [11]. The data given in [11] shows that , in contrast to public opinion, most of the road accidents in 2009 in Croatia with fatalities occured on city and state roads not on highways (Figure 7).

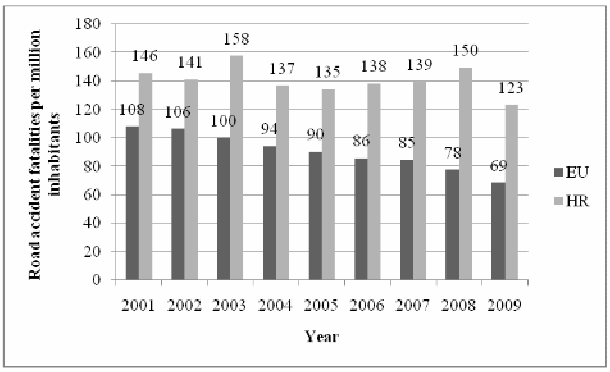

Figure 6. Road accident fatalities per million inhabitants in EU and Croatia, 2001–2009 [10]

Slika 6. Broj poginulih u prometnim na million stanovnika nesrećama u EU i RH, 2001–2009

It is also important to notice that most of the people were killed in accidents on strait parts of the road (46%), and on bends (34,9%), following are crossroads and other places. If the types of accidents are observed, the largest number of accidents with fatalities involved a vehicle that was leaving the carriageway in an uncontrolled way (36%). Concerning the type of vehicle involved in accidents with fatalities the largest number involved cars (63,8%) followed by motorcycles (18,2%) [11]. Most of the accidents occurred during day time in good visibility.

This suggests that there are significant improvements than can be made concerning restraint barriers and support structures for road equipment installed on roads specially when dealing with particularly hazardous places (so called "black spots") both in the city and outside.

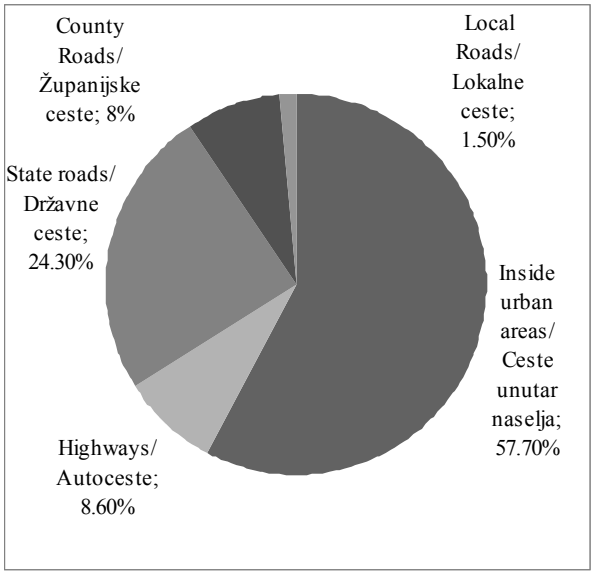

Figure 7. Road accidents fatalities in Croatia per road type, 2009 [11]

Slika 7. Poginule osobe po kategorijama cesta u 2009 u RH

We are witnessing a continuous upgrade in the requirements of safety barriers levels. The EU and individual countries are trying to reduce the number of road accident victims and also the great cost associated with accidents.

The current Croatian requirements for safety barriers is given in the following table [12]

Table 6. Croatian containment level requirements for median and side-strip barriers
Tablica 6. Hrvatski zahtjevi za nivoe zadržavanja zaštitne ograde na trasi ceste

Medians/Razdjelni pojas	
H2	In general
Side-Strips/Rub ceste	
N2	County, local and other roads
H1	State road and a fast city road
H2 - H1	Highways and fast roads

In general there are quite large differences in national requirements concerning the required containment level across Europe at this moment, although there is an obvious increase in the required containment levels.
In the United Kingdom standard TD19/06 requires the containment level N1 on roads with a speed limit < 80 km/h (50 mph), and the containments N2, H1, H2 or H4a on roads with a speed limit ≥ 80 km/h (50 mph) [13].

In the following table (Table 7) a representation of the current German requirements for safety barriers is given [7].

Table 7. German containment level requirements for median and side-strip barriers
Tablica 7. Njemački zahtjevi za nivoe zadržavanja zaštitne ograde na traci ceste

Medians/Razdjelni pojas	
H2	In general
H4B	High risk to run off the road and every day traffic – HGV > 3000 vehicles/day
Side-Strips/Rub ceste	
H1	In general
H2	High danger for third parties (e.g. motorway service areas, structures not designed to withstand a collision) and every day traffic – HGV > 3000 vehicles/day
H4B	High danger for third parties (e.g. motorway service areas, structures not designed to withstand a collision) and every day traffic – HGV > 3000 vehicles/day and high risk to run off the road

Having in mind everything said it can be concluded that in Croatia more attention should be given to installing suitable class barriers according to EN 1317 including motorcycle road restraint systems, and passive safety support structures according to EN 12767 in urban areas and state roads, particularly targeting the so called particularly hazardous places (so called "black spots"). This could lead to a significant reduction of road accidents fatalities.

On the EU level a more uniform set of national rules regarding the installation of barriers, support structures and other road equipment would also be desirable.

REFERENCES

[1] COMMUNICATION FROM THE COMMISSION, European Road Safety Action Programme, Halving the number of road accident victims in the European Union by 2010: A shared responsibility, European Commission, Brussels, 2003
[2] HRN EN 1317-1:2001: Zaštitni cestovni sustavi -- 1. dio: Nazivlje i opći kriteriji za metode ispitivanja (EN 1317-1:1998), DZNM, Zagreb, 2001
[3] HRN EN 1317-2/A1¸:2007: Zaštitni cestovni sustavi -- 2. dio: Vrste izvedbe, testovi sudara prema kriterijima prihvatljivosti i metode ispitivanja sigurnosnih ograda (EN 1317-2:1998/A1:2006), DZNM, Zagreb, 2007

[4] HRN EN 1317-5:2009: Zaštitni cestovni sustavi -- 5. dio: Zahtjevi za proizvod i ocjenjivanje sukladnosti za zaštitne cestovne sustave (EN 1317-5:2007+A1:2008), DZNM, Zagreb, 2009
[5] BS EN 1317-1:2010: Road restraint systems Part 1: Terminology and general criteria for test methods., BSI, London, 2010
[6] BS EN 1317-2:2010: Road restraint systems Part 2: Performance classes, impact test acceptance criteria and test methods for safety barriers including vehicle parapets, BSI, London, 2010
[7] EHLERS, U.; Assessing the need and cost-effectiveness of high containment level safety barriers in Finland, AALTO UNIVERSITY, Espoo, 2010
[8] WHITE PAPER, Roadmap to a Single European Transport Area – Towards a competitive and resource efficient transport system, European Commission, Brussels, 2011
[9] Communication from the Commission to the European Parliament, the Council, the European Economic and Social Committee and the Committee of the Regions, Towards a European road safety area: policy orientations on road safety 2011-2020, European Commission, Brussels, 2010
[10] EU, European Commission, http://ec.europa.eu/transport/road_safety/index_en.htm, European Union, 1995-2011
[11] Republika Hrvatska, Ministarstvo unutarnjih poslova, Bilten o sigurnosti cestovnog prometa 2009., Zagreb, 2010
[12] Republika Hrvatska, Ministarstvo mora, turizma, prometa i razvitka, PRAVILNIK o prometnim znakovima, signalizaciji i opremi na cestama, Narodne novine br. 33/2005, Zagreb, 2005
[13] Highways Agency of England, Design manual for roads and bridges, Volume 2, Section 2, Part 8, TD 19/06, 2006

PASSIVE SAFETY PRODUCTS SAVE LIFES – REAL FACTS FROM WIMED EXPERIENCE IN POLAND

Zdzisław Dąbczyński

Predavanje - *Presentation*

Cijelo predavanje nalazi se na priloženom CD-u.

The whole presentation is on the attached CD.

WIMED Oznakowanie Dróg Spółka z o.o.
ul. Tarnowska 48, 33-170 Tuchów, Poljska
tel. +48 (14) 65 25 247; fax +48 (14) 65 23 452
e-mail: info@wimed.pl www.wimed.pl

ZIP poles for public lighting with regard to EN 12767 – Passive Safety of Support Structures for Road Equipment

Demeter PRISLAN [1)]
1) B.Sc.Ec., representative Safety Product, ICC Demeter Prislan s.p., **Slovenia**
demeter.prislan@siol.net

Keywords
Passive safety
ZIP pole
public lighting
energy absorption
safety level

Ključne riječi
pasivna sigurnost
ZIP stup
javna rasvjeta
absorbcija energije
stupanj sigurnosti

Review article
Public lighting poles should comply with and conform to the European standard EN40. The EN40 standard covers technical issues such as dimensions and installation of the poles but does not however deal with passive safety. The European standard EN12767 is used to establish the rating of passive safety for support structures for road equipment. EN12767 has been used to determine the rating the ZIP pole has achieved. ZIP poles have been developed , designed and manufactured to ensure that through their energy absorbing ability to yield they are able to slow and stop a vehicles with minimum consequence to the occupants and the surrounding area.

ZIPpole stupovi za javnu rasvjetu prema EN 12767 - Pasivna sigurnost nosivih struktura cestovne opreme

Pregledni rad
Stupovi javne rasvjete moraju biti u skladu stupovi sa zahtjevima europske norme EN 40. Europska norma EN 40 odnosi se na tehničku problematiku kao što su dimenzije i postavljanje stupova, ali se istovremeno ne bavi pasivnom sigurnošću. Europska norma EN 12767 se koristi za određivanje nivoa pasivne sigurnosti nosivih struktura cestovne opreme. EN12767 koristi se za određivanje nivoa pasivne sigurnosti ZIPpole stupova. ZIPpoles su razvijeni, projektirani i proizvedeni kako bi svojom sposobnošću upijanja energije bili u stanju usporiti i zaustaviti vozila sa najmanje posljedica za putnike i okoliš.

Introduction

The European standard EN 12767 – Passive Safety of Support Structures for Road Equipment evaluates two parameters which categorize the support structures of road equipment which are: category of energy absorption in case of vehicle impact and the level of safety for the occupants in the vehicle. This is achieved in a controlled environment with, defined conditions and the specified equipment using the prescribed procedures.

Energy absorption

The seriousness of the occupants' injuries is a direct result of the impact into an obstacle on or at the roadside such as a support structure and the speed of the vehicle involved. If we consider safety, such support structures could be integrated in a way that they absorb or disperse the energy in a case of a vehicle impact. The prescribed European standard creates a common base for testing of a vehicle crashing into support structures and or roadside equipment. European standard has three categories of passive safety for support structures:

- High energy absorbing (HE)
- Low energy absorbing (LE)
- Non-energy absorbing (NE)

The support structures that absorb the impact and resultant energy thereby slowing down the vehicle significantly and thus decrease the risk of a secondary impact .This secondary impact could involve vehicles, pedestrians or any other objects in the immediate vicinity. Structures that do not absorb the impact fully allow the vehicle to proceed with lower speeds but still have the ability to cause damage. Such support structures enable lower primary risk for the occupants but do however pose a bigger risk through secondary collisions into obstacles in vicinity of the primary impact.

Symbols/Oznake

ASI	- Acceleration Severity Index - Indeks ubrzanja na ozbiljnost posljedica	LE	- Low Energy absorption - Niska apsorpcija energije
THIV	- Theoretical Head Impact Velocity - Teoretska brzina glave u trenutku sudara	NE	- Non Energy absorption - Bez apsorpcije energije
HE	- High Energy absorption - Visoka apsorpcija energije		

Table 1. Energy absorption category according to the EN12767

Tablica 1. Nivoi apsorpcije energije prema EN12767

Impact speed, v_I km/h	50	70	100
Energy absorption category	Exit speed, v_e km/h		
HE (high)	$v_e = 0$	$0 \leq v_e \leq 5$	$0 \leq v_e \leq 50$
LE (low)	$0 < v_e \leq 5$	$5 < v_e \leq 30$	$50 < v_e \leq 70$
NE (none)	$5 < v_e \leq 50$	$30 < v_e \leq 70$	$70 < v_e \leq 100$

ZIP pole = HE

The standard determines the category of energy absorption in relation to three different initial speeds and their related exit speeds with their maximum and minimum limits. Support structures for which exists no request for efficiency regarding the passive safety are marked with a category 0.
The support structures which do not deform in case of a vehicle impact or they deform just minimally, that is, all those where the complete energy of collision overtakes the vehicle and the occupants, are not classified in the passive safety support structures at all. Such support structure is, for example, a rigid lighting column. The consequences of a collision could me immense (figure no. 1).

Figure 1. One of many crashes with tragic consequences

Slika 1. Jedan od mnigih sudara s tragičnim posljedicama

Levels of occupant safety

There are four levels of occupant safety specified. Level 1, 2 and 3 – in this order – present an increase of occupant safety which means lowering the effect of the impact into support structure. For these levels of safety a test has to be performed:

- at 35 km/h, to verify the sufficient functionality of support structures at low speed and
- At speed classes of impact speed (50, 70 and 100 km/h) as given in a table no. 1.

Level 4 includes a non-harmful support structures that are assumed to cause only minor damage. A simplified test at a certain speed class should be done and the difference between impact speed and exit speed may not be more than 3 km/h. [1]

All tests must be done with light weight cars for the reason that the level of impact severity in respect to the

occupant safety in such type of cars is ensured. The test vehicle must be a standard passenger car with inertial mass of 825 kg ± 40 kg, with maximum allowed ballast 100 kg, test dummy of 78 kg ± 5 kg and other characteristics described in the article 6.2.1 of the mentioned standard. [1]

To determine the level of occupant safety two parameters are used:

- ASI (Acceleration Severity Index) and
- THIV (Theoretical Head Impact Velocity),

both in regard to the class of impact speed and the category of energy absorption. The ASI and THIV are calculated in accordance with EN 1317-1.
For a given combination of the energy absorption category and occupant safety level, the ACI and THIV values, rounded in accordance with 6.12 [1], shall not exceed the maximum values specified in Table 2 for both the low impact speed and the high impact speed tests.

ASI

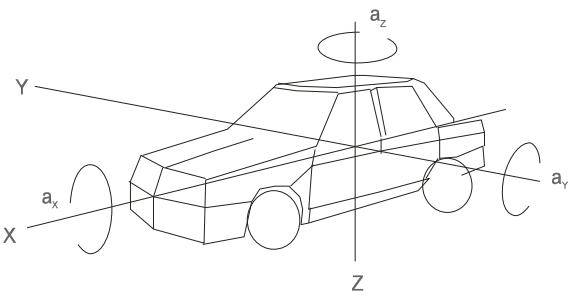

THIV

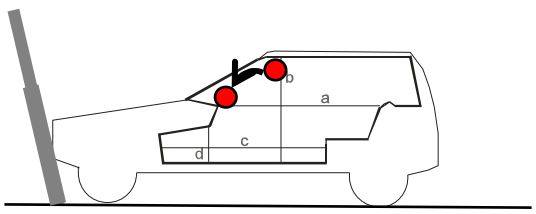

Figure 2. Schematic drawing of the components measured to evaluate the ASI and THIV values

Slika 2. Shematski crtež izmjerenih komponenti za procjenu ASI i THIV vrijednosti

Different demands and evaluations are taken into account beside the category of occupant safety to determine the type of support structures for road equipment whereas following parameters are taken into consideration:

- Expected risk of accidents damage or harm and possible calculation of cost and benefit,
- Type of the road and it's geometry,
- Characteristic speed of a vehicle on a certain location,
- Presence of other objects, constructions, trees or pedestrians,
- Presence of different systems for lowering the speed.

In such way the road authorities on different levels of administration (state, provincial, regional, municipal) specify the request for a certain level of passive safety of support structures. These decisions could be different in different regions or states and they depend very much on a consciousness of decision takers, that is, how much are they aware about the need for passive safety on the roads. For instance, having in mind the increase of passive safety of the roads, the Flemish Road Administration decided to install the ZIP poles:

- On all roads where the allowed speed is over 50 km/h and where are no guardrails in front of the lighting poles,
- On all roads where the allowed speed is under 50 km/h but the lighting columns must be closer than 2m from the edge of the pavement and there are no guardrails in front of the columns,
- On all roundabouts where the speed is not limited to 30 km/h and
- In places where a big possibility for a vehicle to crash into the pole exists: roads leading to roundabouts, roads between roundabouts, curves, crossings with sharp angles, etc.

Lately the installation of ZIP poles became interesting also on the entrances and exits of the highways because there is no need anymore for guardrails in front of the columns if "safe" columns are used. This enables the investor to save money on the guardrails as well as on land needed for the infrastructure. Of course the guardrail can not be omitted if there are other obstacles which need to be protected but also in this case a saving on land can be achieved because the column can stand close to the guardrail (no need for the prescribed distance between the guardrail and column).

Even further step in (beside other measures for higher safety on the roads) encouraging the authorities and investors to prescribe and use passive safe infrastructure elements were done by ETSC document speaking about European Road Safety, mentioning also so called "forgiving roadside" (2.3. – Safer Infrastructure). [2]

Based on tests successfully undertaken and completed the producer has obtained the certification for the product, its category and the level of occupant safety. (Figure no. 3)

Table 2. The evaluated ASI and THIV values

Tablica 2. Procjenjene ASI i THIV vrijednosti

Energy absorption categories	Occupant safety level	Speeds			
		Mandatory low speed impact test - 35 km/h		Speed class impact tests 50, 70 and 100 km/h	
		Maximum values		Maximum values	
		ASI	THIV km/h	ASI	THIV km/h
HE	3	1,0	27	1,0	27
HE	2	1,0	27	1,2	33
HE	1	1,0	27	1,4	44
LE	3	1,0	27	1,0	27
LE	2	1,0	27	1,2	33
LE	1	1,0	27	1,4	44
NE	3	0,6	11	0,6	11
NE	2	1,0	27	1,0	27
NE	1	1,0	27	1,2	33

ZIP poles have achieved level3, which means the highest safety for the occupants.


OCAB CE OCBS
CE1148 CE1148

1148 - CPD - 20080603

SAFETY-PRODUCT in its factory of PULLE

CE-Certificate: List of Approved Products

Products	Qualities and categories	Dimensions
Harmonised standard under reference: hEN 40-5 : 2002		
ZIPPOLE (6 m to 12 m) as top pole or with bracket (up to 2.5 m) with concrete foundation below ground level following Quality Handbook of SAFETY-PRODUCT (Report: "safety-product verslag EN 40 08-06") (Report: "safety-product verslag 12ZP2-10C2-2,5") (drawings enclosed in next pages) with passive safety evaluated by physical tests according to EN 12767:2007 "Speed Class = 100" "Energy Absorption Category = HE" "Occupant Safety Level = 3"		

Figure 3. Example of a CE certificate for the poles that correspond to EN 12767

Slika 3. Primjer CE atesta za stupove prema EN 12767

The product - principle

The reason that ZIP pole reaches the highest safety for occupants and the highest absorption of energy lies in its innovative design and construction. The cross section of a ZIP pole is nine angles and in the longitudinal direction is conical. It is made of steel plate. The main differentiator of the pole is that it is constructed of

pliable yet strong steel and is not welded but riveted. This construction enables the column to be strong enough for functional use, this means that it can support the lamp or other equipment but at the same time, in case of a vehicle impact, it starts flattening gradually, so that it changes shape from almost round into a ribbon which means that the crumpling of a column overtakes the impact force of a vehicle. This construction enables the energy absorbing principle to perform no matter the height the column might be hit. Even if a vehicle is launched into the pole at one or two meters above the ground the characteristics of the pole remain the same as if being hit at ground level. ZIP poles had already been tested in accordance with EN 12767 in 2008 and passed. [3]

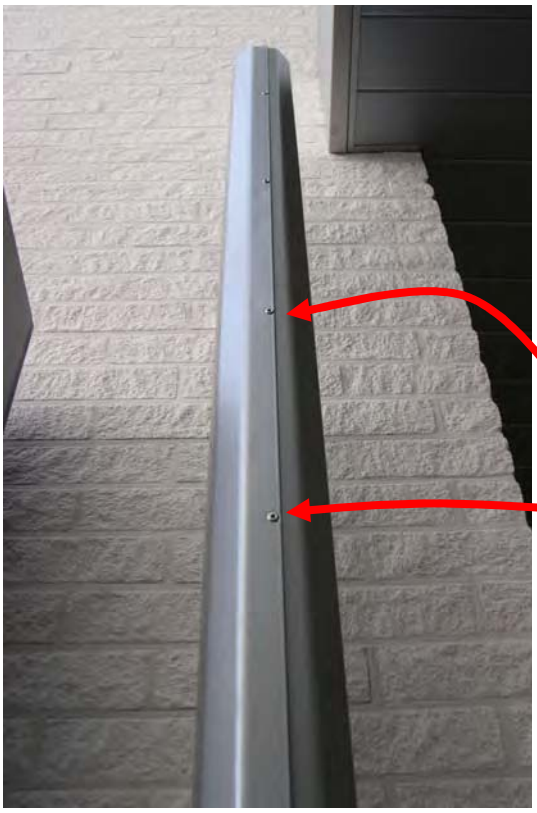

Figure 4. Construction detail

Slika 4. Detalj konstrukcije

The verification of ZIP pole was done also in Slovenia in the centre for safe drive Španik, Murska Sobota on September 11th, 2009. The aim of the tests was the comparison of the effects in case of a car crash into a conventional (energy non-absorbing column) and then into the ZIP pole (energy absorbing column). The tests were not performed in strict accordance with the EN 12767 standard (the speed was slightly lower than 50 km/h and the point of the impact was moved from the centre of the vehicle). The main aim was a comparison of crash effects with the same type of vehicle and different poles. The test was performed by Mr. Jože Škrilec, B. Sc. Traffic. Comparative crash test with ordinary column and ZIP pole proved that the ZIP pole is much safer. The time duration of impact is longer, maximum slow down at impact is significantly lower which all increases the safety of occupants in case of a crash. ZIP poles yield and absorb more during the impact and what is even more important, they deform gradually, which means that the peaks of slow down are less extreme in comparison with the conventional column. This means that the potential injuries of occupants as well as the damage to the vehicle would be significantly less compared to impact into a conventional column. [4]

Figure 5. Function principle – impact of a car flattens the pole

Figure 5. Princip djelovanja – udarac vozila u cijelosti deformira stup

Figure 6. Crash into conventional pole – almost immediate stop (green car) and crash into the ZIP pole – gradual slow down (red car)

Slika 6. Sudar s konvencionalnim stupom – gotovo trenutno zaustavljanje (zeleni vozilo) i sudar sa ZIPpole stupom – postepeno usporavanje (crveno vozilo)

Conclusion

ZIP poles proved to be extremely efficient and safe. They are ranked in the high energy absorbing class of impact with a vehicle and they guarantee the highest occupant safety level. Beside this ZIP poles have lower CO_2 footprint because of cold production and less material used so therefore they are ECO friendly. ZIP poles also provide a possible advantage with regards scales of economy. The prices are very similar to conventional poles. This by implication means that the community does not need to pay more to bring passive road safety to an improved level. Taking into account that a big part of the public lighting presents the expenses for the installation, lamps, maybe decorative elements, the small differences (sometimes smaller than 10% value) can not be an excuse to omit the use of the passive safe ZIP poles. This fact becomes even more important especially considered at a State level because by preventing deaths, casualties and critical injuries the health insurance/road accident fund would generate significant savings thus lowering the burden on the State budget and therefore assisting tax payers.

REFERENCES

[1] ...: EUROPEAN STANDARD EN 12767:2007: *Passive safety of support structures for road equipment – Requirements, classification and test methods,* Approved by CEN on 23 September 2007, Brussels 2007. www.cen.eu

http://esearch.cen.eu/Details.aspx?id=4523024

[2] …: ETSC – European Transport Safety Council: *Future Road Safety in the EU At Stake? ETSC Response to the EC Communication "Towards a European Road Safety Area: Policy Orientations on Road Safety 2011 – 2020", Written By Antonio Avenoso and Ellen Townsend*, September 2010. www.etsc.eu

www.etsc.eu/documents/ETSC%20Response%20to%20EC%20Communication_%2022%20Sept%202010.pdf

[3] …: *Technical documentation on ZIP pole,* SAFETY PRODUCT, Pulle 2010. www.zippole.com

[4] ŠKRILEC, J.: *Zaključno poročilo: Poskusni trki vozil MS 2009 Zippole – klasičen drog*, Murska Sobota 2009. skrilec.joze@gmail.com

EN12767. PASSIVE SAFETY OF SUPPORT STRUCTURES FOR ROAD EQUIPMENT

Miles Dadson
Principal Engineer – HAVOC Facility
Safety Development

+44 (0)24 7635 5274
+44 (0)7887 632657

Miles.dadson@mira.co.uk

Predavanje - *Presentation*

Cijelo predavanje nalazi se na priloženom CD-u.

The whole presentation is on the attached CD.

10 YEARS WITH EN 12767 AND ZERO VISION

Lattix AS, Norway
Kim Heglund
Managing Director
Phone: + 47 906 72 911
kim.heglund@lattix.net

Predavanje - *Presentation*

Cijelo predavanje nalazi se na priloženom CD-u.

The whole presentation is on the attached CD.

i

Application of reverse engineering process in mold manufacturing industry

Luka CELENT[1)], ***Dražen BAJIĆ***[1)] ***and Sonja JOZIĆ***[1)]
1) University of Split
Faculty of Electrical Engineering, Mechanical Engineering and Naval Architecture, R. Boškovića 32, Split, Croatia
Sveučilište u Splitu
Fakultet elektrotehnike, strojarstva i brodogradnje, R. Boškovića 32, Split, Hrvatska

luka.celent@fesb.hr; drazen.bajic@fesb.hr; sonja.jozic@fesb.hr

Keywords
Reverse engineering
CAD
Surface creation
Mold
Three-dimensional printing

Ključne riječi
Reverzno inženjerstvo
CAD
Kreiranje površine
Kalup
Trodimenzionalno printanje

Original scientific article
This paper presents reverse engineering approach in molds making. Conventional forward engineering for mass produced parts that employ molds, is often too expensive and does not complete the time requirement. Therefore this approach has a negative effect on the economy of production. In order to solve this problem, manufacturing industry is forced to implement a reverse engineering approach due to its significant advances and practical application in this field.
Reverse engineering process in molds making industry, presented in this paper, involves the use of 3D scanner as a device to capture and digitize the data from the existing object. Measurement data are acquired by 3D stereo-photogrammetric scanning. Processing the measurement data by CATIA V5 software a CAD model was created. The analysis and modifications of design are preformed on that CAD model. Due to the improvement of design, additional machining used in making the initial object, was avoided. Molds correspond the modified CAD model were made using 3D printing technology.

Izvorni znanstveni rad
Ovaj rad predstavlja novi pristup u industriji izrade kalupa, korištenjem Reverznog Inženjerstva. Konvencionalno, antegradno inženjerstvo u masovnoj proizvodnji koja uključuje kalupe, je vrlo često preskupo i ne ispunjava vremenske uvjete isporuke. Ovaj pristup time negativno utječe na profitabilnost proizvodnje. U svrhu rješavanja ovog problema, proizvodna inustrija je prisiljena uvesti novi reverzno inženjerski pristup u proizvodnji, zahvaljujući njegovim značajnim prednostima i praktičnoj primjeni u ovom području. Proces reverznog inženjerstva u industriji izrade kalupa predstavljen u ovom radu, obuhvaća korištenje 3D skenera kao uređaja za dobivanje podataka od već postojećeg objekta i njihovu digitizaciju. 3D fotogramatskim skeniranjem su prikupljeni parametri na temelju kojih je u programu CATIA V5 kreiran CAD model. Analize i izmjene dizajna su izvršene na tom CAD modelu. Poboljšanim dizajnom se uspjela izbjeći dodatna obrada korištena prilikom izrade već postojećeg objekta. Kalupi modificiranog CAD modela su izrađeni korištenjem 3D printera.

1. Introduction

Reverse engineering (RE) is the process of taking the existing physical model and reproducing its surface geometry in three-dimensional (3D) data file on a computer-aided-design (CAD) system.
RE process is now accepted as a necessary phase in manufacturing for it provides the achievement of prescribed quality with significant cost reduction as compared to conventional forward approach. The main difference between conventional forward engineering and reverse engineering is that the former is an explicit physical implementation process from high-lever abstract concept to design, whilst the latter is an inferential process that is obtained by adjusting and modifying the feature parameters to approach an object model [1].
There is an increasing pressure on manufacturing industry to develop new ways to make their production more cost effective. Introduction of RE approach was very successful and resulted in giving maximal benefit of invested money. In RE process, a physical object is translated in mathematical model allowing the adjustments and modifications in order to optimize the product concept before manufacturing. Methods of RE have different application areas for extracting data from the existing object for which the documentation doesn´t exist, recovery of a damaged part, modification of model, inspection and analyses of model etc [2].
The part of the metalworking industry that is probably subjected to the fastest changes as a response of ever increasing demands is die/mould industry. Intricate geometry and sculptured surfaces make die/mold design and manufacturing very demanding and difficult engineering task. For example, molds are composed of functional and support components. In genera more than 60% of the production time of a mold is spent to manufacture the functional parts [3]. With application of RE the product development times are rapidly compressing. For the existing parts RE approach can speed up research and development of products, shorten

the cycle from design to manufacturing and allows realization of some modern design concepts [4].
In general, development of a new casting broadly comprises three distinct phases: model design, molds development, and casting production [5]. Most firms now make use of CAD programs for solid modeling and shape optimization. Creating a 3D model of the part is a time-taking task, but essential for computer-aided casting development. For existing parts, the solid modeling time can be minimized by reverse engineering: scanning the part geometry using a contact or non-contact (laser) scanner and using software programs for mold design.
The very important tools in this process are different scanning and CAD systems, used to capture and digitize the object surface geometry. The CAD model representing the geometric features and other properties of the original object is reconstructed in CAD system.

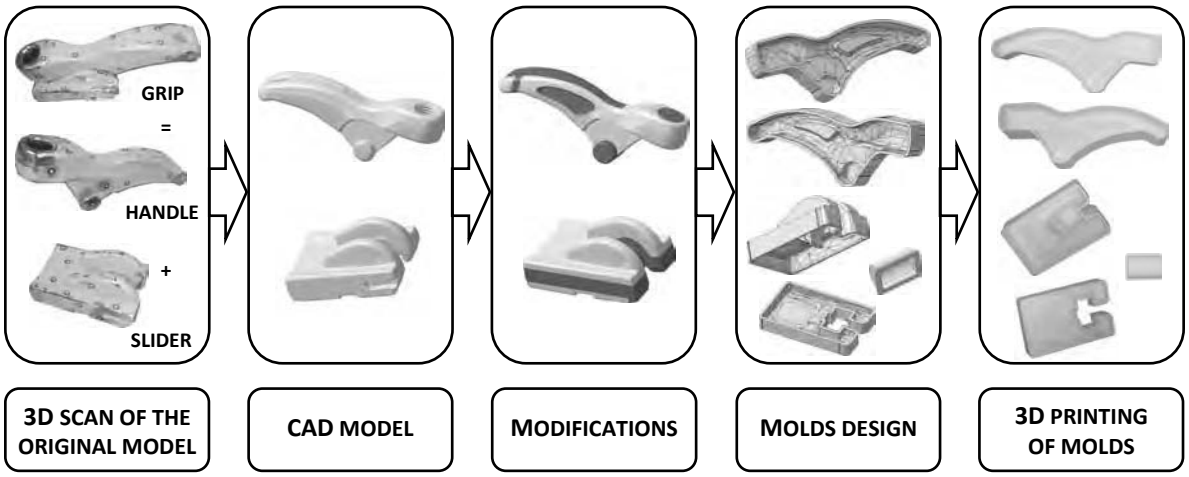

Figure 1. General steps of RE on grip model

Slika 1. Faze procesa reverznog inženjerstva na modelu stege

2. Phases of Reverse Engineering process on grip model

RE process was performed on the original model of the grip used in shipbuilding industry. The grip consists of two parts, the handle and the slider. The request for modification of the original grip model came as a result of specific order for a particular model of the ship.
The objective of the process is to be able to generate model-to-CAD and CAD-to-model reconstruction of the original model for future usage. The goal of the first phase of RE is to capture or recreate the geometry of the object by digitization. Strategy for digitization of the object depends on complexity of the surfaces [6]. As the original grip has a relatively complex shape and small dimensions, the RE of grip model digitization was performed by 3D stereo-photogrammetric scanning using measurement volume of 65mm. During this process, the system records information about the surface in the form of numerical data-generates a point's cloud matrix (3D-coordinates) [7]. This approach can provide high-quality overall geometry as well as increased resolution and accuracy of selected details.
The obtained point cloud data is then imported to CATIA V5 software to develop the 3D model and after some specific modifications, finally design the molds. The molds were made using 3D printing technology. In order to get the final product, RE process is followed by the casting of plastic into the printed molds. Plastic models are than used to get sand molds for metal casting of the final product.

3. Reverse Engineering in CATIA

The use of numerous systems to develop digital products from physical prototypes is complex and costly, leading to delays in product development. There are many software about RE, like Geomagic, Surface, Imageware, and like normal 3D modeling software also included the function of reverse engineering.
CATIA RE makes possible quickly capture and enhance physical prototype shapes, making the 3D virtual model the design reference. It also provides powerful technologies embedded within CATIA that allow the easy manipulation of points cloud or meshes, while quickly transforming them into 3D surface shapes.

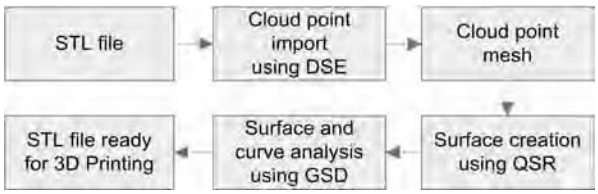

Figure 2. The process of RE in CATIA V5 software

Slika 2. Proces reverznog inženjerstva u programskom paketu CATIA V5

This paper uses CATIA V5 because of its great combination function about surface design, modeling design, reverse design and etc. In RE design three modules were used: Digitized Shape Editor (DSE), Quick Surface Reconstruction (QSR), Part design (PD) and Generative Shape Design (GSD). The process of RE in CATIA used in this article is shown in Figure 2.

3.1. Surface creation

To solve the problem of surface creation in building the model of grip, certain requirements were taken into consideration. The purpose of the object, the required accuracy and the quality of the patch layout of the surface were considered and consequently the CATIA software was used.

In order to create surface a points cloud acquired by 3D stereo-photogrammetric scanner was tessellated by CATIA software into a STL mesh. Building a surface from the STL mesh requires an extensive analysis and a good quality of STL file [8].

Rough and noisy parts on the surface of the mesh were avoided and twisted or in any other way corrupted triangles were prevented and quality of the layout was ensured by closing all small holes. Mean surface deviation was checked and the Surface detail was set to 4000. Due to a rough edge of the mesh free edge tolerance was set to higher value of 1mm, also the full internal tangency was checked. Satisfying layout of the sub-surface was gained.

3.2. CAD model analysis and improvements

Reconstructed CAD model was analyzed in order to make certain adjustments based on the requirements of function. From examination of the initial model it is obvious that the final product was obtained using the additional machining. Two great modifications were made on handle, allowing realization of modern concept design of final product (Figure 3). Compared to the initial scanning object, the handle was lengthened for 10 mm to suit the required function better. Further, 9 mm pocket was added to make savings on material and to reduce the product final weight without any deterioration of its function.

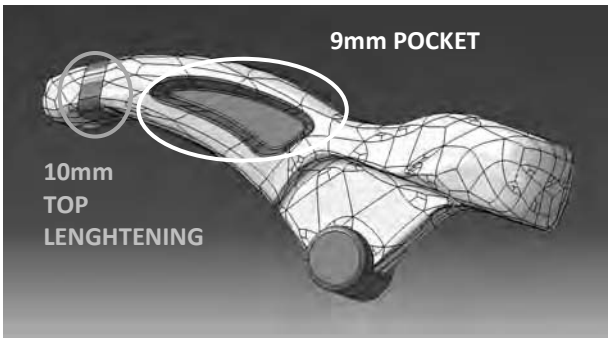

Figure 3. Main handle modifications

Slika 3. Glavne modifikacije na modelu ručke

The slider was also improved considering manufacturing facilities but especially quality specifications. These improvements were enabled by decreasing of the molds parting line for 5mm and by adjustments of the corresponding geometric features and other parameters (Figure 4).

Due to these modifications, additional machining of the final product was avoided, making the process of production less lasting and more cost effective.

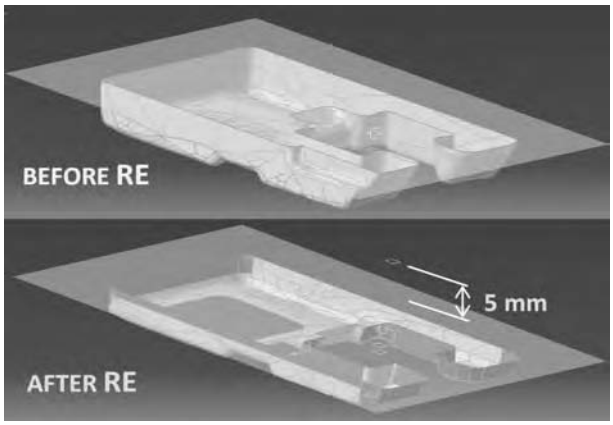

Figure 4. Avoiding additional machining of the slider using different position of molds parting line

Slika 4. Izbjegavanje naknadne strojne obrade klizača pomicanjem razdjelne ravnine na odgovarajuću poziciju

3.3. Molds design

The mold is made according to the modified CAD model (Figure 5). With some objects this can be accomplished by creating one mold for the entire object. However, most molds are made from at least two pieces. The handle mold consists of two and the slider mold of three pieces.

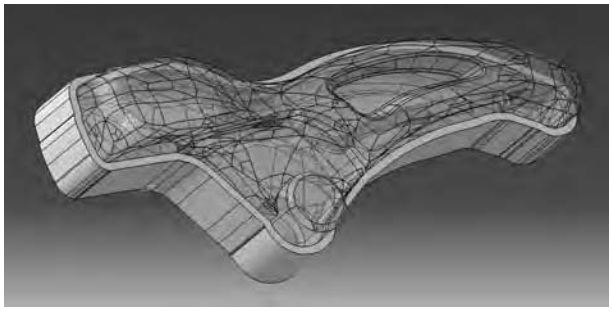

Figure 5. Obtaining the molds from the modified CAD model using PD and GSD module in CATIA

Slika 5. Dobivanje kalupa iz modificiranog CAD modela korištenjem PD i GSD modula u CATIA-i

The most importante decision in mould design is about the parting line. This separation between two or more segments is necessary to create the mould cavity and also to remove the manufactured part from the mould.

The demand to avoid the additional mechining led to different solution for the same shape, moving the parting line of the slider 5mm belowe the initial one. This affects and is affected by part orientation, design of the mold and the number of cavities in the mould. Variation of design depended on customer requirements considering the specific use of the product and its manufacturing cost.

4. 3D printing of the molds

Technique for creating moulds directly from a 3D model is called Direct Shell Production Casting (DSPC) and was developed by Solingen Technologies, Inc. [6]. DSPC uses 3-D printing to create a ceramic mould.

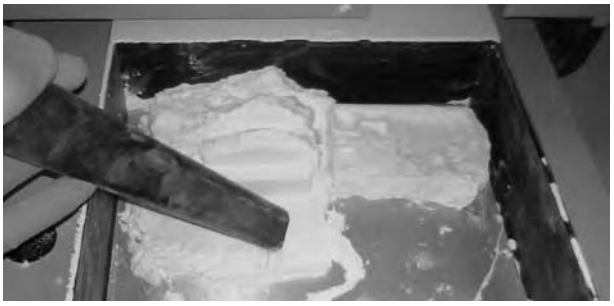

Figure 6. Removing of loose powder with vacuum cleaner

Slika 6. Uklanjanje neupotrebljenog praha

First step is to import an STL format, 3D data file into ZPrint® software. By executing the command to start printing, a 3D model is emerging from the bottom up one cross-section at a time. A thin layer of ceramic powder is spread and then an ink jet print head deposits a silicate binder onto the powder in the shape of the part. When printing is complete , using vacuum cleaner a 90% of loose powder should be removed and recycled for future use (Figure 6) .

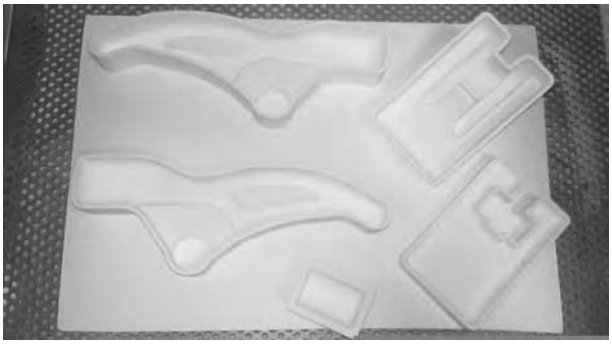

Figure 7. Final molds parts

Slika 7. Gotovi dijelovi kalupa

After the models were extracted from the printing area the remaining powder was removed from the models using lightly compressed air, in fully enclosed chamber that vacuums away powder as it goes (Figure 7). In order to finish and strenghten the models, molds were cured with Z-Bond impregnation liquid.

5. Conclusion

Today we are witness of ever increasing demands in manufacturing industry. Conventional methods can`t follow this development and are no longer acceptable.

This paper shows some possibilities of use and benefit from utilizing the RE-methodologies and techniques in molds production process. The integration of RE approach compresses the product development times compared to conventional method, and enables for faster manufacturing of any complicated shaped sand moulds. Any changes in design can be easily updated in the backup 3D CAD model considering customer requirements, quality specifications and manufacturing facilities.

It can be concluded that application of RE approach reduces manufacturing cost of all processes from development of the mold to mass production of the object for increasing the competition ability in the market.

REFERENCES

[1] PUNTAMBEKAR, N.V.; JABLOKOW, A.G.; SOMMER, H.J.: *Unified review of 3D model generation for reverse engineering,* Comput. Integrated Manuf. Syst. (1994) 7 (4), 259-268

[2] YUAN, X.; ZHENROG, X.; HAIBIN, W.: *Research on integrated reverse engineering technology for forming sheet metal with a freeform surface,* Journal of Materials Processing Technology (2001), Vol. 112, 153-156

[3] FALLBOHMER, P.; ALTAN, T.; TONSHOFF, H.K.; NAKAGAWA, T.; *Survey of the die and mold manufacturing industry,* Journal of Materials Processing Technology (1996), Vol. 59, 158-168

[4] ZHANG, Y.; LIU, H.: *Application of Rapid Prototyping Technology in Die Making of Diesel Engine,* Tsinghua Science and Technology (2009), Vol. 14, 127-131

[5] SURESH BABU, T.; THUMBANGA, R.D.: *Reverse engineering, CAD\CAM & pattern less process applications in casting-A case study,* International Journal of Mechanics (2011), Vol. 5, 40-47

[6] HONG-TZONG, Y..: *Reverse Engineering of the engine intake ports by digitization and surface approximation,* International Journal of Machine Tools and Manufacture (1997), Vol. 37, 855-971

[7] DOKOVIC, M.; KOPAC, J.: *RE (reverse engineering) as necessary phase by rapid product development,* Journal of Materials Processing Technology (2006), Vol. 175, 398-403

[8] RYPL, D.; BITTNAR, Z.: *Generation of computational surface meshes of STL models,* Journal of Computational and Applied Mathematics (2006), Vol. 192, 148-151

Feasibility study of a novel device for separate collection and treatment of solid urban waste

Giuseppe PIGLIAPOCO [1)]**,**
Massimo ROGANTE [2)]
1) Studio Legale Avv. Pigliapoco,
Via M. Batà , 21
I-62100 Macerata, **Italy**
2) Rogante Engineering Office,
Contrada San Michele, 61
I-62012 Civitanova Marche, **Italy**

avv.pigliapoco@libero.it
main@roganteengineering.it

Keywords
Domestic appliance
Refusal
Waste
Recycling

Ključne riječi
Kućna upotreba
Otpad
Smeće
Recikliranje

Professional paper

In the present study a system is illustrated for the diversified collecting of the refusals to use in the initial phase of production of the same.
The system is composed of various forms to create a small appliance, and it can be employed in domestic circle or in the restaurants sector, or where refusals are produced in general.
The system introduces the following advantages: to already stimulate the diversified collecting of the refusals in phase of production; the reduction of dimension and volume of the refusals with a first triturating; to prepare the material for the successive industrial treatments of recycling; to pre-treat some typologies of material decomposable refusals.

Studija izvodljivosti novog uređaja za odvojeno prikupljanje i tretman krutog gradskog otpada

Stručni rad

U ovoj studiji prikazan je sustav za prikupljanje raznovrsnog otpada, kao i korištenje istog u početnoj fazi nastajanja otpada.
Sustav je sastavljen od različitih dijelova koji omogućavaju sklapanje urađaja za odvajanje otpada, a koji se može koristiti u domaćinstvu ili u restoranima, odnosno svuda gdje nastaje otpad.
Sustav uvodi slijedeće prednosti: stimuliranje prikupljanja raznovrsnih ostataka već u fazi nastajanja; smanjenje dimenzije i volumena ostataka već kod prve faze odvajanja, priprema materijala za industrijski tretman recikliranja; rana obrada razlaganjem pojedinih vrsta otpada.

1. Introduction

The separate collection of solid urban waste, since many years, represents a more growing problem at the point to create strong inconveniences and also social conflicts. The incinerators and the introduction of other new disposal systems certainly lightened the use of the dumps but the remarkable increase of the waste has presented the urgent necessity of a differentiated collection and, if the case, the re-use of the same litter.
A novel modular system has been studied for the diversified collection of the refusals, made of more forms to generate a small appliance (see Fig. 1).
The field of application of this appliance results very wide; in particular, it can be adopted:
- in domestic circle, to reduce and to decompose the different refusals produced by a family;
- in the restaurants sector, to reduce and pre-treat, above all, the damp solid refusals;
- in the commercial sectors, to reduce the volumes of refusals of some typologies.

Figure 1. Device for separate collection of solid urban waste.

Slika 1. Uređaj za prikupljanje i razdvajanje krutog otpada

In the following chapter the operation of the appliance are illustrated and described, as well as the various devices for the treatment and the grinding of the main components of the domestic refusals.

2. Description of the device

The device is composed of five independent modular systems to treat and to grind the following elements of refusal that are normally produced in domestic circle:

- damp solid refusals;
- bottles of glass;
- papers and cardboards;
- bottles and objects in plastics;
- cans in aluminium.

These modules can be placed in the traditional recessed position configuration in the sectional kitchen and/or separately.

The operational forms of the appliance have the following dimensions:

- height 800 mm
- depth 700 mm
- width 150 - 200 mm

in order to form an appliance of general standard width having the following dimension:

- 450 mm (joining 3 forms of 150 mm);
- 600 mm (joining 4 forms of 150 mms or three of 200 mm);
- 900 mm (joining 3 forms of 200 mm together with two of 150 mm).

On the frontal part of every form of the product the following elements are placed:

A - superior door inside which the refusals are thrown;

B - central part where the command panel with indication on the state of operation of the mechanism is placed;

C - inferior drawer where the treated refusals ready to be disposed are picked up.

Fig. 2 shows the household appliance with the introduction door of the refusals opened, while Fig. 3 shows the household appliance with the open inferior drawer.

Figure 2. The household appliance with the introduction door of the refusals opened.

Slika 2. Kućni uređaj s otvorenom ulaznom ladicom za prihvat otpada

Figure 3. The household appliance with the open inferior drawer.

Slika 3. Kućni uređaj s otvorenom ladicom

The mechanisms for the treatment of the various main elements are different among them because they treat products having very different treatment problems. The operational forms of treatment of the various components of the refusals are one independent from the other. The disposition of the single mechanisms can be performed according to two followings hypotheses illustrated:

I hypothesis

The mechanisms are connected with a shaft that transversally crosses the single forms, operated through a special reduction by an electric motor, as shown in Fig. 4.

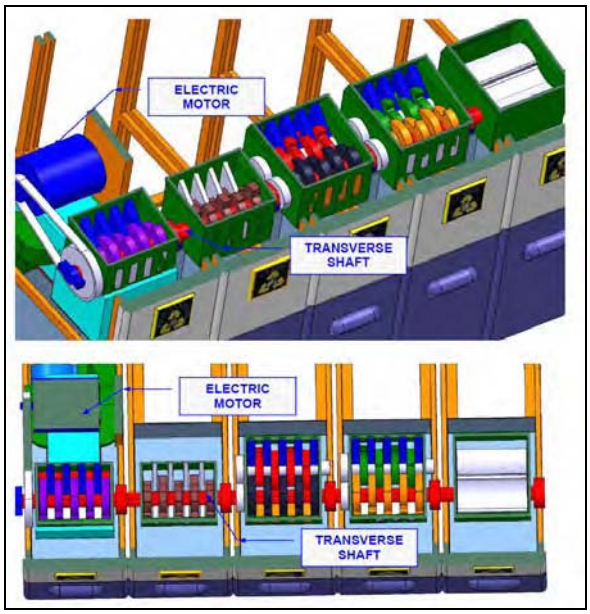

Figure 4. Scheme of the first hypothesis of the single mechanisms' disposition.

Slika 4. Shematski prikaz primarne ideje rasporeda jednog uređaja

II hypothesis

The mechanisms of treatment of the various refusals are placed with longitudinal axle in comparison to the form and they are operated, through special gears, from a transmission shaft that crosses the various forms and takes power from an only electric motor. In this hypothesis, in the operational phase only one mechanism is operated at a time corresponding to the interested form to the treatment of the refusal, operated by the transversal shaft through a connection with a joint friction having an electromagnetic coupling. The motor should have a power of around 800 W, operating at a rotation speed of around 1400 rpm.

Fig. 5 shows the disposition of the five forms, while Fig. 6 the coupled mechanisms.

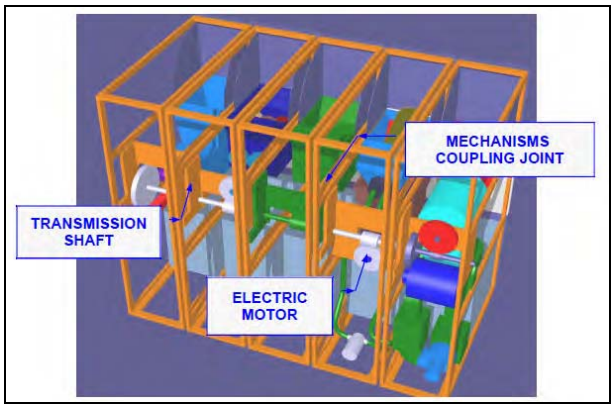

Figure 5. Scheme of disposition of the five modules.

Slika 5. Shematski prikaz rasporeda pet modula

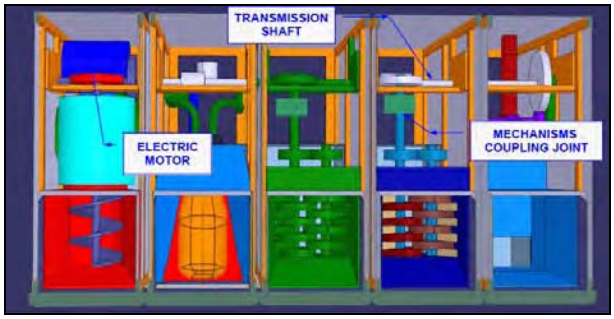

Figure 6. Scheme of the coupled mechanisms.

Slika 6. Skupni shematski prikaz uređaja

The form for the treatment of the damp solid refusals is essentially composed of the followings functional parts:

- a triturating system of the damp solid refusals in order to reduce their volume;
- a desiccation system in order to remove the present damp on the refusals.

This form operates as in the following phases:

- Introduction of the refusals inside the treatment system through the opening of the superior door. By closing the superior door, the treatment cycle of the refusals begins.
- Trituration of the refusals to reduce their volume. The trituration happens through a cutting device able to reduce the treated product to a uniform dimension. The product obtained by the trituration passes in the container for the execution of the following treatment of desiccation.
- Desiccation of the refusals with elimination of the damp. The system of desiccation is composed by a closed circuit of air so constituted:
    - centrifugal fan for the execution of the air circulation
    - air heating system
    - filtration system for the laying of the vapours formed in the passage of the warm air to contact with the product. The product remains in the desiccation container until it doesn't reach a damp content such to be not more degradable.
- Discharge of the refusals in the container.
- Extraction of the refusals from the container. Once the drawer present in the inferior part of the form is filled, it is necessary to extract the pouch full of refusal.

The form for the treatment of glass refusals (e.g., bottles and jars) is essentially composed from the followings functional parts:

- a washing system of the glass containers with the purpose to eliminate the perishable substances enclosed in the same containers;
- a trituration system in order to decrease the volume of the objects.

This form operates as in the following phases:

- Introduction of the glass elements inside the treatment system through the opening of the superior door. By closing the superior door, the cycle of treatment of the element begins.
- Washing of the containers with elimination of the residues. The washing system is constituted by the following components:
    - a taking device of the mouth of the universal container;
    - a pump for water injection at high pressure;
    - a discharge system of the water with the residues to be eliminated.
- Trituration of the refusals in order to decrease the volume of the objects. The system is constituted by two counter-rotating shafts on which some rings are connected having irregular outline, that shatter the glass objects during the rotation. The glass fragments directly fall on the collecting container.
- Extraction of the refusals from the container. Once filled the drawer present in the inferior part of the form, it is necessary to extract the pouch full of refusal.

The form for the treatment of paper refusals (e.g., cardboard boxes, and newspapers) is essentially composed of a trituration system having the function to

decrease the volume of the objects. This form operates as in the following phases:

- Introduction of the paper objects inside the treatment system through the opening of the superior door. By closing the superior door, the cycle of treatment of the objects begins.
- Trituration of the refusals. The system is constituted by two counter-rotating shafts on which some blades are connected having irregular outline that cut the paper objects during the rotation. The pieces of cut paper directly fall in the collecting container. Different geometries of the cut blades are brought with which it is possible to get diverse sizes of the grinded material. the cutting blades must be realized with a special steel that, after a very complex and delicate process of tempering, it has to reach the following characteristics: complete quenching, with little difference of hardness between the surface and the inside, thus allowing different re-grindings; raised value of resilience that guarantees an elastic steel under very severe operative conditions, with very high mechanical loads on the knives; raised hardness that guarantees low levels of wear with critical material such as metals and dirty refusals. When the blades are wearied, they can be re-grinded quite many times before being replaced.
- Extraction of the refusals from the container. Once filled the drawer present in the inferior part of the form, it is necessary to extract the pouch full of refusal.

The form for the treatment of the plastic refusals (e.g., plastic bottles, containers and envelopments) is essentially composed, also in this case, of a trituration system having the function to decrease the volume of the objects. This form operates as in the following phases:

- Introduction of the plastic objects inside the treatment system through the opening of the superior door. By closing the superior door, the cycle of treatment of the objects begins.
- Trituration of the refusals in order to decrease the volume of the objects. The system is constituted by two counter-rotating shafts on which some cutting blades are connected having irregular outline, which cut the plastic objects during the rotation. The pieces of cut plastic directly fall on the collecting container. Concerning the blades, see the considerations above reported.
- Extraction of the refusals from the container. Once filled the drawer present in the inferior part of the form, it is necessary to extract the pouch full of refusal.

The form for the treatment of aluminium refusals (e.g., cans, aluminium containers and aluminium sheets) is essentially composed, also in this case, of a compaction system having the function to decrease the volume of the objects. This form operates as in the following phases:

- Introduction of the aluminium objects inside the compaction system through the opening of the superior door. By closing the superior door, the cycle of treatment of the objects begins.
- Compaction of the refusals in order to decrease the volume of the objects. The system is constituted by a crushing piston that advances inside the compression chamber. At the end of the compaction phase, the compacted object falls in the collecting container.
- Extraction of the refusals from the container. Once filled the drawer present in the inferior part of the form, it is necessary to extract the pouch full of refusal.

The following accessories can be installed in the complete device:

- a system to perform hygienization treatments of the various forms;
- an automatic system for the replacement of the plastic pouches in the respective containers

Fig. 7 shows a scheme the complete device.

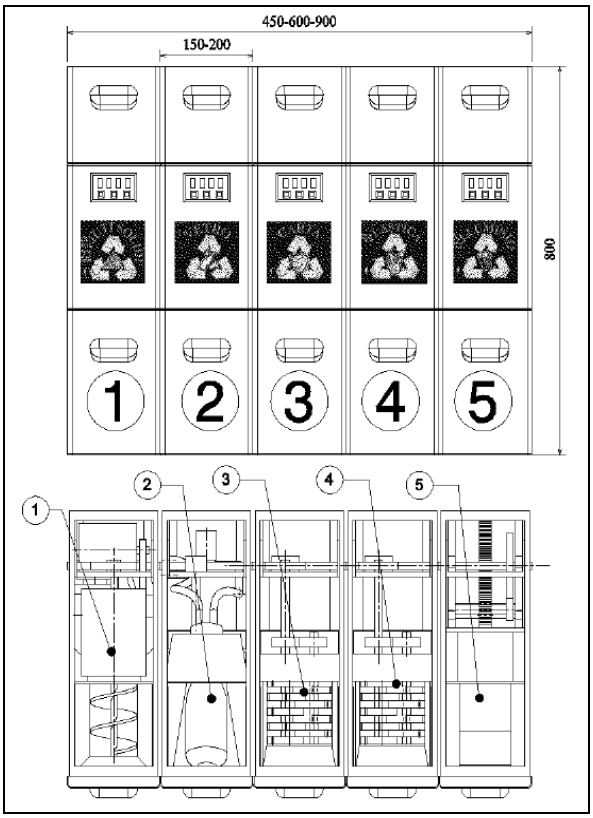

Figure 7. Scheme of the complete device.

Slika 7. Shematski prikaz cijelog uređaja

Conclusions

A novel device to collect, treat, compress, grind and reduce of volume the urban solid refusals in a differentiate way the refusals already at the initial phase of their production has been illustrated. The appliance is a practical mean to reduce and recover at the source the urban solid refusals and to avoid the difficult situation that currently it occurs concerning the disposal or their incineration. Such appliance has, inside, triturating and compression mechanisms in order to reduce the volume and to singly recover dampness, glass, plastics, paper and cans.

It appears evident that the aforesaid invention would allow eliminating the serious problems of disposal of the urban solid refusals to which our society succeeds in facing with a lot of difficulties and expenditure of money. Concerning the damps, for instance, it must be said that once grinded and dried, they will be of notably inferior volume and when they are put in the dump they don't require particular treatments for their degradability. The refusals that will be transferred to dump will be well little thing in comparison to today's massive structure, with great environmental and economic advantages both for the State (or the States and the Territorial Authorities), both for the single families.

This household will have different dimensions dependently on its assignment (at home, in a public house, in a hotel or in a restaurant, or also in substitution of the current collection devices placed on the roads), therefore its structures or its single forms can be suitable to the single demands. We estimate that at least the 80% can be reached in changing the refusal collection and treatment procedure, beginning also a further change with respect to the past and with an appreciable result, due to the great advantages obtainable at a social scale. The intervention of Municipalities and other local Boards in compensating the resulting simplifications and energy saving at a general level, by favouring the users, would be fundamental.

REFERENCES

[1] PIGLIAPOCO, G.: *Elettrodomestico per lo smaltimento dei rifiuti solidi urbani*, Brevetto per modello di utilità N° 0000263833, Ufficio Italiano Berevetti, Jan. 20, 2010.

[2] PIGLIAPOCO, G.: *Raccolta differenziata: Pigliapoco, come sarà in futuro?*, Vivere Macerata., Amsterdam, 2010, web page http://www.viveremacerata.it/index.php?page=articolo&articolo_id=237218, accessed on 04/07/2011.

[3] AGOSTINELLI, S.: *Smaltire alla sorgente: un'idea che funziona*, Regioni e Ambiente, 5 (2004), 55. Web page http://www.regionieambiente.it/pagine/pdf/05lugago2004/ReA7_8_2004_15.pdf, accessed on 04/07/2011.

Cements for nuclear industry: a feasibility study of neutron-based investigations

Massimo ROGANTE[1)]**,**
Anastasia SELEZNEVA[2)]
1) Rogante Engineering Office,
I-62012 Civitanova Marche, **Italy**
2) Ural Federal University
19, Mira Str., 620002 Yekaterinburg,
Russian Federation
main@roganteengineering.it

Keywords
Cement
Polymers
Radioactive waste
Industrial Applications of Neutron Techniques

Ključne riječi
Cement
Polimeri
Radioaktivni otpad
Industrijska primjena neutronskih tehnika

Professional article
Safety, lifetime monitoring and nuclear waste management are a main concern for the nuclear installations and they require the knowledge of the real state of materials and components, with the aim to guarantee the higher levels of reliability and control severe natural and plant–centred events. Study of dense cements, ceramics and associated materials (for instance, cement stones) is significant to create novel advanced components for nuclear–safety related structures, with high functional properties (such as ageing and cracks' formation resistance, hardness, durability, stability of mechanical modules and ecological criteria) also to be considered for corrosion resistive coatings of nuclear waste containers.
In this paper, some examples concerning different types of cements suitable for nuclear industry are reported and their investigability and analyses by neutron techniques are discussed, in order to assess key parameters, e.g. porosity, fractal dimensions, size distribution and other characteristics (open, closed pores, cracks) at the scale from 1 Å to 100 Å, responsible of the materials' performance.
The result can translate into optimization of consistency, design of operating conditions and procedures, supporting to enhance quality and safety levels.

Cementi za nuklearnu industriju: studija o provedivosti neutronski temeljenih istraživanja
Stručni rad
Sigurnost, nadzor vijeka trajanja i upravljanje nuklearnim otpadom glavna su briga u nuklearnim postrojenjima, te zahtijevaju znanje o realnom stanju materijala i komponenti, a u svrhu jamstva visokih stupnjeva pouzdanosti, nadzora opasnih prirodnih pojava, kao i nezgoda unutar postrojenja. Proučavanje cementa povećane gustoće, keramika i pripadajućih materijala (npr. cementnog kamena) je značajno u stvaranju novih naprednih komponenti za sigurna nuklearna postrojenja, s visokom vrijednostima svojstava (otpornost prema starenju i nastajanju pukotina, tvrdoća, trajnost, stabilnost mehaničkih svojstava i ekoloških kriterija). Isto tako u obzir treba uzeti kvalitetu zaštitnih prevlaka otpornih na koroziju kod kontejnera s nuklearnim otpadom.
U ovom članku, navedeni su neki primjeri različitih tipova cementa pogodnih za nuklearnu industriju. Mogućnost njihovog istraživanja i analize pomoću neutronskih tehnika obrađene su u cilju određivanja ključnih parametara kao što su: porozitet, dimenzije fraktala, raspodjela veličine, te drugih karakteristika (otvorenost, zatvorenost pora, pukotine) u dimenzijalnom rasponu od 1 Å do 100 Å.
Rezultati mogu koristiti za optimizaciju postojanosti sustava, projektiranje operativnih uvjeta i procedura, podršku povećanju kvalitete i stupnjeva sigurnosti.

1. Introduction

Nuclear installations should involve, in general, the most advanced levels of reliability for materials and components, either in the plants' parts, or in the nuclear wastes storage devices.
Radioactive wastes are by-products of commercial and research nuclear reactors operation and their related fuel cycle, as well as residuals of radioactive isotopes adopted in the medical (for diagnoses and treatments), defence (fabrication and tests of nuclear weapon, naval propulsion), industrial, agriculture and research fields [1]. Nuclear wastes can be divided into the following categories: high level waste (HLW), intermediate-level waste (ILW), low-level waste (LLW). HLW is highly radioactive and contains long-lived radionuclides generating considerable decay heat: it is usually spent

Symbols/Oznake

HLW	- high level waste - visoko radioaktivan otpad	PGAA	- prompt gamma activation analysis - brza gama aktivacijska analiza
ILW	- intermediate-level waste - srednje radioaktivan otpad	PGNAA	- prompt gamma neutron activation analysis - brza gama neutronska aktivacijska analiza
LLW	- low-level waste - nisko radioaktivni otpad	SANS	- small angle neutron scattering - mali kut neutronskog rasipanja
n	- neutron - neutron		**Greek letters/Grčka slova**
ND	- neutron diffraction - neutronska difrakcija	(n, γ)	- neutron capture reaction - zapis neutronske reakcije
NR	- neutron radiography - neutronska radiografija	γ	- γ ray - gama zraka
PAV 22	- trademark of Rhodia Co. - marka proizvoda tvrtke Rhodia	γ	- γ phase of Al_2O_3 - gama faza iz Al_2O_3

nuclear fuel or the product resulting from its reprocessing. The long-term results of radiation on waste form solids is a key concern in the performance appraisal of the long-term containment strategy. The radiation dose related to the spent nuclear fuel and due to the in-reactor neutron irradiation, for instance, is considerable, as well as the post-disposal radiation damage to waste form glasses and crystalline ceramics [2]. ILW includes substantial quantities of long-lived radionuclides with unimportant generation of decay heat. LLW includes substantial quantities of short-lived radionuclides that decay to low levels within decades. Approximately the half of the entire conditioned radioactive waste quantity from nuclear installations is produced during the decommissioning phase. A proper management of radioactive wastes is a main task, which embraces various activities such as waste treatment (e.g., chemical processing and solidification into waste shapes), transport, storage and disposal. The latter activity should be carried out dependently on the waste category and involves the environmental monitoring of radionuclides releases [3].

Various materials have been studied, in the last years, to produce radioactive waste storage devices according to the regulations set by the competent authority. Spent fuel is generally vitrified prior to being sealed. Cement boxes filled with grout, made especially from Portland cement mixed with appropriate additives, are used to encapsulate a range of other wastes. Cements are typically used in conditioning ILW and LLW. Fly ash powders or blast furnace slag mixed with cement make a combination chemically stable, proven to be long lasting and suitable with the majority of wastes' sorts. The cement offers a barrier to the escape of radioactive or dangerous species by entomb the waste in a low permeability material; the chemical reactions during the cement pastes hardening, in some cases, help immobilizing harmful species incorporating them into the lately forming cement phases [4]. Nevertheless, the diverse nature of nuclear wastes means that, preferably, cement binder systems should be accessible to deal with definite needs of dissimilar categories of waste varying in terms of radioactivity, physical appearance and chemical nature [5].

Alternative cement formulations made with calcium aluminate, magnesium and calcium phosphate, calcium sulpho-aluminate, as well as alkali-activated systems and geopolymers have been considered and studied – see, for instance, novel low pH cement blends based on the hydration of MgO [6].

Concerning metallic wastes such as aluminium and uranium, they can be chemically reactive, starting a corrosion process inside the cement, favouring the cracking of the grouting material and the generation of flammable hydrogen gas, thus allowing water penetration into the grout mass. High-molecular-weight polymers have been studied, to encapsulate these particular types of nuclear waste, retaining adequately the radioactive elements and avoiding corrosion. Poly(carbonate urethane) and poly(bisphenol a-coepichlorohydrin), radiation-resistant polymers, have been also considered, as possible candidate materials for the radioactive waste containment: the maximum waste activity embeddable into these polymers and the dose rate distribution of the waste drum have been evaluated by Monte Carlo simulations of the mechanical properties' variations for 15, 30 and 300 years after embedding [7].

2. Methods

Conventional investigations of cements, including those for nuclear industry, use classical methodologies to obtain information on aspects mainly related to microstructure, fatigue behaviour and computational mechanics. These investigations rely essentially on standard tests, theoretical studies, and simulation-based analyses.

The radionuclide composition and distribution in high- and regular-density concrete specimens exposed to neutron and gamma irradiation as well as radioactive contamination was assessed, e.g., to supply essential information on the management of decommissioning waste, concrete decontamination and the behaviour of radionuclides in cement -based engineered barriers [8]. Porosity, for instance, is a key parameter for cement, affecting mechanical and heat-insulation properties. This factor is usually assessed by using gravimetric techniques, gas and liquid porosimetry (e.g., mercury intrusion porosimetry) and acoustic methods: an acoustic-electric method was also studied, which established the interrelation between porosity and the characteristics of electric and acoustic responses to their pulsed mechanical excitation [9]. Various studies are being carried out, moreover, subjecting weathered materials to diverse stresses and conditions and using modal-based simulations; the aim is to obtain indication to predict the cement's behaviour after ageing and improve nuclear waste containers.

Neutron techniques have come to the fore recently as effective non-destructive methods for characterising materials and components across a range of disciplines and they can represent a fundamental answer to the need to extend material life and prevent ageing-related degradation. They reveal significant properties and allow the assessment of responses to external influences over the sample's entire volume [10, 11]. What differentiates neutron techniques from other investigation tools is the capability to non-destructively capture information about the material's micro- and nano-physical structures down to ~1Å (0.1 nm) [10]. Neutrons are able to distinguish between different isotopes, thus neutron techniques are important tools also for the analysis of radioactive materials.

Small angle neutron scattering (SANS) accurately and completely characterises materials at the micro and nano levels, providing statistically precise information averaged over a macroscopic volume. In particular, the following parameters relative to the scattering objects (defects) can be monitored: diameter, concentration, volume fraction and area of interface. The theoretical basis of the SANS technique can be found in various references [10, 12-15].

Neutron radiography (NR) allows penetrating a sample through a neutron beam, which is attenuated (according to the basic law of radiation attenuation) by the investigated material – also by some light materials such as hydrogen, and lithium - and detected by an imaging device. The obtained information is related to the material and structure inside the specimen. NR allows visualising and measuring material distribution within macroscopic samples, as well as defining water's movement through the investigated cements. NR images of concrete structures are also helpful to validate conventional measurements. The theoretical basis of the NR technique can be found in various references, e.g. [10, 12, 16 and 17].

Prompt gamma activation analysis (PGAA) is a relatively new nuclear analytical method based on the detection of characteristic prompt gamma photons that originate in (n,γ) nuclear reactions. The principles of the method have been well known for decades and industrial applications are currently in development. Every atomic nuclei, apart from ^{4}He, may undergo a (n,γ) reaction with different probabilities. The energies of the emitted gamma photons are characteristic for each given isotope, while the intensities of the gamma peaks are proportional to the amount of a given isotope. This phenomenon allows the use of a quantitative elemental (isotopic) analysis method known as PGAA or PGNAA [18]. PGAA gives information on the sample as a whole: neutrons can penetrate the surface and lower layers of the material, so PGAA does not distinguish between the "bulk" and "surface" composition of a sample. The theoretical basis of the PGAA technique can be found in various references [10, 18-21].

Neutron diffraction (ND), complementary to synchrotron X-ray diffraction, is able to supply information on the crystalline phase of materials, including cements, providing data related to the specimen's bulk and helping the study of the alterations and degradation processes. The theoretical basis of the ND technique can be found in various references, e.g. [10, 12].

3. Materials investigation and discussions

A feasibility study has been carried out by Rogante Engineering Office for the investigation by SANS of a cement with added polymer and γ Al_2O_3. Polymer concrete is defined to be cement-based concrete with the addition of various high-molecular compounds as aqueous dispersions. Polymers using in concrete allows changing the structure of cement stone towards the crucial direction. Two active components can be mentioned: mineral binding agent and organic matter. Binding agent and water forms cement stone which joints particles of aggregate together to make monolith; in the meanwhile, during removing water from concrete, polymer forms a thin layer on the surface of pores, cement and aggregate nodules, this layer possessing good adhesive behaviour.

When designing the composition of polymer cements one need to ensure the following conditions:

- Maximal rate of Portland cement hydration. It is known that when polymer additions are present,

especially with high polymer/cement ratios, Portland cement partially plays the role of inert filler.

- Long aggregative stability and favourable conditions for film formation of polymer dispersions.
- Optimal correlation between crystalline and amorphous phases in the hardened cement stone, ensuring high resistance both to brittle failure and plastic collapse.

In the composite binding, material polymer component and mineral binder are selected to combine them efficiently and let them show their advantages, amplifying the strong points. The main requirement to polymer addition is to retard the process of cement stone hardening with the least possible rate. Cement neo-formations make the crystalline - coagulation structure. The rigid mineral skeleton formed strengthens in depressed defect points (pores, cracks) with polymer. It leads to the creation of composite material with improved strength and elasticity, owing to articulated joint of hydrates with more flexible particles, nets and films of strong elastic organic polymers possessing adhesiveness. The main properties of concrete influenced by polymer are:

- Strength. The addition of polymer to cement increases bending and tensile strength greatly, the compressive strength is enlarged as well. Strength is one of the most important characteristics in the terms of discussing structural properties of material. Strength values, for such heterogeneous material as polymer cement, can be evaluated to determine the phase composition.
- Abrasive resistance. The research of polymer cements showed that their abrasive resistance enhances considerably with the increase of polymer rate. Polymer acts as a binder that prevents tearing of cement stone components from the surface.
- Deformability. The elasticity modulus of concrete usually decreases with increasing of polymer/cement ratio.

A research carried out by the Solid State Chemistry Institute of the Ural Federal University is devoted to find out the interaction between cement, polymer and Al_2O_3 (γ type) [22-25]. Firstly, γ Al_2O_3 is produced in the laboratory by using the process at 600°C. The following reaction takes place:

$$AlCl_3 \cdot 6H_2O + H_2O \rightarrow \gamma\ Al_2O_3 + HCl + H_2O. \quad (1)$$

Fig. 1 shows a micro photo of γ Al_2O_3 obtained by aluminium chloride thermo–hydrolysis.

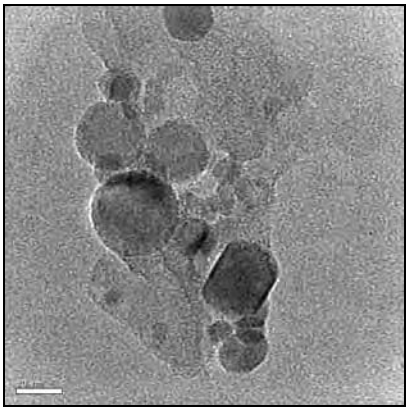

Figure 1. Micro photo of γ Al_2O_3 obtained by aluminium chloride thermo-hydrolysis (line is 20 nm).

Slika 1. Mikro fotografija γ Al_2O_3 razvijenog pomoću toplinske hidrolize u aluminijevom kloridu (duljina linije je 20nm)

Then the produced material is joint grinded in planetary-type mill to the average size of 70-90 nm. Fig. 2 shows size distribution after joint grinding in planetary mill.

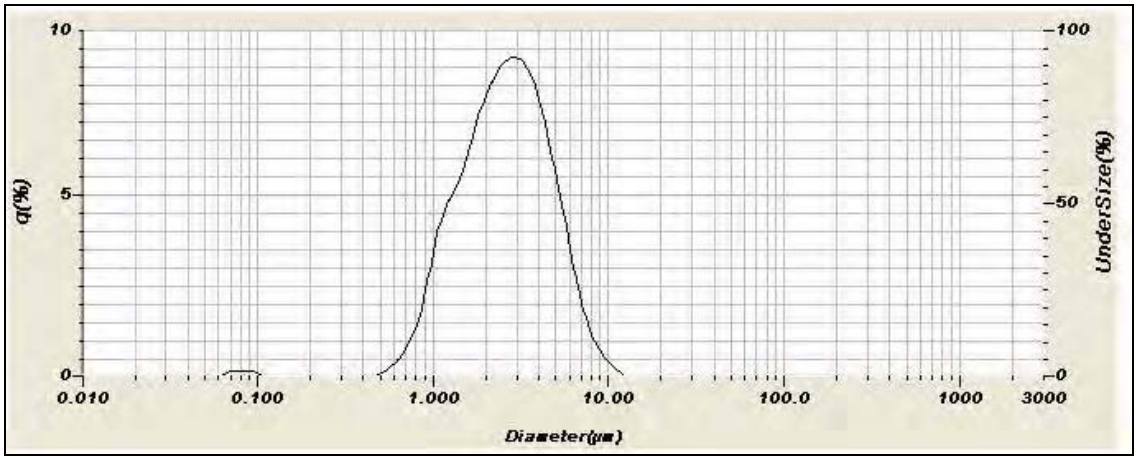

Figure 2. Size distribution after joint grinding in planetary mill

Slika 2. Dimenzionalna razdioba nakon obrade brušenjem

Both ways of polymer mixing are investigated, the first on being joint grinding in polymer dispersion and the second being dry blended. The nature of interaction is supposed to be either physical or chemical one. From the physical point of view, polymer cements' hardening includes the combination of two opposite processes: Portland cement clinker hydration and autohesion of polymer dispersion. On the one hand, mineral binding material can harden only in presence of water and film formation occurs with drying. As for chemical point of view, the γ Al_2O_3 grains can be the centres of clinker minerals crystallization. Nanoscale investigations of cement stone, therefore, are very important to determine the interaction mechanism. Study of cements and related materials seems to be fundamental, moreover, to create novel advanced components for building industry and also for the improvement of nuclear waste containers, with high functional properties such as hardness, durability (i.e., the cement's aptitude to resist the infiltration of liquid and oxygen), resistance to ageing, cracks' formation, stability of mechanical modules and ecological criteria.

Specimens with different additives ratios have been considered for a SANS investigation. The chemical composition includes: ordinary Portland cement, Rhoximat® PAV 22 (vinyl acetate and vinyl versatate) copolymer resin and Al_2O_3, with different γ Al_2O_3 / PAV 22 polymer cement ratios, the water/cement ratio remaining stable. Fig. 3 shows a sample.

Figure 3. Portland cement samples with added nano Al_2O_3 (γ type) mixed with Rhoximat® PAV 22 polymer. Dimensions are 60×10×10 mm.

Slika 3. Uzorak iz Portland cementa sa dodatkom nano Al_2O_3 (γ tip) pomješan s Rhoximat® PAV 22 polimerom. Dimenzije uzorka su 60×10×10 mm.

These samples are usually submitted to the following tests: bending and compressive strength, water absorption and density. The main problems to be investigated by SANS include the following aspects:

- Researches of hydration processes, through the contrast variation method, using light and heavy water to understand the mechanisms of water molecules association and their structuring in ceramics' matrix in the formation process of cement stone, as dependent on the addition of special entities (nano-particles, polymers, low molecular components modifying hydrogen bonds, such as salts, acids and bases);
- Observation of kinetics related to water reactions and nanoscale migration (localization) for short (seconds) and long (hours, days) times in connection with strength, hardness at microscopic level of cement stone;
- Study of cement stone porosity;
- Determination of fractal dimension, size distribution and other characteristics (open, closed pores, cracks) at the scale 1–100 Å and at large distances 102–103 Å using Ultra–SANS.

Polymer cement compositions find wide application in industry nowadays. Since these compositions possess increased bending strength, water and frost resistance, high adhesive properties, low abradability and porosity, they can be used as construction materials of high quality, such as corrosion resistive coatings, plasters and insulation. The material object of this SANS study can be in principle considered also for corrosion resistive coatings of nuclear waste containers.

The achievable results are expected to supply information concerning, in particular, porosity, determination of fractal dimension, size distribution and other characteristics (open, closed pores, cracks). These results could contribute to study the influence of adding polymer and γ Al_2O_3 to cement compositions, helping monitoring some important characteristics of the considered material.

Some examples concerning different other types of cements - including those suitable for the nuclear sector - and their investigation by neutron techniques are reported as follows.

NR was used to study cracks in concrete samples. Digital radiographs were obtained by the direct method with a gadolinium converter screen and they allowed visualizing cracks, with better results in comparison with digital X-ray radiographies [26]. A cement-based waste-form was analysed by NR, in order to characterise this material for disposal in a repository for radioactive wastes. Imaging was able to show the pore size distribution as well as the amount of cracking. The rate of the water penetration was measured by using NR together with conventional sorptivity: in particular, it was evidenced the capability of cracks to fast distribute water through the cement specimens [27]. The concrete's natural drying process influences notably its features and performances (e.g., durability). Concrete specimens, wet cured for one day and covered on all the sides but one, were investigated by NR in order to monitor the water movement inside the material, to quantify the measured water content and porosity and to compare the results with conventional gravimetrical data [28]. The concrete's durability can be measured by assessing some characteristics such as permeability, porosity and sorptivity. A study was carried out, with the following purposes: to consider the NR ability to achieve quantitative data for porosity and sorptivity

related to concrete, in comparison with the results from traditional methods; to analyse the effects that water to cement ratio and curing time have on the concrete's durability [29]. A cement standard used for the qualification of chemical laboratories of cement factories was analysed by PGAA, completing the data achieved during round robin tests of several laboratories using classical analytical chemistry, atomic absorption spectroscopy, X-ray fluorescence spectroscopy, gravimetry, etc. The PGAA results showed good agreement with the cement's reference values. PGAA allowed also determining a few trace elements, which did not appear in the certification of the standard [21]. Neutron activation analysis was used to assess the concentration of trace elements normally present in concrete shielding (mainly in cement), accountable of high radioactivity of a NPP shielding after decommissioning. Diverse cement specimens were irradiated with neutron beam and analyzed with γ-ray counting system. It was found that the radioactivity from certain elements (Ce, Co, Cs, Eu, Fe, Hf, Sb, Sc, Ta and Tb) has a main role after a long cooling time or NPP decommissioning [30]. Composition and microstructural changes of cement pastes when heating up to 620 °C and cooling subsequently, in different conditions, have been monitored by simultaneous ND data acquisition. High temperatures above the 300 °C, in fact, can involve alterations of the mechanical properties (e.g., compressive strength, elastic limit and fluency resistance. The analysis of the obtained ND patterns consented to identify the main crystal phases: portlandite, ettringite, calcite, lime, hydrated calcium silicate and larnite [31].

Conclusions

Neutron techniques are able to characterize in a non-destructive way cements, allowing obtaining data complementary to those achievable by using traditional examination methods.

A feasibility study has been carried out for a full SANS investigation of Portland cement samples with added nano Al_2O_3 (γ type) mixed with Rhoximat® PAV 22 polymer. SANS can supply, in this case, significant data on basic parameters connected with degradation, fracture and other phenomena, allowing also a more reliable lifetime assessments. Other key works have been reported, finally, demonstrating as well the complementarity between neutron-based methods and the other techniques conventionally adopted.

The results can be used to optimize performances and reliability, supporting to achieve a better quality of cements.

Acknowledgements

E.S. Gerasimova and E.V. Vladimirova are acknowledged for useful discussions.

REFERENCES

[1] GEE, G.W.; MEYER, P.D.; WARD, A.L.: *Nuclear waste disposal*, Encyclopedia of Soils in the Environment, *Elsevier Ltd.*, Amsterdam, 2005, 56-63.

[2] EWING, R. C.; WEBER W. J.; CLINARD, F. W. JR: *Radiation effects in nuclear waste forms for high-level radioactive waste*, Progress in Nuclear Energy, 29 (1995) 2, 63-127.

[3] FORSBERG, C.W.: *Radioactive wastes*, Encyclopedia of Physical Science and Technology - Third Edition, Academic Press, San Diego, 2002, 643-659.

[4] JANTZEN, C.M.; F.P. GLASSER; LACHOWSKI, E.E.: *Radioactive waste-Portland cement systems: I, Radionuclide distribution*,. Journal of the American Ceramic Society, 67 (1984) 10, 668-673.

[5] OJOVAN, M.I.; LEE, W.E.: *An introduction to nuclear waste immobilisation*. Elsevier Ltd., London, 2005.

[6] ZHANG, T.; CHEESEMAN, C.R.; VANDEPERRE L.J.: *Development of novel low pH cement systems for encapsulation of wastes containing aluminium*, International Conference *Decommissioning, Immobilisation and Management of Nuclear Waste for Disposal DIAMOND'09* – Proceedings, York, UK, 2009.

[7] ÖZDEMIR, T.; USANMAZ, A.: *Monte Carlo simulations of radioactive waste embedded into polymer*, Radiation Physics and Chemistry, 78 (2009) 9, 800-805.

[8] KRASZNAI, J.P.: *The radiochemical characterization of regular- and high-density concrete from a decommissioned reactor*, Waste Management, 13 (1993) 2, 131-140.

[9] FURSA, T. V.; SURZHIKOV, A. P.; OSIPOV, K.YU.: *Development of an acoustoelectric method for determining the porosity of dielectric materials*, Russian Journal of Nondestructive Testing, 43 (2006) 2, 95-99.

[10] ROGANTE, M.: *Applicazioni Industriali delle Tecniche Neutroniche*, Italian Workshop for *Industry Industrial Applications of Neutron Techniques*, Proc., Civitanova Marche, Italy, 2008.

[11] ROGANTE, M.; ROSTA, L.: Nanoscale characterisation by SANS and residual stresses determination by neutron diffraction related to materials and components of technological interest, SPIE Proc. 5824 (2005), 294-305.

[12] ROGANTE, M.: *Caratterizzazione, mediante scattering neutronico, di materiali e componenti per l'impiantistica nucleare ed industriale*, PhD thesis, University of Bologna, Italy , 1999.

[13] WILLIAMS, C.; MAY, R.P.; GUINIER, A.: *Small-Angle Scattering of X-rays and Neutrons*, Characterisation of Materials, Lifshin E., ed., "Materials Science and Technology", vol. 2B, VCH Verlagsgesellschaft, Weinheim (1994), 611-656.

[14] RIETVELD, H.M.: *Line profiles of neutron powder-diffraction peaks for structure refinement*, Acta Crystallographica, 22 (1967), pp.151-152.

[15] RIETVELD, H.M.: *Profile refinement method for nuclear and magnetic structures*, Journal of Applied Crystallography, 2 (1969), pp. 65-71.

[16] BALASKÓ, M.; ROGANTE, M.: *La radiografia neutronica al servizio dell'industria*, Progettare, 273 (2003), 35-39.

[17] BALASKÓ, M.; SVÁB, E.: *Neutron Radiography in Research and Development*, Nukleonica 39 (1994) 1/2, 3-22.

[18] ROGANTE, M.: *Neutroni per l'investigazione di componenti e materiali industriali*, ICP, 2 (2008), 72-75.

[19] RÉVAY, ZS.; BELGYA, T.; KASZTOVSZKY, ZS.; WEIL J. L.; MOLNÁR G. L.: *Cold neutron PGAA facility at Budapest*, Nuclear Instruments and Methods in Physics Research Section B: Beam Interactions with Materials and Atoms, 213 (2004), 385-388.

[20] RÉVAY, ZS.; MOLNAR, G.L.; BELGYA, T.; KASZTOVSZKY, ZS.; FIRESTONE, R.B.: *A new gamma-ray spectrum catalog and library for PGAA*, Journal of Radioanalytical and Nuclear Chemistry, 248 (2001) 2, 395-399.

[21] RÉVAY, ZS.: *Determining Elemental Composition Using Prompt γ Activation Analysis*, Analytical Chemistry, 81 (2009), 6851–6859.

[22] BAZHENOV, P.I.: *Complex using of mineral raw materials for construction materials production*, Stroyizdat, Moscow, 1986.

[23] State Standard 28013-98. *Mortars for construction. General conditions*. Izdatelstvo standartov, Moscow, 1998.

[24] KRUGLITSKY, N.N.; BOIKO, G.P.: *Phisico-Chemical Mechanics of cementpolymer compositions*, Naukova dumca, Kiev, 1981.

[25] DOMANSKAYA, I.K.: *About specialties of disperse mineral fillers using as the component of construction mixtures*, Sroykompleks Srednego Urala 12 (2002), 42.

[26] PUGLIESI, R.; ANDRADE, M.L.G.: *Study of cracking in concrete by neutron radiography*, Applied Radiation and Isotopes, 48 (1997) 3, 339-344.

[27] McGLINN, P.J.; DE BEER, F.C.; ALDRIDGE, L.P.; RADEBE, M.J.; NSHIMIRIMANA, R.; BREW, D.R.M.; PAYNE, T.E.; OLUFSON, K.P.: *Appraisal of a cementitious material for waste disposal: Neutron imaging studies of pore structure and sorptivity*, Cement and Concrete Research, 40 (2010) 8, 1320-1326.

[28] DE BEER, F.C.; STRYDOM, W.J.; GRIESEL, E.J.: *The drying process of concrete: a neutron radiography study*, Applied Radiation and Isotopes, 61 (2004) 4, 617-623.

[29] DE BEER, F.C.; LE ROUX, J.J.; KEARSLEY, E.P.: *Testing the durability of concrete with neutron radiography*, Nuclear Instruments and Methods in Physics Research Section A: Accelerators, Spectrometers, Detectors and Associated Equipment, 542 (2005) 1/3, 226-231.

[30] MEDHAT, M.E.; FAYEZ-HASSAN, M.: *Elemental analysis of cement used for radiation shielding by instrumental neutron activation analysis*, Nuclear Engineering and Design, 241 (2011) 6, 2138-2142.

[31] CASTELLOTE, M.; ALONSO, C.; ANDRADE, C.; TURRILLAS, X.; CAMPO J.: *Composition and microstructural changes of cement pastes upon heating, as studied by neutron diffraction*, Cement and Concrete Research, 34 (2004), 1633–1644.

Inverted Pendulum Swing up Controller

***David KENNEDY*[1)], *James CONLON*[1)]**
1) Department of Mechanical Engineering
Dublin Institute of Technology DIT Bolton Street, Dublin 1, **Ireland**

Email: David.kennedy@dit.ie

Keywords
Controls
Inverted Pendulum
Open-loop control

Ključne riječi
Upravljanje
Obrnuto njihalo
Regulacija otvorenom petljom

Early information

The inverted pendulum is a classic control problem. The system is open – loop unstable and continuously wants to reach equilibrium by falling over. The system must be stabilised by means of feedback. The developed inverted pendulum system is shown in Figure 1.

In order to balance the pendulum in the inverted position the pivot must be moved continuously to correct the falling pendulum. This is similar to trying to vertically balance a broom on your hand. This interesting control problem is fundamentally the same as those involved in rocket or missile propulsion. The rocket has to balance on its engine as it accelerates. As the rocket tends to fall over, the rocket thrust must be deflected sideways to restore the rockets course. This is just one of many practical applications of the system. This paper describes the technology introduced to achieve this design and development which is now a working piece of demonstration kit for control and mechatronic engineering.

REGULATOR OBRNUTOG NJIHALA

Prethodno priopćenje

Obrnuto njihalo predstavlja klasičan problem upravljačke regulacije. Sustav je tipa otvorene petlje, nestabilan je, te kontinuirano želi postići ravnotežu prevrtanjem. Sustav se mora stabilizirati uz pomoć povratne veze. Razvijeni sustav obrnutog njihala pokazan je na Slici 1.

U cilju uravnoteženja njihala u obrnutoj poziciji, oslonac njihala se mora kontinuirano pomicati da stabilizira padajuće njihalo. To je istovjetno pokušaju da se u vertikalnoj poziciji uravnoteži „metla na ruci". Ova interesantna problematika upravljačke regulacije u osnovi je jednaka kao održavanje smjera rakete i projektila. Raketa se mora uravnotežiti na svom motoru za vrijeme ubrzavanja. Kako raketa ima tendenciju padanja, raketni potisak mora biti usmjeren bočno kako bi vratio smjer raketi. To je samo jedan od mnogih praktičnih primjena sustava. Ovaj članak opisuje primjenjenu tehnologiju regulacije u cilju postizanja daljnjeg razvoja upravljačkog i mehatroničkog inženjerstva.

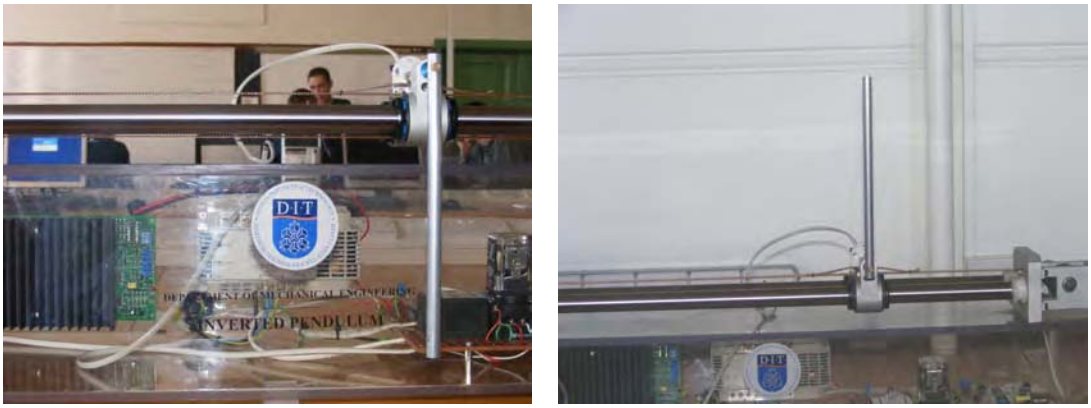

Figure 1. Inverted Pendulum at rest and in active mode

Slika 1. Obrnuto njihalo u mirujućem i aktivnom položaju

Symbols/Oznake

θ	- pendulum angle, radians - kut njihala, radijani
x	- displacement, mm - pomak, mm
y	- displacement, mm - pomak, mm
ω	- frequency, degrees/second - frekvencija, °/s
j	- phase shift - fazni pomak

1. Inverted Pendulum designs

Figure 2. shows a basic schematic of the inverted pendulum.

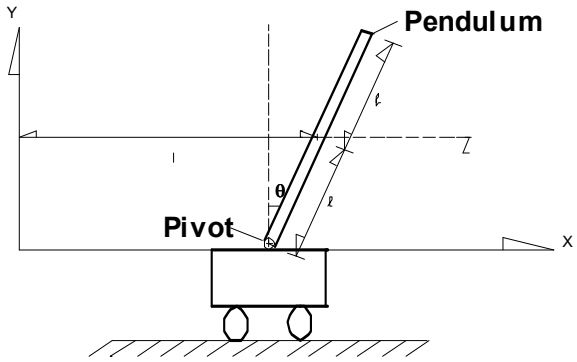

Figure 2. Inverted Pendulum

Slika 2. Obrnuto njihalo

The Pendulum is free to rotate at one end and is fixed to a pivot point at the other. The unit is free to move in the x-axis. This action (velocity, acceleration and deceleration) combined with the mass of the pendulum, creates enough momentum to force the pendulum to rotate and take up the inverted position as shown.

The cart balanced Inverted Pendulum as shown in Figure 3. is the most common. As the pendulum falls one way the motor drives the cart in the same direction to prevent the pendulum from falling over.

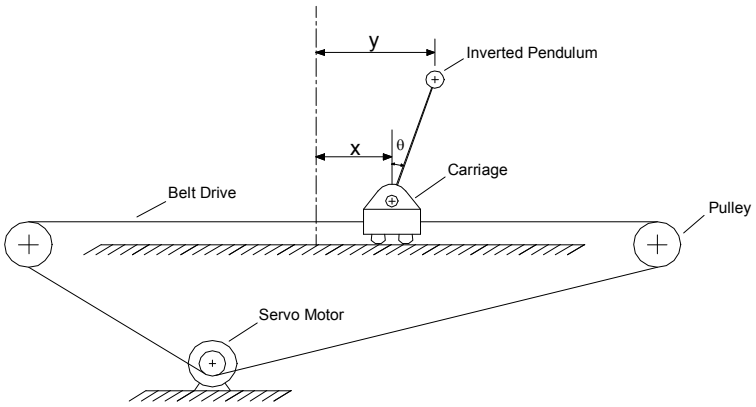

Figure 3. The cart balanced inverted pendulum

Slika 3. Pokretni oslonac uravnoteženog obrnutog njihala

A stabilisation controller keeps the pendulum in the inverted position by sending the appropriate signals to the servomotor. For the servo loop, a potentiometer was used for position feedback and a tachometer on the motor shaft for velocity feedback. A potentiometer was also used to measure pendulum angle θ.

When switched off the pendulum is in the pendant position (hanging down). The purpose of the swing up controller is to swing the pendulum from the pendant position to the inverted position at which point the stabilisation controller takes over to stabilise the pendulum and return the carriage to its desired position on the track.

A simple swing up routine uses strategic cart movements to gradually add energy to the pendulum. This involves placing the cart under closed loop position control. Then a routine is developed to prescribe the cart's movement. This movement is such that the cart does work on the pendulum, in a consistent and efficient manner. It is also important to gradually reduce cart movement amplitude so that the swing up routine delivers the pendulum to the inverted pendulum position with small angular velocity [1].

A swing up strategy suggested by K. J. Åström and K. Furuta [2] was further developed and simplified as follows:

From the resting pendent position:

Switch the system to position control of the cart

Drive the position control system with an appropriate displacement signal to raise the pendulum to above the horizon

When the angle of the pendulum is 'small enough' (with respect to the inverted position) switch to the stabilisation controller to keep the pendulum balanced.

2. Developing a forcing function

Based on Research and investigations of other inverted pendulums completing a swing up routine, the relationship between the movement of the carriage and the pendulum angle was observed. This led to the design and specification of the type of displacement signal that should be applied to the carriage. Based on this, a computer simulation of the motion of the carriage and pendulum was developed.

2.1. Solid edge motion Simulation

A model representing a simplified version of the track, carriage and pendulum was constructed and the solid edge model is shown in Figure 4.

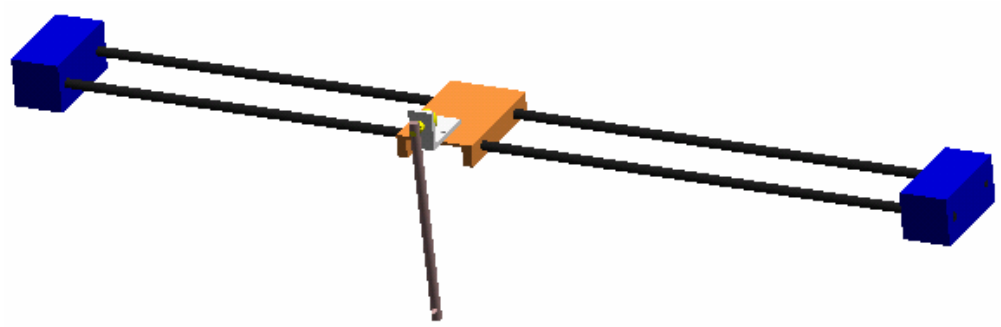

Figure 4. Solid Edge model of a track, carriage and pendulum system

Slika 4. "Solid edge" model vodilica, nosača i sustava njihala

The joints in the model are defined. For example the pendulum is supported by and free to rotate around the potentiometer shaft and the carriage is free to translate along the track. Once the model was constructed, different functions could be applied to the carriage and the motion of the pendulum observed. A harmonic force (sine wave) was applied to the carriage and the motion of the pendulum noted. After some redesign and alteration to the amplitude and frequency of a sin wave it was clear that a sin wave of a certain amplitude and frequency would swing the pendulum to the inverted position. Figure 5 shows a series of images taken from the solid edge program during the computer simulation.

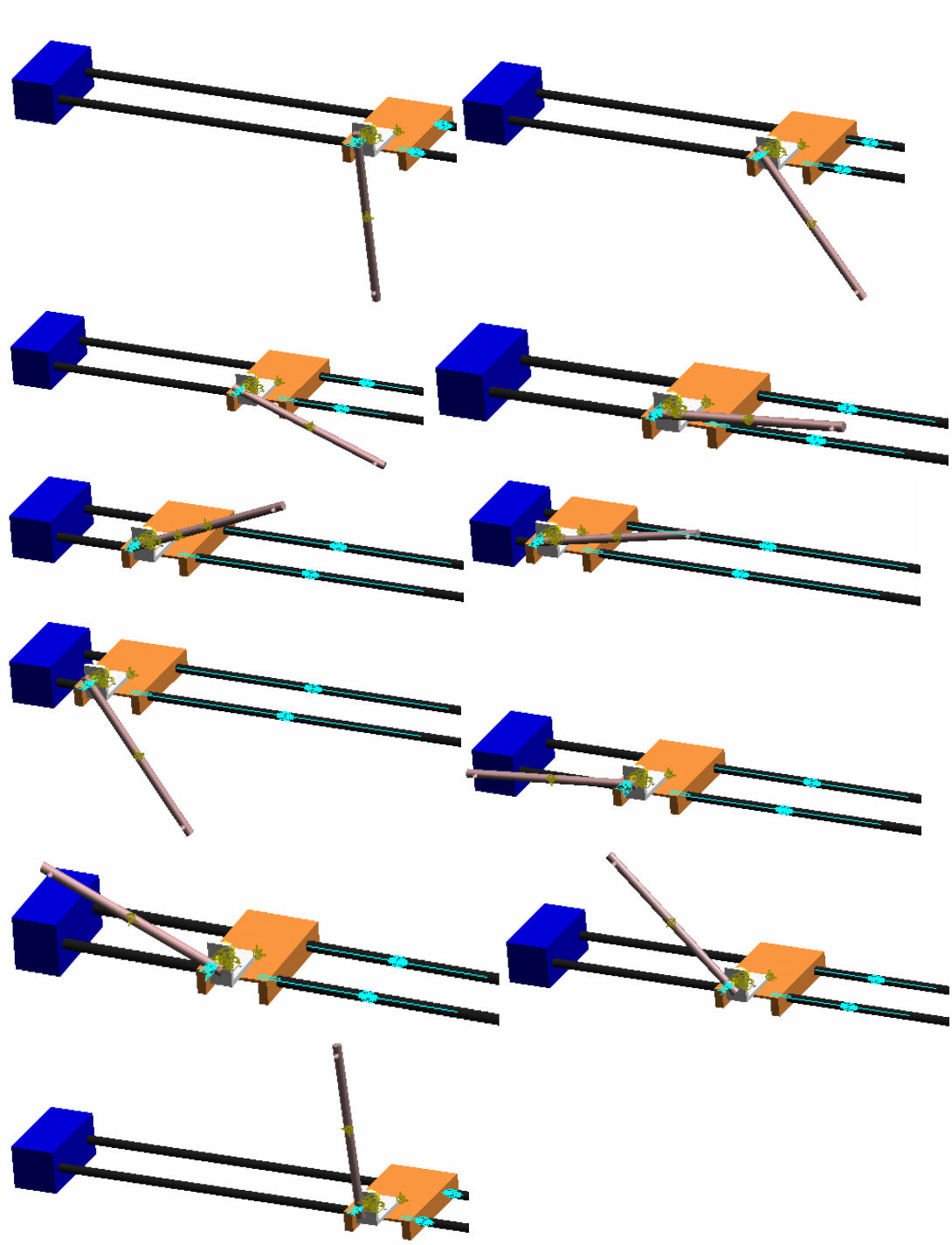

Figure 5. Computer simulation positions of pendulum due to input signals

Slika 5. Računalna simulacija položaja njihala prema ulaznom signalu

Sine waves of varying amplitude and frequency were applied to the cart and optimum values recorded. The optimum values are the values which cause the pendulum to approach the inverted position with as small an angular velocity as possible.

The length of the track sets an obvious limitation on the maximum amplitude that can be applied.

The optimum values for the harmonic function to swing up the pendulum from the pendant position to the inverted position were:

Amplitude = 350mm

Frequency, ω= 232deg/sec

The equation of the harmonic function in solid edge is given by

$$f(t) = A.\sin(\omega.(t-T0)-j)+B \quad (1)$$

Where

A = Amplitude

ω = Frequency

T0 = Offset Time

j = Phase shift

B = Average value

With T0, B and j equal to zero this reduces to the simple function

$$f(t) = A*\sin(\omega.t) \quad (2)$$

Figure 6. shows some of the values for the simulation when applied to Solid Edge.

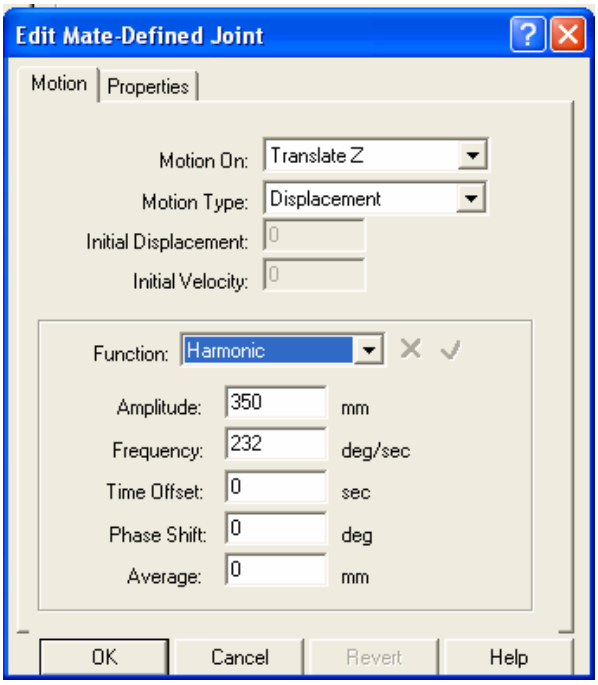

Figure 6. Solid Edge Simulation values

Slika 6. "Solid edge" vrijednosti simulacije

The required carriage movement is sinusoidal, with amplitude (distance) 350mm and frequency 232deg/sec. Different values would be obtained for different carriage and pendulum masses.

The carriage position potentiometer voltage varied from -9.31V to +9.31V over the entire length of track.

Track length = 918mm

Therefore $\frac{18.62V}{918mm} = 0.02V/mm$ of track

Therefore an Amplitude of

350mm = 350mm X 0.02V/mm = 7V

The frequency of 232 deg/sec must be converted to a frequency in Hz.

$$\frac{232\,\text{deg/sec}}{360\,\text{deg}} = 0.644Hz$$

A sine wave generator was used to apply a sine wave of 14V peak to peak with frequency 0.644 Hz to the position loop set point. The response of the pendulum was then observed. These values were fine tuned to improve performance. The tuning process was found to be very simple and straightforward.

The pendulum did swing from the pendant position to the inverted position and did so in a most predictable and repetitive manner.

2.2. Switching Criteria

As the pendulum approaches the inverted position a method of switching between the swing up controller and stabilization controller is required. Three switching criteria were considered.

1. The stabilization controller has a limited region around the 0° (vertical) position in which it can control the pendulum. This is because the stabilization controller is based on the linearised system about the 0° point. If the stabilization controller is switched on when the pendulum is outside this region of attraction the system will not be able to stabilize the pendulum.
2. The pendulum must have an angular velocity below a certain value when the stabilization controller switches on. If the angular velocity is too large it will cause the motor to apply a large force to the carriage to try and "catch" the pendulum, causing the carriage to run out of track.
3. The pendulum should not be allowed to go through the 0° vertical as this would lead the pendulum to perform nonlinear rotation around its pivot with a non zero velocity. The best switching moment occurs when the pendulum is approaching the 0° vertical position with a small angular velocity. The switchover method is illustrated in Figure 7.

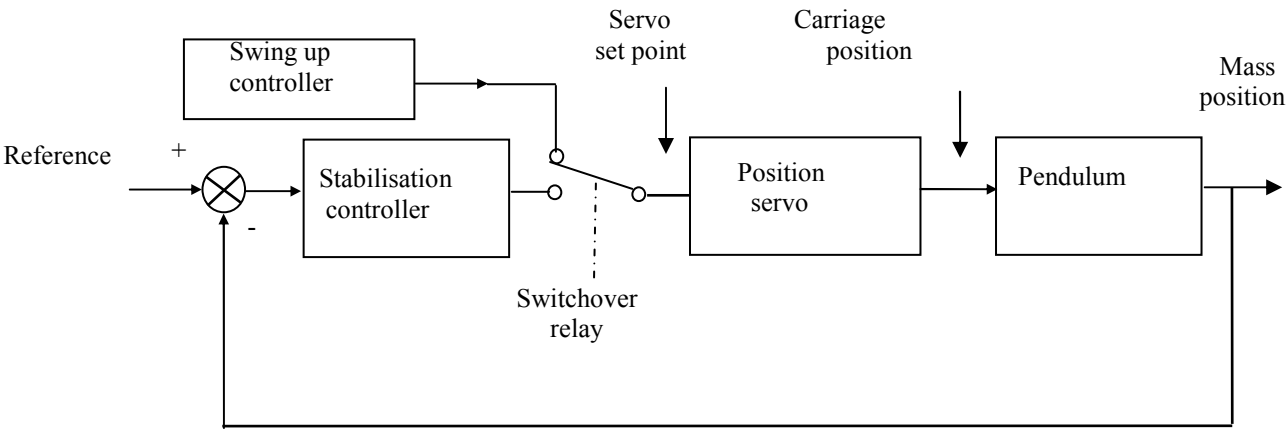

Figure 7. Switch over design

Slika 7. Shematski prikaz regulacije

The literature suggested switching from the swing up controller to the stabilization controller at an angle within + or - 5° of the vertical and an angular velocity of less than 3rad/sec.

It was decided to investigate the possibility of switching from the swing up controller to the stabilisation controller using the pendulum angular position only.

A simple circuit comprising a general purpose 741 operational amplifier configured as a comparator and whose output switched a transistorised relay was designed to control the switch over and this is illustrated in Figure 8.

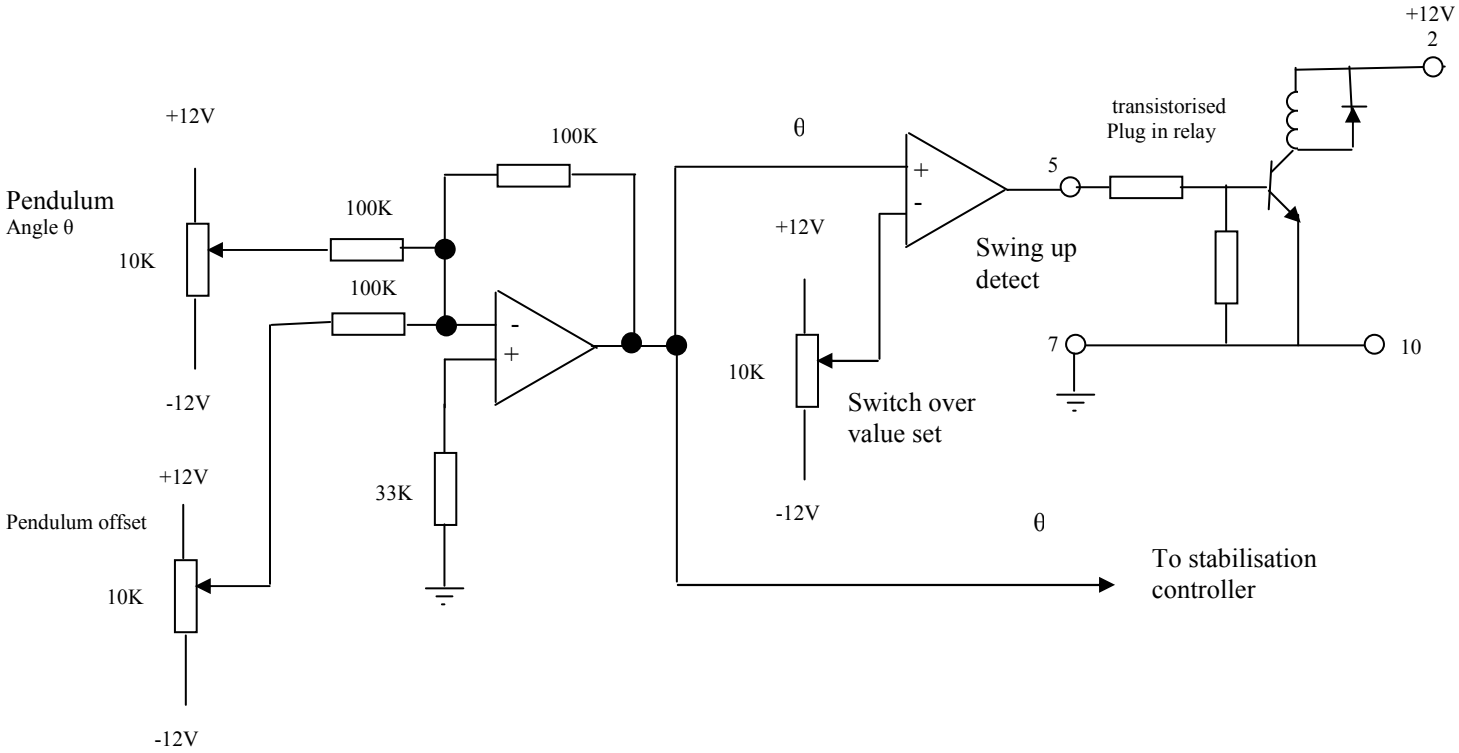

Figure 8. 741 Operational Amplifier

Slika 8. Operacijsko pojačalo

3. Pendulum potentiometer offset

When the pendulum is balanced the output from the pendulum angle potentiometer should be 0 volts. Also, for the swing up controller to operate correctly the pendulum angle signal must always be known. Since the θ potentiometer has a dead zone where no voltage output is available a design modification is required. This dead zone (in the pendant position) is illustrated in Figure 9 (a). To ensure an output signal at all times the potentiometer is rotated such that during swing up from the pendant position to the balanced position an output signal is always present, even when the pendulum swings slightly anti clockwise on swing up. This means that when the pendulum is vertical, the output voltage is not 0 volts. This is illustrated in figure 9 (b). This makes it necessary to subtract a value from the potentiometer such that a value of 0 volts is available when the pendulum is balanced. This was achieved using an inverting summer configuration (IC1) and pendulum offset potentiometer as shown in Figure 8. The pendulum is held in the vertical position and the pendulum offset potentiometer adjusted such that the output from the operational amplifier is 0 volts.

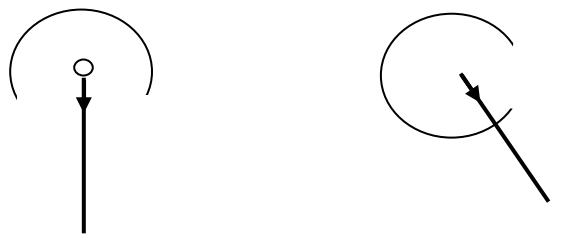

a) Pendant b) Activated

Figure 9. Pendulum position

Slika 9. Položaj njihala

Initially with the pendulum in the pendant position the comparator (IC9)is negatively saturated and the relay is in the position shown allowing the sine wave to drive the motor so as to increase the kinetic energy of the pendulum. As the pendulum moves towards the inverted position the voltage from the pendulum potentiometer gets smaller. When this voltage is less than the voltage on the non inverting input of the comparator the output becomes positively saturated and the relay switches. The relay switches from swing up to balance and the Pendulum remains balanced. The pendulum offset potentiometer was adjusted to achieve optimum switchover. The optimum angle to switchover was larger than expected, approximately 70o from the vertical. The design was completed using an Intersil 8038 function generator chip to generate the low frequency sin wave. The diode was fitted to ensure that only a positive half cycle was applied. This ensures that the carriage always swings up in the same direction

from the middle of the track. The relay connections and function generator are illustrated in Figure 10.

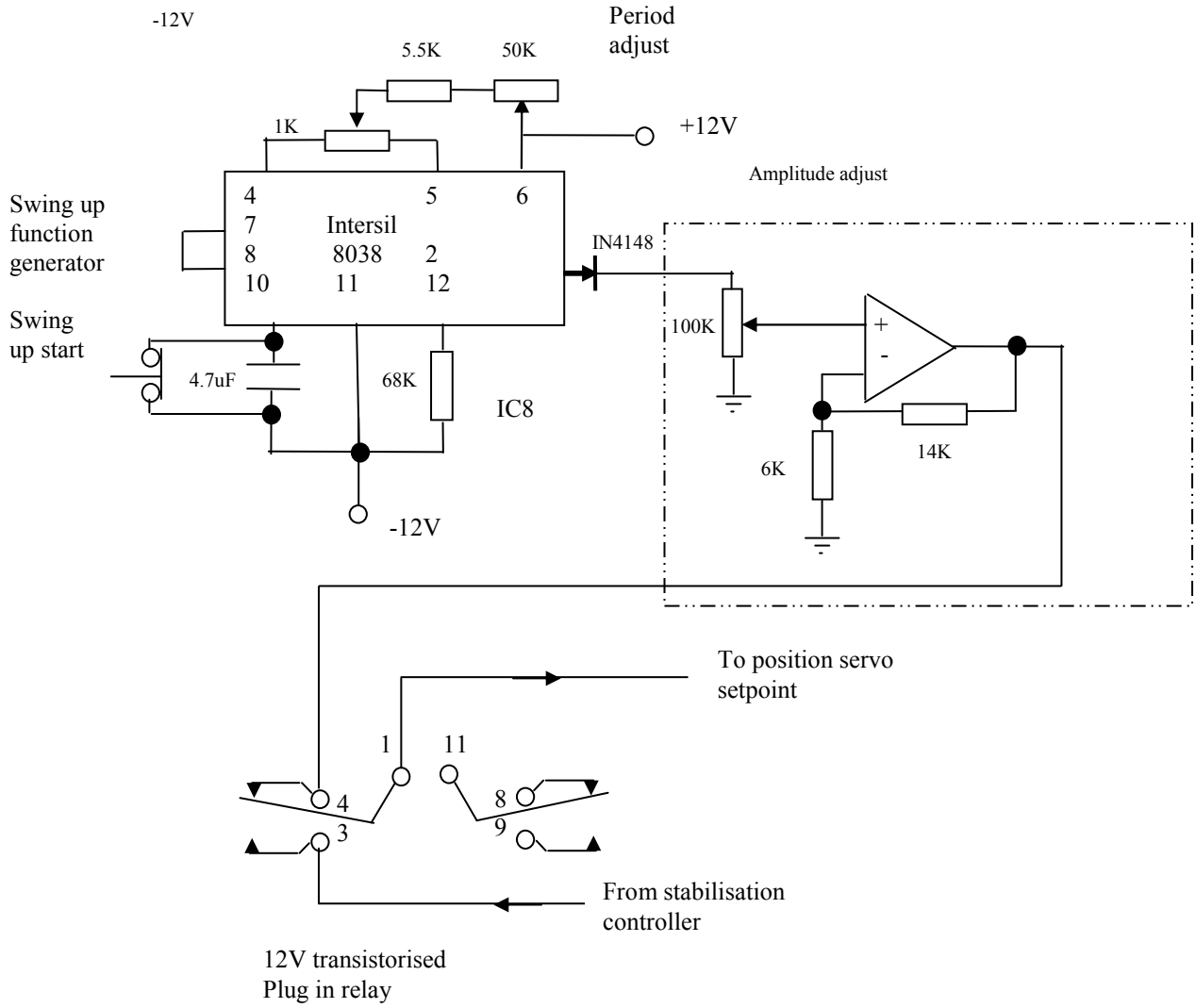

Figure 10. The relay connections and function generator

Slika 10. Relej veza i generator funkcija

4. Conclusions

The swing up controller is efficient and reliable. Its repeatability to swing the pendulum to the vertical position is consistent. The switch over is seamless and the pendulum balances every time. No complex mathematics are required and the circuitry comprises just a sine wave and a relay. The adjustments to tune the system are simple and straight forward.

REFERENCES

[1] GOLTEN, J.; VERWER, A.: *Control System Design and Simulation,* 1991 Mc Graw Hill, London.

[2] ÅSTRÖM, K. J.; FURUTA, K.: *Swinging Up A Pendulum By Energy Control* - Presented at IFAC 13th World Congress, San Francisco, California, 1996.

COMMERCIALIZATION OF KNOWLEDGE ACQUIRED BY R&D OF ADVANCED ENGINEERING MATERIALS

Jaroslav JERZ [1)],
Barbara WILFINGER [2)] ***and***
Robert Christian HULA [2)]

[1)] Institute of Materials & Machine Mechanics, Slovak Academy of Sciences Račianska 75, 83102 Bratislava 3, **Slovakia**

[2)] Institute for Economic Promotion, Austrian Federal Economic Chamber Wiedner Hauptstrasse 63, 1045 Vienna, **Austria**

[3)] Institute of Chemical Technologies and Analytics, Vienna University of Technology Getreidemarkt 9, 1060 Vienna, **Austria**

[1)] ummsjerz@savba.sk
[2)] barbara.wilfinger@wko.at
[3)] robert.hula@tuwien.ac.at

Keywords

advanced engineering materials
knowledge transfer
regional development

Ključne riječi

napredni materijali
transfer znanja
regionalni razvoj

Review article

Research institutions and universities can be a significant factor during an economic recovery by creating new businesses based on advanced technologies developed by R&D activities of their scientists. The mutually beneficial cooperation relationships between research laboratories and private sector funding are unavoidable for recovery efforts. The commercialization of knowledge acquired by basic and applied research in the field of engineering materials and development of advanced technologies for their production and processing fosters the creation of new businesses in the case that various stimulus funding and venture capital are continually in the equilibrium. That is why the excellent material research in the Central European industrial region is a forerunner of a sustainable regional economic and social development.

The technology transfer platform INNOVMAT has been created recently in order to support innovation activities of enterprises from the region Vienna – Bratislava by transfer of knowledge acquired by R&D in the field of advanced engineering materials and related technologies to industrial practice. The main mission of INNOVMAT is to support the development of industrial products with extremely high added value and increase competitiveness of companies with high potential for application of newly developed advanced engineering materials.

The guide to clustering of R&D institutions and universities with the aim to fulfill needs of manufacturing SMEs and multinational industrial companies to increase their innovation capacity and particularly to improve their competitiveness on world-wide markets have been outlined in this contribution.

Komercijalizacija znanja o naprednim materijalima u inženjerstvu razvijenog od R&D-a

Pregledni članak

Istraživačke institucije i sveučilišta mogu predstavljati značajan čimbenik za vrijeme ekonomskog oporavka u stvaranju novih djelatnosti temeljenih na naprednim tehnologijama razvijenim uz pomoć aktivnosti R&D istraživača. Suradnički odnosi temeljeni na principu zajedničke koristi između istraživačkih laboratorija i investitora iz privatnog sektora neizbježni su u nastojanjima ekonomskog oporavaka. Komercijalizacija znanja stečenog temeljnim i primjenjenim istraživanjem na području inženjerstva materijala, kao i razvoj naprednih tehnologija za njihovu proizvodnju i preradu, potiče stvaranje novih djelatnosti. To je razlog zašto je vrhunsko istraživanje materijala u industrijskoj regiji Centralne Europe preduvijet za održivi regionalni ekonomski i društveni razvoj. Platforma prijenosa tehnologije INNOVMAT stvarana je nedavno u cilju podrške inovacijskim aktivnostima tvrtki iz regije Beč – Bratislava prijenosom znanja dobivenim iz R&D-a na području naprednih materijala u inženjerstvu i pripadajućih tehnologija za industrijsku praksu. Glavni zadatak INNOVMAT-a jest podrška razvoju industrijskih proizvoda s ekstremno visokom dodanom vrijednosti i povećanje konkurentnosti tvrtki s visokim mogućnostima primjene novorazvijenih naprednih materijala u inženjerstvu.

U ovom radu istaknut je vodič u povezivanju R&D institucija i sveučilišta, s ciljem zadovoljavanja potreba proizvodnje SMEs-a i povišenja inovacijskih kapaciteta multinacionalnih industrijskih kompanija, te posebno njihove konkurentnosti na svjetskim tržištima,.

1. Introduction

The basic and applied research in the field of engineering materials in the Central European industrial region has been recently, in spite of its huge potential for its sustainable development, in an emergent and fragmented phase. The cross-border technology transfer platform INNOVMAT (www.innovmat.eu) has been therefore created in Austria and Slovakia with the aim to surpass these limitations and transfer potential benefits of the knowledge acquired by material research and technological development to the industrial sector. The main objective of this recently established scientific and technological regional platform is to integrate the scientific groups that work in this field in the region of Vienna – Bratislava, so they contribute to the critical level necessary to generate knowledge in applied research of engineering materials. This knowledge will be used preferably by regional SMEs for development of commercial products with high added value. The main activities of the platform INNOVMAT are structured in following steps:

- ✓ to initiate the cooperation between Austrian and Slovak R&D institutions in identification of potential industrial applications for newly developed engineering materials and advanced technologies for their production;
- ✓ to support industrial production of innovative products produced using engineering materials as well as advanced technologies for their production and processing;
- ✓ to increase the innovative potential and competitiveness of industrial enterprises in the region of Vienna – Bratislava using high-tech acquired by R&D in the field of advanced engineering materials.

a) b) c)

Figure 1. Examples of products with extremely high added value developed by IMMM SAS and successfully applied in industry

Slika 1. Primjer IMMM SAS proizvoda sa ekstremno visokom dodanom vrijednošću i njihova uspješna primjena u industriji

2. Knowledge transfer to industrial practice

Since the 1990s, the knowledge transfer from scientific institutions and universities to industry has become one of the key priorities for policy makers worldwide marked by some influential documents of the OECD which created a policy rationale for technology transfer (OECD 1999), an attention for the variety of transfer mechanisms employed in university-industry relations (OECD 2002), technology-specific diversity of knowledge interactions of industry with universities across economic "clusters" (OECD 2000) and the patenting and licensing of public research organizations (OECD, 2003). In Europe, the Lisbon Agenda (2000) has set the pace for an intensified focus of European science and innovation policymakers on the university-industry knowledge interactions (e.g. European Commission 1995, 2000). Since then, the policy attention for university knowledge transfer has only intensified to one of the key areas of innovation policy (e.g. EC 2004, 2005, 2007) [2].

The central mission of knowledge transfer organizations is to ensure an increase in the efficiency of the transfer of research and development results so as to achieve a maximum benefit for the society. Transfer of knowledge is an important function, which requires the professional management. This function must be adequately secured by resources, by a long-term commitment of providing an access to the necessary funds and expertise. In formulating the mission in a particular case, various aspects may be taken into account and the key aspect should be determined which should play the most important role in knowledge transfer activities:

- ➢ providing the transfer of results of the publicly-funded research into new products and services for the public use and nationwide benefits;
- ➢ promoting regional economic development and increasing the employment rate;
- ➢ for universities and research institutions – promoting the development, maintaining institutes and the faculties, increasing the level of educational process and training of PhD students;
- ➢ creating new or improving existing relations with industry;
- ➢ generating new sources of funding for universities or research institutes based on the sponsored research;
- ➢ increasing the consultancy and expertise opportunities for universities and research institutes;

- ensuring the provision of services for the protection and commercialization of intellectual and industrial property;
- acting actively in order to facilitate the creation of spin-out businesses, scientific and technological parks, incubators and others;
- creating conditions for effective implementation of the knowledge, innovations, technologies and the results of R&D activities from universities and research institutes to industrial practice, etc. [3]

In order to be able to improve the relevance and effectiveness of knowledge transfer policy in the field of engineering materials, a more in-depth understanding of how the actual process itself operates, is required. The aim of this contribution is to fill this void. This paper therefore follows the approach to knowledge transfer along two dimensions. It is characterized from both academic and industry perspectives.

There are two different channels for transferring of knowledge acquired by R&D activities in the field of engineering materials and advanced technologies for their production and processing from scientific institutions and universities to industrial enterprises:

- *Technology Push* – The scientists start research activities and technological development unaffiliated on a specific field. When the research activities lead to new engineering material or process, an economic partner for the implementation and commercialization is in need.

3. Support of innovations in Central European region

The technology transfer platform INNOVMAT was created in 2010 in order to support innovation activities of enterprises in the region Vienna – Bratislava by transfer of knowledge acquired by R&D in the field of advanced engineering materials and related technologies to industrial practice. **Figure 2** shows graphic design of INNOVMAT platform web page.

INNOVMAT combines both abovementioned channels for transferring of knowledge acquired by R&D. The partners in such an innovation system are called "Demand Side" and "Supply Side" where the first one means the industrial enterprises and the second one means the scientific institutions. There are three major forms of mechanisms through which the supply side (the scientists from R&D institutions) transfers knowledge. Firstly, there is the traditional academic dissemination of research results through formal academic channels such as scientific publications in journals and conference proceedings. The second similarly traditional academic type of transfer is the training of academically skilled labour force. Policy instruments or regulation related to these two forms of mechanisms are represented in the science and

- *Demand Pull* – Problems are coming from day-to-day business demand of scientific partner. The experience of the commercial partner guides the research activities and leads to a new development.

The main difficulties in all kinds of knowledge transfer are located at the intersection between economic and scientific partners:

- *acquisition* – finding the best – or at least even any – partner;
- *communication* – technical vs. business language;
- *implementation* – intellectual property rights, licensing contracts, financing, etc.

The theoretical aspects of knowledge transfer is highly controlled by the perspective and scientific methods used (economics, political sciences, sociology, psychology, etc.). The knowledge transfer could just mean the implementation of a market-ready invention or even go as far as basic research in cooperation with an enterprise. Therefore the focus can reach from short-term to long-term effects. Accordingly there is no generally accepted definition for knowledge transfer. **Figure 1** shows examples of successful industrial applications of materials developed by the Institute of Materials & Machine Mechanics SAS published on INNOVMAT web page (a – aluminium alloy component of Camshaft Adjustment System of BMW engine, b – aluminium foam crash energy absorber of Audi Q7, c – aluminium foam crash box of railway carriage).

higher education policies of most European countries. The third type of knowledge transfer mechanisms entails the commercialization of knowledge, which forms the focus of INNOVMAT activities. The commercialization of knowledge can involve many different knowledge transfer channels and mechanisms, either formal channels such as patenting and licensing of acquired know-how and creating of spin-offs, but also various informal channels such as consulting, mobility of science-industry researchers, etc. European knowledge policy includes the incentives that try to stimulate and improve the knowledge transfer interactions that involve the commercialization of scientific research. The Austrian – Slovak cross-border platform INNOVMAT for transfer of knowledge focused on the application of advanced engineering materials established by financial support of European Regional Development Fund is the typical example of such very profitable initiative.

The platform INNOVMAT provides gathering of useful information about R&D activities in the field of material science in the region Vienna – Bratislava. At present, it has been created by co-operation of 6 institutions (2 Economic Chambers, Institute of the Slovak Academy of Sciences, 2 Technical Universities, and private automotive cluster):

- Institute for Economic Promotion, Austrian Federal Economic Chamber, Vienna, Austria (www.wifi.at)
- Slovak Chamber of Commerce and Industry, Bratislava, Slovakia (www.scci.sk)
- Institute of Materials & Machine Mechanics, SAS (www.umms.sav.sk)
- Vienna University of Technology, Austria (www.tuwien.ac.at)
- Slovak University of Technology, Bratislava, Slovakia (www.stuba.sk)
- Automotive Cluster – West Slovakia (www.autoklaster.sk)

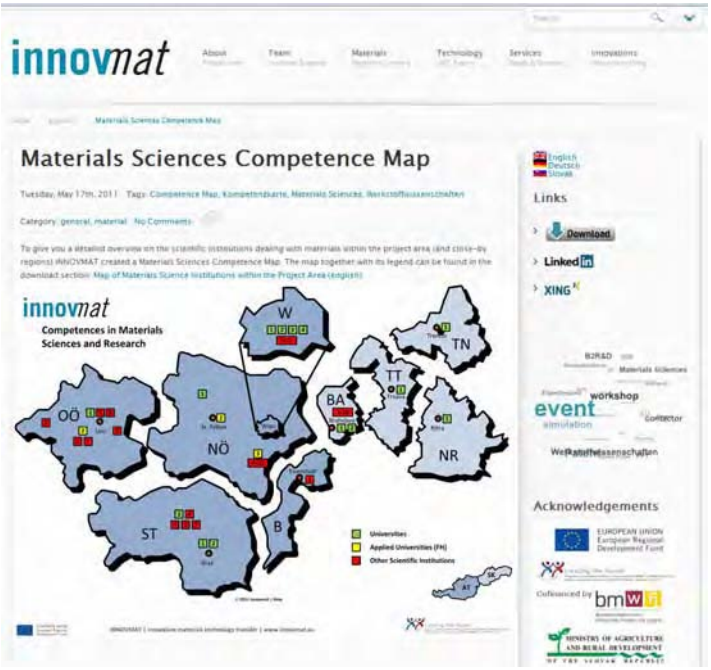

Figure 2. Graphic design of INNOVMAT web page (http://www.innovmat.eu)

Slika 2. Grafički prikaz WEB stranice INNOVMAT (http://www.innovmat.eu)

4. Networking of INNOVMAT experts

INNOVMAT enables very efficient system for linking of scientists and experts from the academic community and the industrial enterprises, effectively provides transfer of knowledge and more rational purchase of equipment, realization of complex R&D projects, etc. The aim of these networking activities is to get in touch experts with key target groups and persons and to inform them about activities of INNOVMAT platform. The both LinkedIn and Xing professional networks are successfully utilized for this purpose. LinkedIn (http://www.linkedIn.com) is the largest social business network in Europe mostly used by English speaking people. This is why it suits very well both Austrian and Slovak partners of INNOVMAT platform to get in touch with key targets in their professional area. Xing (http://www.xing.com) is the largest German speaking social business network. This is why it suits best for targeting Austrian key persons and groups interested in cooperation with experts of INNOVMAT platform [5].

Both LinkedIn as well as Xing professional networks provide the ability to use own recently established "INNOVMAT groups" (**Figs. 3** and **4**), where interested persons are involved in providing and sharing information and serving them in business areas of INNOVMAT platform.

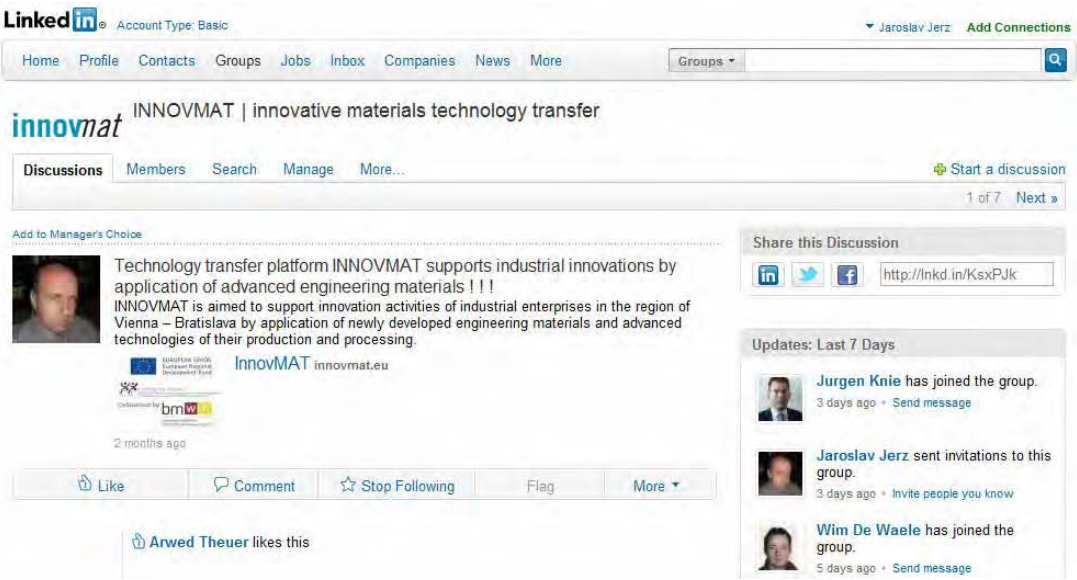

Figure 3. Networking of scientists and experts active in the field of engineering materials and accompanying technologies by means of professional social network LinkedIn (http://www.linkedin.com)
Slika 3. Mreža znanstvenika i stručnjaka aktivnih na polju inženjerstva materijala i pratećih tehnologija uključenih u profesionalnu društvenu mrežu LinkedIn (http://www.linkedin.com)

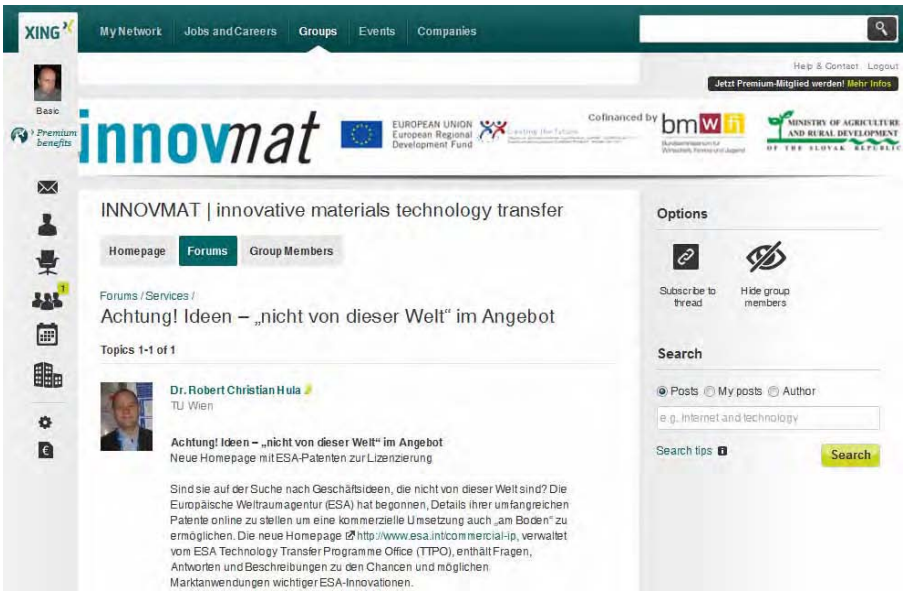

Figure 4. Dissemination of information related to the platform activities through INNOVMAT group created on largest German speaking social business network Xing (http://www.xing.com)
Figure 4. Širenje informacija koje se odnose na aktivnosti INNOVMAT grupe stvorene na najvećoj njemačkoj govornoj društvenoj poslovnoj mreži Xing (http://www.xing.com)

5. Conclusions

The mission of INNOVMAT is to consolidate material research in the Central European region as a forerunner of a sustainable economic and social development by invigorating a technology transfer platform which boosts the connections between the different actors of the innovation system:

- ✓ to accelerate economic development by R&D of engineering materials,
- ✓ to strengthen the knowledge generation stages in this scientific field and its transfer to the industry,
- ✓ to support development of industrial products with extremely high added value,
- ✓ to increase competitiveness of companies with high potential for application of newly developed advanced engineering materials,
- ✓ to link together enterprises, research institutions and industrial regions, etc.

The role of INNOVMAT is to promote the participation of regional companies, especially SMEs in innovative projects. The fostering of knowledge transfer means to align missions of industrial enterprises with high innovative potential and to create synergy effects.

Many new innovative engineering materials and advanced technologies developed by IMMM SAS, TU Vienna and STU Bratislava have been successfully applied in various industrial fields. Development of innovative products in the region of Central Europe supported by technology transfer platform INNOVMAT is systematically focused preferably on those with great potential to achieve particularly high added value thanks to effectively utilized know-how. Achieving global sustainability is a major challenge for the nearest future and that is why international cooperative research, development and knowledge transfer of modern engineering materials to industrial practice is unavoidable.

Acknowledgement

The article was elaborated within the project "Establishment of a cross-border platform for technology transfer focused on the application of advanced engineering materials in the region of Vienna – Bratislava" co-financed by the European Regional Development Fund under the program of Slovak-Austrian cross-border cooperation 2007-2013.

REFERENCES

[1] JERZ, J.: Research, Development and Technology Transfer (R & D & TT) in the Field of Engineering Materials and Related Technologies, Advances in Technology, Education and Development, Wim Kouwenhoven (Ed.), 2009. ISBN: 978-953-307-011-7, INTECH,
Available from:
http://sciyo.com/articles/show/title/research-development-and-technology-transfer-r-amp-d-amp-tt-in-the-field-of-engineering-materials-an.

[2] http://www.dime-eu.org/files/active/0/SC-session4B-vanderSteen-et-al.pdf.

[3] LINCZÉNYI, R.; VRATNÝ, Š.; LINCZÉNYI, A. and KOPKÁŠ, P.: The reader of ERDC project final conference "Research Clusters in Central Europe". Bratislava: BIC Bratislava, Ltd., 2010, p. 27-36. ISBN 978-80-970393-6-3.

[4] JERZ, J.: Modern Engineering Materials for Design of Sustainable Products. In Strojarske tehnologije i konstrukcijski materijali. Split: Hrvatsko Društvo za strojarske tehnologije, 2010, p. 60-68. ISSN 1847-7917.

[5] VACLAV, M.: Communications – Concept for Xing & LinkedIn. – Krems/Donau: werbetopf – social media & sales GesbR, 2011.

Cross-border platform INNOVMAT for technology transfer focused on the application of advanced engineering materials in the region of Vienna – Bratislava

IMPROVED TRIBOLOGY FOR HOT ALUMINUM FORMING BY ANODIZATION

Vjekoslav FRANETOVIĆ [1)]***, James G. Schroth***[2)]
1) Retired from Department of Materials Science,GM Research and Development Center, Warren, MI 48090, USA
Now at University Center for Professional Studies, Mechanical Engineering Design, Kopilica 5, 21000 Split, **Croatia**
2) Department of Materials Science, GM Research and Development Center, Warren, MI 48090, **USA**
vfraneto@oss.unist.hr

Original scientific paper

Abstract: The technology of Quick Plastic Forming (QPF), which has been developed by General Motors, facilitates the forming of complex panels from aluminum sheet at high temperature (450°C). Although this process has formability advantages over conventionally stamped aluminum or steel, there are still no fully satisfactory solutions for the problem of aluminum transfer to the steel tool during forming. In this work we show that the process of anodizing aluminum prior to forming greatly diminishes the interaction of aluminum with steel at QPF forming temperatures. Significantly improved tribological behavior of the aluminum surface after anodization was shown on a laboratory scale with flat-on-flat reciprocating bench experiments.

Poboljšanje triboloških svojstava anodizacijom aluminijskih limova za vruce formiranje

Izvornoznanstveni članak

Sažetak: Tehnologija „Brzog plastičnog formiranja (oblikovanja)" (BPF), koja je razvijena u General Motors-u, olaksava formiranje kompleksnih ploča od alumijskog lima na visokim temperaturama (450°C). Premda ovaj proces ima prednosti prilikom formiranja pred konvencionalnim ispresavanjem aluminija ili čelika, jos uvijek ne postoje potpuno zadovoljavajuca riješenja za problem prijenosa aluminija na čelični kalup za vrijeme formiranja. U ovom radu mi pokazujemo da proces anodiziranja aluminija prije formiranja znatno umanjuje interakciju alumnija sa čelikom pri temperaturi BPF. Značajno poboljsano tribolosko ponašanje aluminijske površine nakon anodizacije je pokazano na laboratorijskom nivou sa reciprocnim laboratorijskim eksperimentima, ravno-na-ravno".

Keywords
Manufacturing/Metalworking Tribology
Automobile production
Dry Lubrication Friction
OxidativeLubrication
Anodization
Adhesion.

Ključne riječi
Proizvodno/Metalo-prerađivačka tribologija
Proizvodnja automobila
Trenje suhog podmazivanja
Oksidno podmazivanje
Anodizacija (anodna oksidacija metala)
Adhezija.

1. Introduction

Quick Plastic Forming (QPF) technology was developed by GM to form complex aluminum sheet panels for parts that could not be produced with conventionally stamped aluminum or steel. Adherence of the aluminum sheet to the tool during forming is a critical problem for this high temperature forming process. Such transfer of aluminum to the steel tool requires frequent, expensive, and time consuming repolishing of the tool. Development and improvement of QPF by changes in the process and forming parameters have been documented in numerous research reports [1-5] and patents issued by GM researchers.

Those prior efforts centered on providing tool surfaces that were largely non-reactive toward the aluminum sheet at elevated temperature. A second approach (implemented in combination with the first one) focused on lubricating the aluminum sheet in a manner that would decrease friction during forming to minimize forming strains and to avoid aluminum/tool adhesion and subsequent panel damage.

A recent new experimental approach used to investigate QPF tribology involves flat-on-flat reciprocating bench testing [6-8]. This sliding test simulates the tribological behavior of the aluminum(panel)/steel(tool) sliding pair at the QPF temperature with the intention of replicating the behavior of interacting surfaces, including the presence of lubricants on aluminum and/or coatings on the tool. During the development of the QPF process, many lubricants and coatings were tried in an effort to avoid transfer of aluminum to the tool with time. Some of the lubricants and coatings chosen to minimize friction and/or delay metal-to-metal contact (adhesion)

have been investigated by this bench testing technique [7-9]. No fully satisfactory combination was found.
The surface treatment presented herein consists of anodizing of the aluminum sheet to improve the tribological performance of the forming system. This is the first attempt to improve tribological performance through an alteration of the sheet surface. In this approach, a barrier layer (Al_2O_3) is produced on the aluminum sheet that tends to isolate the reactive aluminum metal from the tool surface. The tribological performance of such treated aluminum was tested by the flat-on-flat reciprocating test at low sliding speed.

Symbols/Oznake

FC	- Friction Coefficient	*IFC*	- Initial Friction Coefficient
GM	- General Motors	*SSFC*	- Steady State Friction Coefficient
AA5083	- Aluminum Alloy 5083	*TTC*	- Time to contact, s
QPF	- Quick Plastic Forming	*EPMA*	- Electron Probe Microanalysis
AISI P20	- mold quality alloy steel	*BSE*	- Back scattered electrons
CP	- Contact potential (electric), V	*BN*	- Boron nitride

2. Experimental

2.1. Anodizing treatment

Aluminum anodizing is the electrochemical process by which aluminum is converted into aluminum oxide (Al_2O_3) over the surface of a component [10]. The process produces a thicker and tougher layer than the naturally occurring protective oxide. In industry the anodizing process provides a durable and cost effective finish for aluminum that increases corrosion and wear resistance, increases electrical insulation, and offers an excellent base for secondary coating, coloring, and lubricity aids [11,12].
From among the different anodizing types available, the Sulfuric Anodizing method was chosen to oxidize 5083 aluminum sheet in an electrolyte containing 17% sulfuric acid (H_2SO_4) in distilled water at room temperature.
This form of anodizing generally yields coatings less than 25µm thick. Alloy 5083 aluminum sheet (1.2 mm thick) was cut to fit the specimen stage on the Plint machine (Figure1). The sheet was then connected to the positive terminal of the voltage source and immersed in the electrolyte bath. A current density of 15A/ft^2 was applied to achieve "soft anodizing" of the sheet, which yields a more porous and softer coating than "hard anodizing", which yields a harder oxide layer.
For the purpose of these experiments, the duration of the applied electrochemical process was varied in order to obtain different thicknesses of aluminum oxide, while the current density was balanced to stay in the range of soft anodizing. The resulting oxide coating thicknesses on the test samples ranged from 3.9 to 23.6 µm (Table 1).

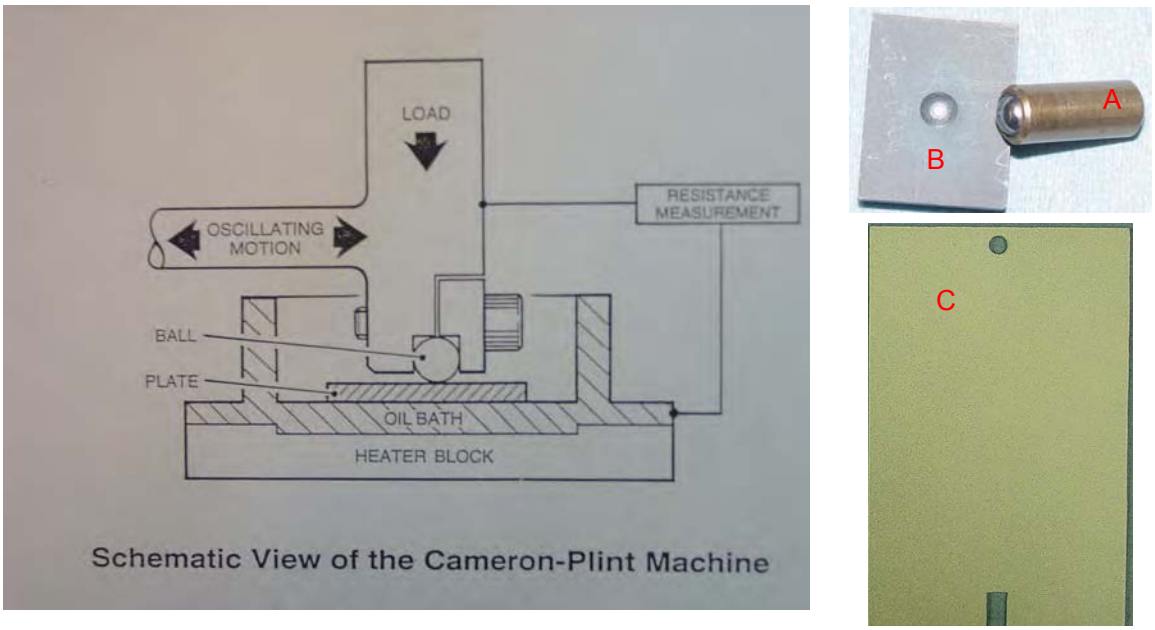

Figure 1. Instead of the ball in the original Plint drawing, the pin (A) ending with movable ball, which fits in the dimple on the back of the tool specimen B, was inserted in the Plint holder. The edges of the tool specimen face were rounded. C shows the Al plate, which was screwed directly on specimen stage (oil bath was not used).

Slika 1. Umjesto kuglice na originalnom Plintovom crtežu umetnut je u Plintovom držaču cilindar (A) sa pokretnom kuglicom na kraju, koja odgovara rupici na stražnjoj strani uzorka kalupa B. Rubovi lica uzorka kalupa su zaobljeni. C označava Al pločicu, koja je pričvščena direktno na postolje uzorka.

Table 1. Results of the tribological evaluation of anodized aluminum sheet compared to BN lubricated sheet.

Tablica 1. Rezultati triboloskog istraživanja anodiziranog aluminijskog lima u usporedbi sa BN podmazanim limom.

Layer over Al sheet	Oxide thickness (µm)	BN thickness (µm)	Failure time (s)	TTC (s)	FC at TTC	SS FC
None (pure Al)	~0.0	~0.0	5	0	NA	NA
BN only	~0.0	9.9	211	157	0.25	0.184
BN only	~0.0	9.9	88	77	0.31	0.238
BN only	~0.0	8.4	43	33	0.24	0.160
thick ox.layer, only	20.1	0.0	Not failed in 800s	More than 800s	NA	0.289
thick ox.layer + BN	22.0	12.9	Not failed in 1,200s	More than 1,200s	NA	0.231
thick ox.layer+BN	23.6	7.9	Not failed in 1,000s	More than 1,000s	NA	0.223
thin ox.layer, only	9.9	0.0	Not failed in 680s	669, but NA	0.27	0.241
thin ox. Layer + BN	9.5	10.2	Not failed in 1,500s	More than 1,500s	NA	0.231
thin ox.layer + BN	8.9	9.4	Not failed in 2,000s	More than 2,000s	NA	0.225
the thinnest ox. layer + thinnest BN	3.9	5.9	Not failed in 700s	More than 700s	NA	0.212

2.2. Flat-on-flat reciprocating testing at low sliding speed

Reciprocating Cameron Plint testing is a well known bench method for the investigation of the tribological performance of two interacting surfaces [13]. During this testing program, the friction coefficient (FC), operating temperature, applied load, and electric contact potential (CP) are automatically recorded.

The contact potential, which is measured between the two sliding material samples (one fixed and the other reciprocating against it), is an indicator of the insulating layer (lubricant or chemically formed layer) or the

occurrence of metal-to-metal contact between this pair. When the contact potential is maximum, there is an insulator present between the two interacting surfaces. When the contact potential drops toward zero, that change indicates the beginning of metal-to-metal contact between the two surfaces and the friction coefficient is expected to rise from that point onward. The steady state friction coefficient (the average of the oscillating curve) in the first stage of the run (Figure 2), indicates stable conditions between the two sliding surfaces through the regime where the friction laws are valid. The steep increase of the friction coefficient that occurs after metal-to-metal contact indicates the onset of adhesion. In that range of sudden friction coefficient increase, material is likely to be transferred from the softer to the harder surface.

Recently, the flat-on-flat reciprocating Plint method was used to investigate the tribological characteristics of an AA5083/P20steel pair, where the aluminum sheet is fixed and P20 steel specimen is cycled back and forth, Figure 1. A description of the machine and experimental setup as well as the detailed test procedure has been described earlier [6,7]. The advantages of a low sliding speed versus the speeds used in previous flat-on-flat methods [6,13], was also explained earlier [7, 8].

In the QPF production process, the aluminum panel is coated with boron nitride and the tool covered by a coating to avoid or delay direct metal-to-metal contact and the occurrence of adhesion, and to facilitate forming of the panel by decreasing the friction coefficient.

The aluminum sheet tested herein was covered by a controlled thickness of aluminum oxide with the anodizing process. Some sheets were additionally covered with thin or thick BN layers (Table 1). The flat AISI P20 steel sample was used to simulate the die material. The Plint flat-on-flat reciprocating tribological tests were run at 450oC, with a load of 50N, and at a frequency of 0.1 Hz. The tests were terminated at the point where a steep rise in friction was observed. That point is indicative of unacceptable transfer of aluminum to the tool [7,8].

The recorded friction coefficient (FC) and contact potential (CP) curves were evaluated in order to extract specific values of time and FC that characterize the tribological behavior of the reciprocating steel/aluminum sliding surfaces. The graph in Figure 2 shows the results of a typical flat-on-flat experiment at 0.1 Hz for the BN-lubricated aluminum sheet. The arrows in the graph refer to the characteristic tribological values extracted from the test. The pertinent characteristics were defined in a previous report [7] and were determined for each test:

(a) Initial friction coefficient (IFC),
(b) Steady state friction coefficient (SSFC),
(c) Time to contact (TTC),
(d) Friction coefficient at time to contact (FC at TTC), and
(e) Time to tribological failure of sliding pair (Failure time),

The analysis of the tribological test results was also elaborated earlier [7].

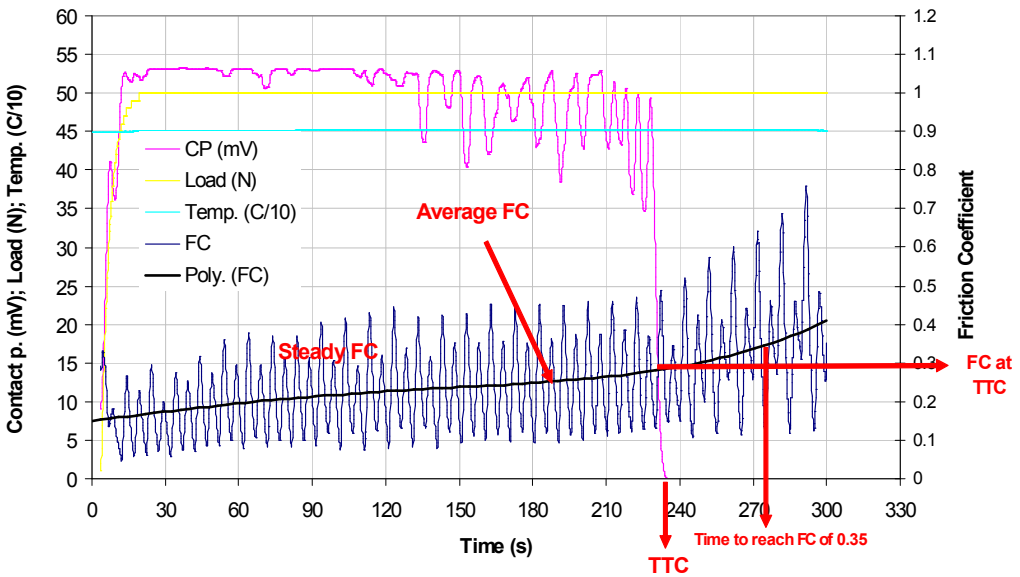

Figure 2. Friction coefficient, contact potential, load, and specimen temperature as functions of time for one typical flat-on-flat reciprocating Plint experiment at 0.1 Hz.

Slika 2. Koeficijent trenja, kontaktni potencijal. opterećenje i temperatura uzorka kao funkcije vremena za jedan tipični ravno-na-ravno recipročni Plintov eksperiment kod 0.1 Hz.

2.3. Specimen appearance

The tested tool specimens and aluminum sheets were examined optically to detect occurrence of aluminum transfer to the tool and damage to the aluminum sheet.

Electron probe microanalysis (EPMA) was also used to analyze the surface of the steel tool specimens after testing. X-ray maps of Al, O, B, N, and Fe, together with corresponding back scattered electron (BSE) images, were taken from the tool specimen surfaces to detect those elements on the tool after testing.

3. Results and discussion

Three different oxide layers, having thicknesses of approximately 20, 10, and 4 μm, respectively, were applied to the aluminum sheet with a sulfuric acid anodization process. The oxidized aluminum sheets were tested with various applied BN thicknesses ranging from ~6 to 13 μm, Table 1. For the purpose of comparison, additional aluminum sheets covered only by the BN lubricant were also tested. In summary, three groups of experiments were run:

1. P20 steel sliding against untreated AA5083 covered only by the BN lubricant (used as a baseline),
2. P20 steel sliding against anodized AA5083 sheet without lubricant,
3. P20 steel sliding against anodized AA5083 sheet with differing thicknesses of BN lubricant.

The results from the test program are presented in Table 1 and Figures 3-9. In these experiments, soft anodization treatment of the aluminum sheet eliminated the transfer of aluminum to the steel tool over much longer time periods than had been observed for prior work with non-anodized aluminum.

3.1. BN-coated and bare aluminum

The results obtained from untreated aluminum samples with 8.4 and 9.9 μm BN lubricant thicknesses, respectively, were used to establish a behavior baseline for comparison with the oxidized, and oxidized+BN samples (Table 1, Figures 3-8). Similar samples had been used in previous work to investigate variations in BN thickness and steel tool surface [7] and for comparison with alternate lubricants [8]. Also, the test run with P20 steel against unlubricated aluminum sheet was used to show the benefit of BN lubricant alone. While the unlubricated aluminum sheet suffered tribological failure in just a few seconds, Figure 3a, the beneficial influence of BN lubricant pushed back the failure event in one typical experiment with BN covered sheet to nearly 90 seconds, Figure 3b. The accompanying damage to the sheet surface as well as the transfer of aluminum from the sheet to the tool specimen are readily seen in the photo insets within the graphs (the light area all over the tool specimen in Figure 3a, and the light traces in Figure 3b). The inset photo in Figure 3b actually shows the welded aluminum on the tool specimen surface.

The friction coefficient curve exhibited a high average friction coefficient and very high amplitude oscillations of the measured friction in the case of bare aluminum, which is the result of very high static friction (direct metal-to-metal contact). In contrast to this behavior, the BN lubricated sheet showed a much lower average friction coefficient, a much lower amplitude of FC and a relatively steady FC (until the BN was displaced), that is, until the CP dropped to zero (metal-to-metal contact). After that point there was a steep rise in the FC that coincided with tribological failure and transfer of aluminum to the tool (note the traces of Al on the tool specimen in the inset). A steep rise in FC was routinely correlated with the observed transfer of Al to the actual tested tool specimen in order to more accurately determine the failure time.

The failure time for BN-coated sheets were 43, 88, and 211 seconds with the corresponding steady state FC's calculated to be 0.16, 0.24, and 0.18, respectively. The IFC was somewhat lower than the SSFC and the TTC followed the behavior of the failure time as was shown earlier [8]. This variation in characteristic values resulted from the difference in the initial BN thickness (8.4 and 9.9 μm) and the uniformity of the sprayed BN layer over the aluminum sheet.

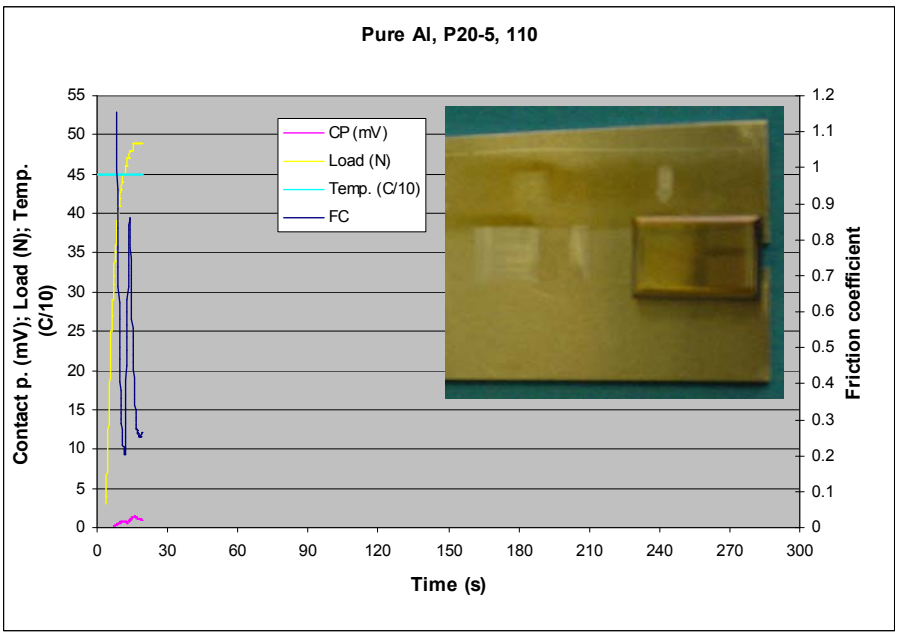

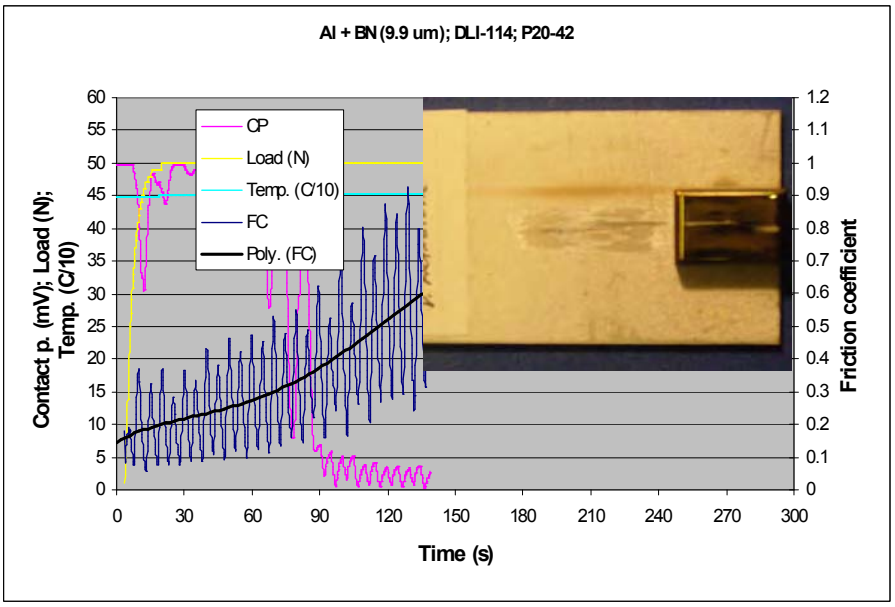

Figure 3. Friction coefficient, contact potential, load, and specimen temperature as functions of time for a) pure aluminum, and b) production used BN covered sheet. Inserts in both cases show aluminum transferred to the tool specimen.

Slika 3. Koeficijent trenja, kontakt potencijal, opterečenje i temperatura uzorka kao funkcije vremena za a) čisti aluminij i b) lim prekriven sa BN, koji se upotrebljava u proizvodnji.

3.2. Anodized aluminum sheet

The aluminum sheets oxidized by an anodization process displayed much better tribological performance than the previously tested aluminum surfaces. The calculated characteristic values are presented in Table 1. The graphs showing the friction coefficient behavior as a function of time are shown in Figures 4 and 5. For the purpose of comparison, two FC–time graphs corresponding to two tests of Al sheet coated only with BN are also shown in the same Figures.

Figure 4a is the same as Figure 3b, but with the longer time scale needed to show the oxidized sheet test. Figure 5a represents one of the best tribological performers among any of the tested BN-covered sheets (it was uniformly sprayed with BN aerosol in the laboratory).

The aluminum sheets anodized to develop 9.9 and 20.1 µm thick oxide layers did not suffer tribological failure at all during the prolonged tested time, which is shown by the steady and low FC up until the end of the tests, 680 and 800s, respectively. No sign of sudden FC increase indicated that the tested tribo-pair was sliding within the same regime (constant FC) and did not pass into a regime of uncontrolled plastic deformation. Correspondingly, the insets in the graphs, which show the tool and aluminum sheet surfaces, do not show any transferred aluminum on the tool specimen. The interpretation of the CP behavior in these experiments, where both sheet sides were anodized, is not equivalent to the case where the sheet is covered by an insulator on only one side (e.g. BN) and therefore is not emphasized in this discussion. For the same reason the FC at TTC is not defined ("NA" in Table 1). The SSFC calculated for the oxidized sheets was generally higher than for the sheets lubricated with BN alone. However, despite the lower lubricity, the oxide layer prevented aluminum transfer between the sheet and tool.

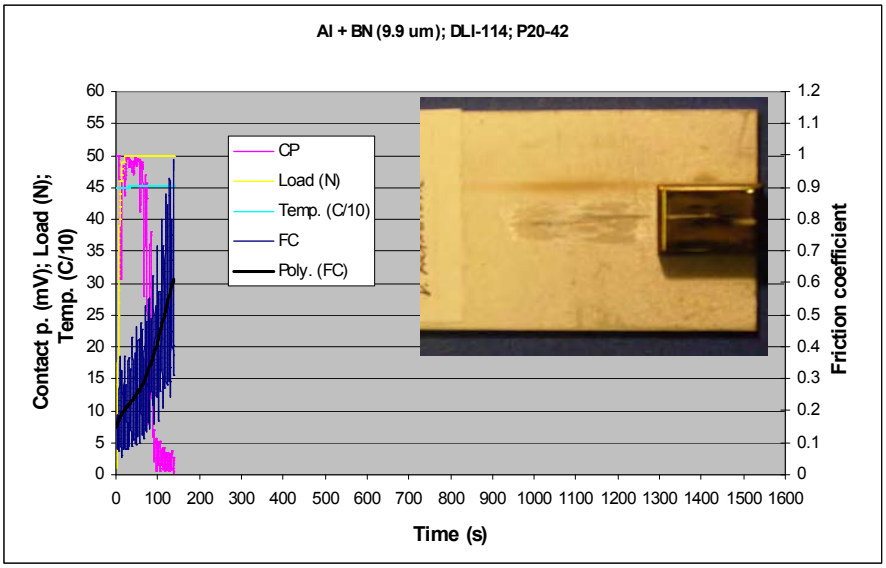

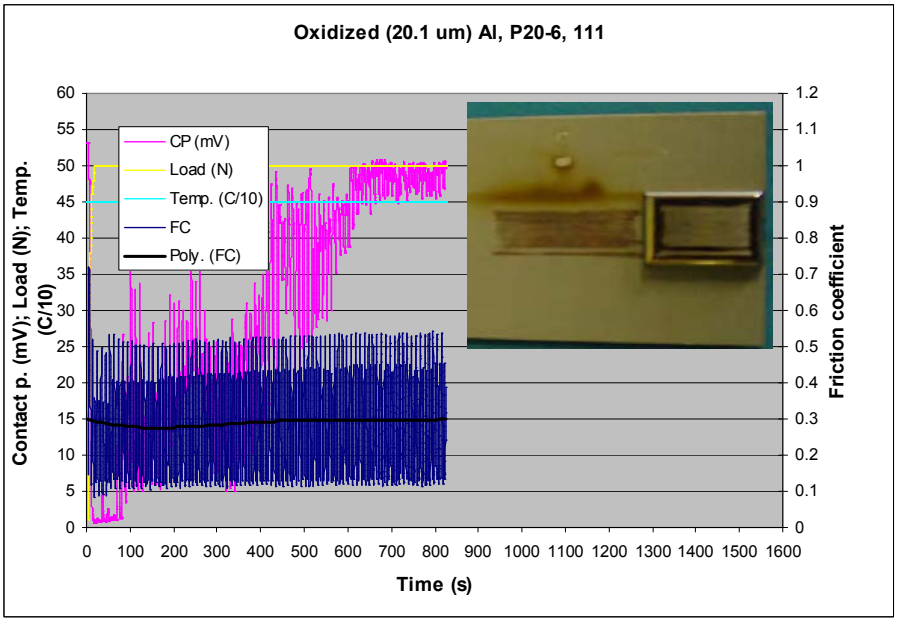

Figure 4. Friction coefficient, contact potential, load, and specimen temperature as functions of time for a) production used BN covered sheet, and b) anodized Al plate having 20.1 µm thick oxide. Inserts show in a) welded Al to the tool, and in b) no transferred Al to the tool.

Slika 4. Koeficijent trenja, kontakt potencijal, opterečenje i temperature uzorka kao funkcije vremena za a) lim prekriven sa BN, koji se upotrebljava u proizvodnji i b) anodizirana Al pločica koja ima 20.1 µm debeli oksid. Umetci prikazuju u a) zataljeni Al za uzorak kalupa i u b) uzorak kalupa bez prenesenog Al.

In conclusion, the oxidized sheet with a 10-20 µm thick oxide surface layer exhibited an extension of the specimen failure time to 7 to 8 times that of the "classically" lubricated (with boron nitride) aluminum sheet (Figure 8), without any signs of transferred Al on the tool specimen following the prolonged test time. Thus the aluminum treated in the described manner essentially eliminated (or significantly delayed) the onset of adhesion.

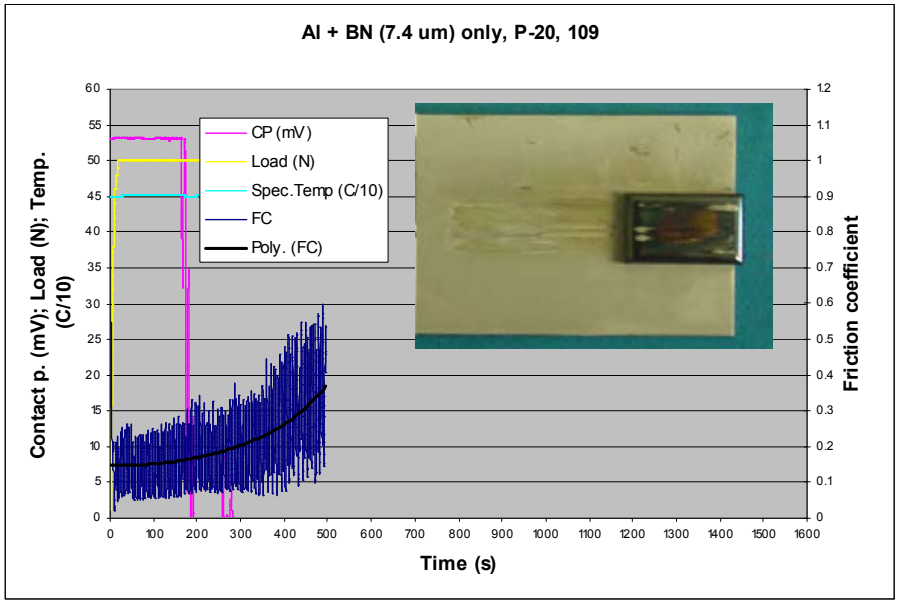

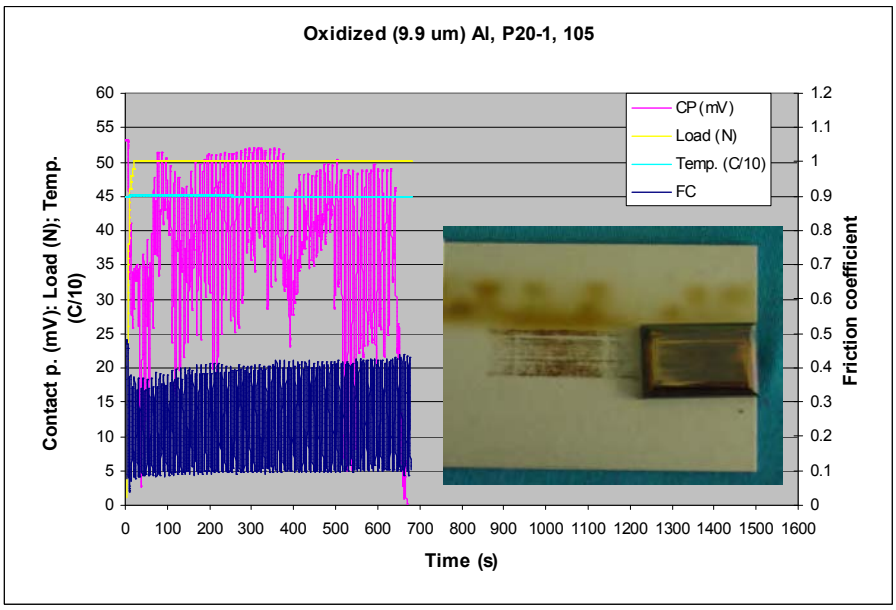

Figure 5. Friction coefficient, contact potential, load, and specimen temperature as functions of time for a) uniformly BN aerosol covered plate in laboratory, and b) anodized Al plate having 9.9 µm thick oxide. Inserts show in a) welded Al to the tool specimen, and b) no transferred Al to the tool.

Slika 5. Koeficijent trenja, kontakt potencijal, opterečenje, i temperatura uzorka kao funkcije vremena za a) jednoliko prekrivenu pločicu u laboratoriju sa BN aerosol i b) anodiziranu Al pločicu koja ima 9.9 µm debeli oksid. Umetci prikazuju u a) zataljeni Al na uzorku kalupa i b) uzorak kalupa bez prenesenog Al.

3.3. Anodized aluminum sheet lubricated with BN

The anodized aluminum sheets covered by BN layers of different thicknesses exhibited even better tribological performance than oxidized plates run without a solid lubricant.

The characteristic values from flat-on-flat tribological testing are presented in Table 1. and in Figures 6-8.

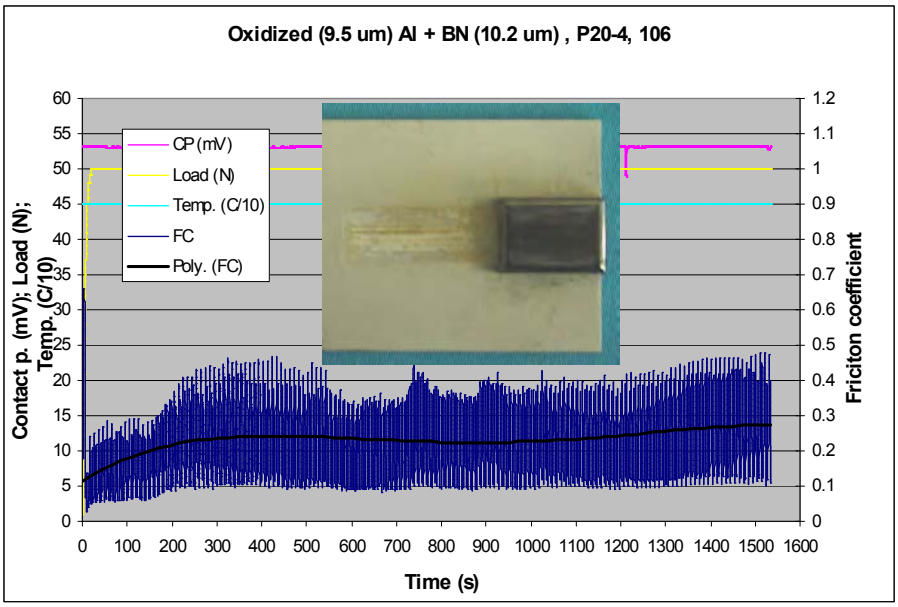

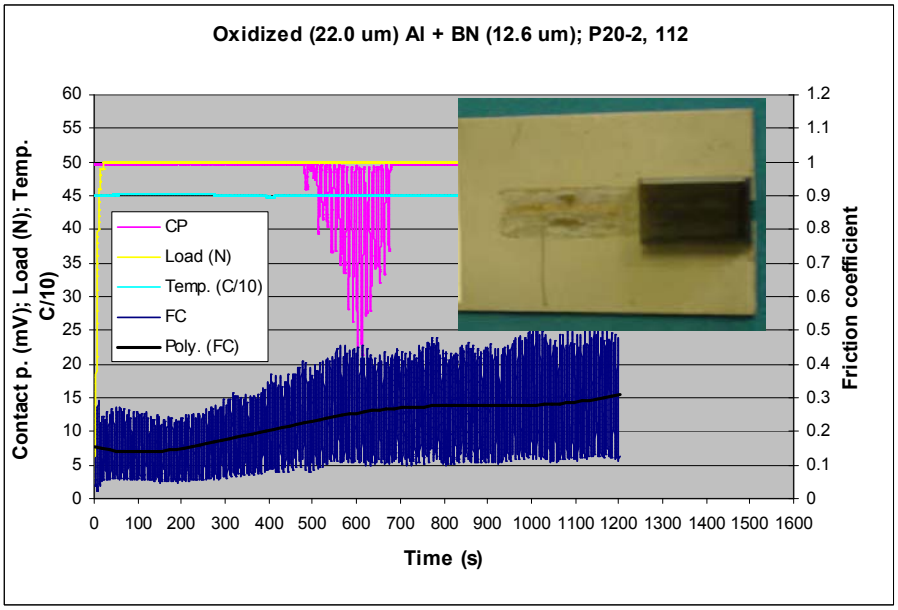

Figure 6. Friction coefficient, contact potential, load, and specimen temperature as functions of time for plates a) oxidized (9.5 µm) + BN covered (10.2 µm), and b) oxidized (22.0 µm) + BN covered (12.6 µm). Inserts show no transferred Al to the tool specimens.

Slika 6. Koeficijent trenja, kontakt potencijal, opterečenje i temperatura uzorka kao funkcije vremena za pločice a) oksidirane (9.5 µm) + prekrivene sa BN (10.2 µm) i b) oksidirane (22.0 µm) + prekrivene sa BN (12.6 µm). Umetci prikazuju uzorke kalupa bez prenesenog Al.

The graphs in these Figures show the FC and CP behavior during the test as a function of time. Again, for the purpose of comparison with aluminum sheet covered by BN only, the FC–time graph obtained from one such typical test is shown with the same time scale as the oxide+BN covered sheet in Figure 7a.

The aluminum sheets covered by 9.5 μm thick oxide + 10.2 μm BN and 22.0 μm + 12.6 μm thick BN did not suffer tribological failure during the prolonged test times of more than 1500s and 1200s, respectively, Figure 6. The FC remained steady and relatively low right to the end of the test. Since no sudden friction increase was observed during the test time, it is reasonable to assume that aluminum sheet treated in such a manner should demonstrate even longer endurance times without tribological failure. In support of the above conclusion, no sign of transferred Al was observed during the optical examination of the tool specimens (shown in Figure 6). Yet, these tribo-pairs were not sliding completely within the same regime (constant FC) as in the case of the unlubricated anodized sheet. The SS FC is generally lower (Table 1) than in the case of oxide only, and the IFC was always lower at the beginning of the test of all oxide+BN sheet experiments (Figures 6 and 7) as compared with the anodized-only sheets for which the average FC was constant.

This can be explained as the effect of the BN lubricant decreasing the average FC at the beginning of sliding interaction of two surfaces until the lubricant is displaced. From that point on, the average FC starts to increase as more oxide surface becomes exposed. This effect can even be correlated with small differences in initial BN thickness. For the 5.9 μm BN layer, the duration of relatively low FC was about 120 seconds; for the 10.2 μm BN thickness, the FC remained low for nearly 200 seconds; and for 12.6 μm BN layer, FC remained low for ~350 seconds (Figures 6 and 7).

The nature of the surface structure of the aluminum oxide grown over aluminum during anodization can be beneficial in the presence of lubrication because this porous structure acts as a kind of storage media for the applied lubricant. Something similar has been experienced in the oil-lubricated cylinder bore of a combustion engine, where the bore is honed with the purpose of creating tiny valleys in the bore structure.

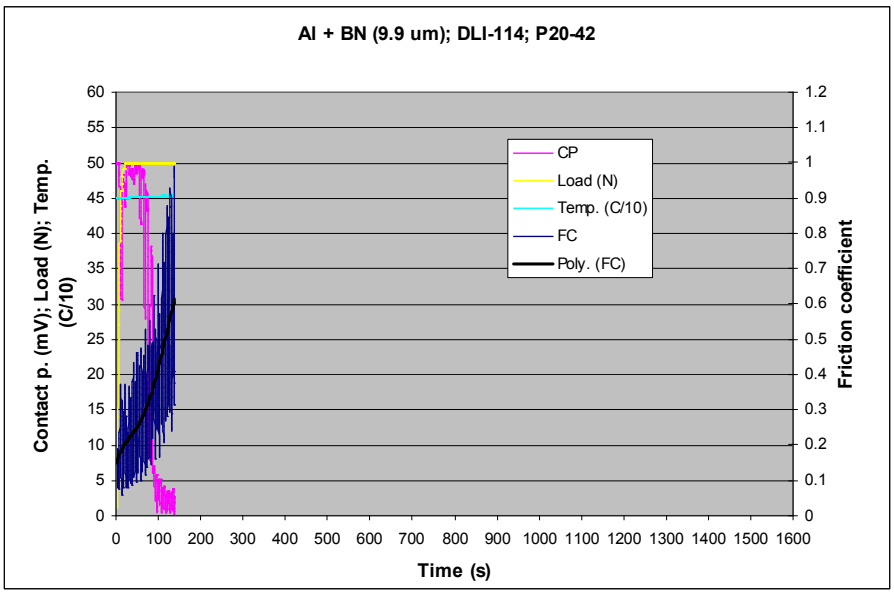

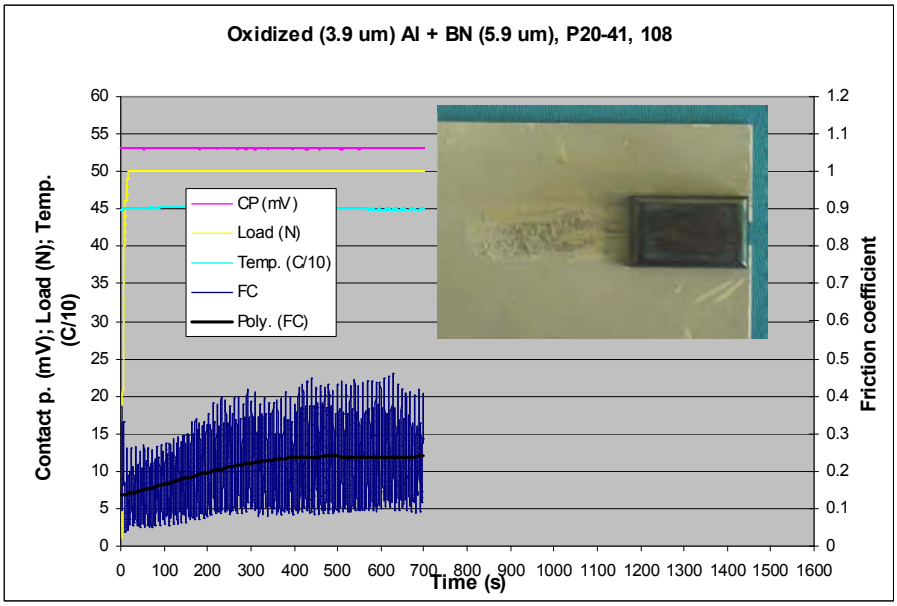

Figure 7. Friction coefficient, contact potential, load, and specimen temperature as functions of time for a) production used BN covered sheet, and b) lightly oxidized (3.9 µm) + covered by the thinnest BN ever used. Insert in b) shows no transferred aluminum to the tool specimen.

Slika 7. Koeficijent trenja, kontakt potencijal, opterečenje i temperatura uzorka kao funkcije vremena za a) lim prekriven sa BN, koji se upotrebljava u proizvodnji i b) lagano oksidirani (3.9 µm) + prekriven sa najtanjim BN koji je ikada upotrebljen. Umetak u b) prikazuje da nema prenesenog aluminija na uzorak kalupa.

These tiny valleys act as reservoirs for the oil and enhance the lubrication during ring-bore sliding.

TTC and FC at TTC were not defined in these experiments due to the inability to track metal-to-metal contact (i.e. the sheet specimen was surrounded with an insulating layer).

Finally, a very thin oxide layer of only 3.9 µm covered with a very thin BN layer of 5.9 µm showed an endurance 8 times higher than that for bare aluminum with a thicker (9.9µm) BN layer (Table 1, Figures 7b and 8). The sheet covered with the very thin oxide and BN layers did not suffer tribological failure during the test time of 700 seconds. Optical examination (photo inset in Figure 7b) did not reveal any aluminum transferred to the tool specimen. The tribological performance of the aluminum sheet treated in this manner exceeded that of any of the QPF bench experimental trials to date on BN-based lubricants.

EPMA analysis of the steel tool surface after testing showed no aluminum transfer to the tool surface

following testing against both oxide- and (oxide+BN)-covered sheet. This result confirmed the appearance noted from the optical examination of the tool specimen surfaces. One typical EPMA analysis of the thinnest oxide+thinnest BN layer is shown in Figure 9. There is a striking difference in the amount of aluminum found on the tool surface after testing between the BN-covered sheet and the sheet first anodized to a thin level of oxide and covered with a thin layer of BN.

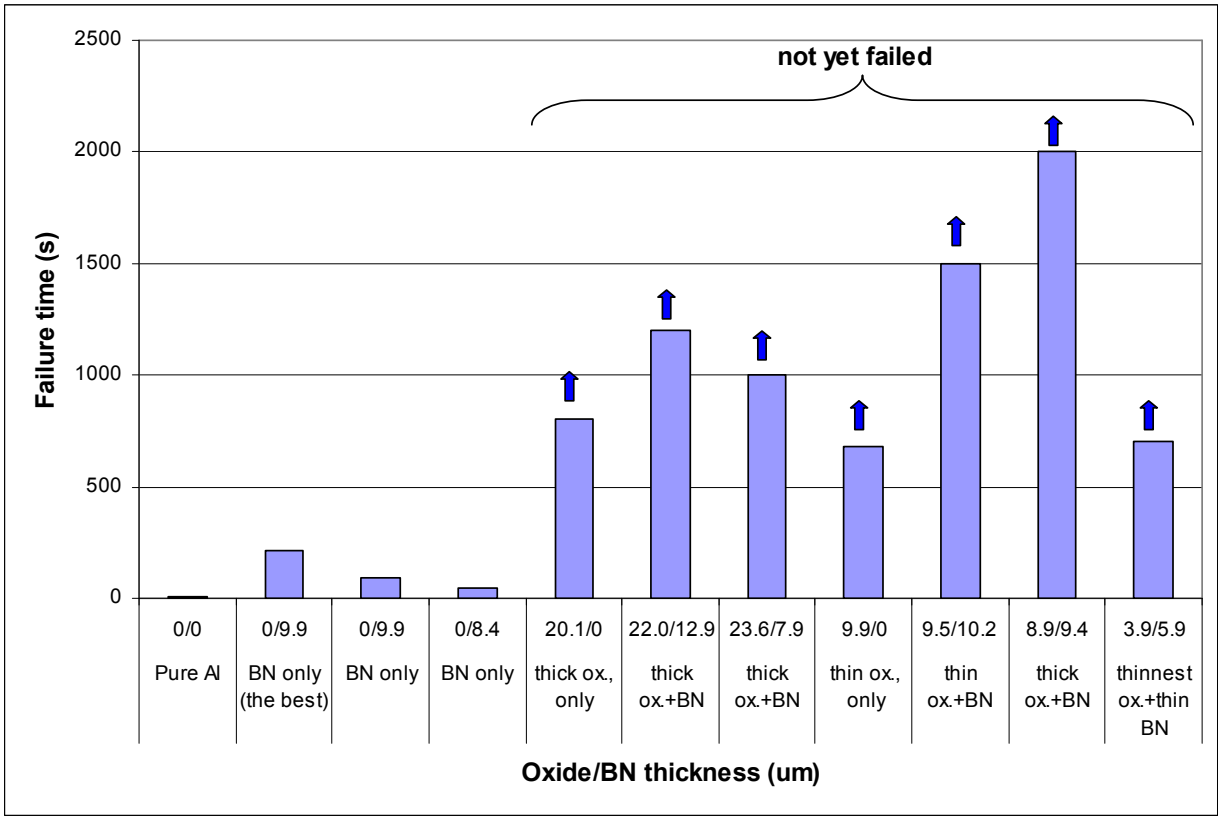

Figure 8. Time to tribological failure for aluminum sheets with various oxide/BN coating combinations. None of the anodized specimens had failed at the time that the tests were stopped.

Slika 8. Vrijeme do triboloskog otkazivanja za aluminijske limove sa različitim kombinacijama oksid/BN prevlaka. Nijedan od anodiziranih uzoraka nije otkazao za vrijeme do kada su testovi prekinuti.

For the case of the BN-coated non-anodized aluminum, an abundance of transferred aluminum along with indications of welding are seen in the x-ray image taken from the tool surface in Figure 9a. The BSE image (Figure 9b) shows the corresponding layer of transferred aluminum (dark area). In sharp contrast to this behavior, negligible traces of aluminum were found on the tool surface in the case of the thin-oxide+thinnest-BN covered sheet. For this case, the dark area on the corresponding BSE image (9d) shows a BN-covered tool specimen with surface species that were confirmed by the corresponding x-ray maps of B and N.

In conclusion, the oxidized aluminum sheet covered by even a small amount of BN is an excellent tribological performer, exhibiting an 11 to 15-fold improvement in test times compared to the non-oxidized BN-covered aluminum sheet. The anodized aluminum sheet with or without a very light BN layer demonstrated the longest endurance of all the P20/Al tribo-pairs tested in this laboratory [6-9]. It is important to note here that the limits of endurance of such treated specimens under various conditions still have to be determined.

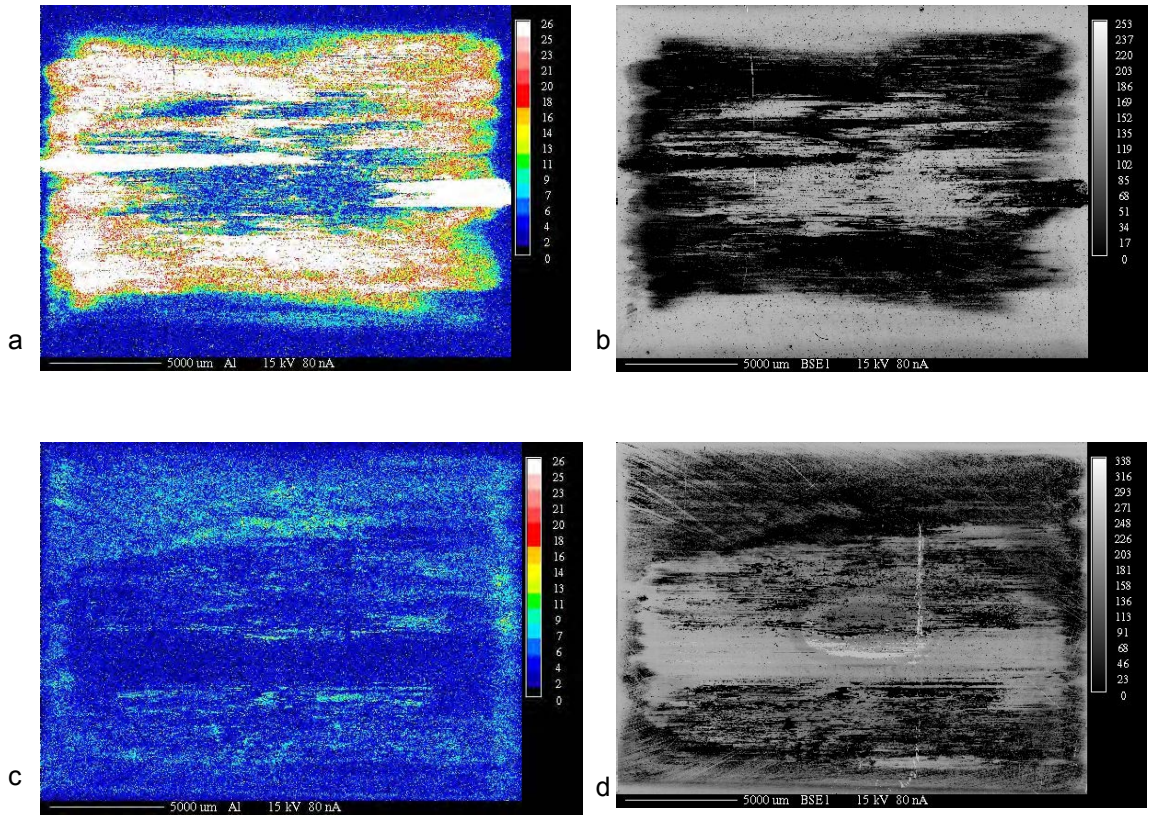

Figure 9. EPMA showing: a) X-ray map of Al and b) corresponding BSE image of the tool specimen surface, which was run against Al plate + BN, only; c) and d) the same for the tool run against oxidized Al plate + very thin BN layer.

Slika 9. EPMA koji prikazuje a) mapu X zraka za Al i b) odgovarajuću BSE sliku površine uzorka kalupa, koji je klizio preko Al pločice + samo BN; c) i d) Isto za uzorak kalupa, koji je klizio preko oksidirane Al pločice + vrlo tanki BN sloj.

3.4. Possible sources of the anodizing effect

For the anodized 5083 aluminum sheets, the softer metal is covered by a naturally well-bonded and very hard layer (Al_2O_3) that is stable at high temperature. There are at least three beneficial characteristics of this composite structure.

First, this structure eliminates the occurrence of the "cheese and knife" situation [14] that occurs when a much harder partner (steel tool) slides against the softer member under high load. Conditions in such a regime (typical conditions in the QPF process) are far away from ideal friction where the "friction laws" are valid. In this case, the soft material suffers not only elastic flattening of asperities, but also plastic deformation and rupture that leads to the transfer of material from the soft partner (soft aluminum at high temperature) to the much harder sliding partner (tool surface).

When this happens, the initial roughness of the sheet has no practical importance and resistance to cutting and sticking is determined above all by the tensile and shear strength of the weaker solid [15]. By applying the hard and well bonded oxide over aluminum by anodization, the interactions between the underlying aluminum and tool material are largely excluded. The lubricated oxide does not bond with the tool material in a manner sufficiently strong to rupture the underlying soft aluminum alloy. Thus, anodized aluminum would eliminate the transfer of aluminum to the tool and subsequent panel damage during QPF forming.

The second benefit of the anodized panel surface in the QPF process is the barrier nature of this coating that a priori eliminates the initial metal-to-metal contact that can ultimately lead to adhesion. It is widely accepted that any adhered layer that prevents metal-to-metal contact promotes a reduction of the friction between the two interacting metal surfaces and delays adhesion [16].

The third beneficial characteristic of the anodized coating is the natural surface structure of electrochemically-grown aluminum oxide. The additional layer is porous and offers an excellent base for lubrication and coloring [11,12]. The latter possibility may not be important for the QPF production system since an acid wash is used to remove the oxide created during high-T exposure, so it is believed that the anodized layer may naturally be removed in the current production system and will not interfere with any post-form processing steps. However, during forming the porous character of the grown oxide may provide depots for the solid lubricant and additionally decrease the

friction coefficient and improve the tribological performance.
Finally, it is worth noting that the implementation of this process might be improved economically by oxidizing the aluminum surface in a controlled-moisturizing chamber under an elevated temperature rather than through the electrochemical anodization process. It remains to be investigated if such an aluminum surface would exhibit similar tribological advantages.

3.5. Benefits associated with anodized panels

The results of this work suggest the following:
1. Anodizing of aluminum blanks could improve the tribological system for Quick Plastic Forming or warm forming of aluminum and prevent/minimize the transfer of aluminum from the aluminum panel to the steel tool. Such transfer currently necessitates a frequent, expensive, and time consuming repolishing of the tool working surface.
2. Also, since this process produces a relatively steady and low friction coefficient between the aluminum and steel surfaces, it is also expected that the process could improve the reproducibility of panel forming, and help to eliminate (or at least minimize) fractures of the panel in critical locations, or alternatively reduce forming cycle time.
3. Additionally, since the benefits of anodization have remained even when only small amounts of BN are used, the cost of the BN eliminated from the process can be used as an offset to the cost of blank oxidation along with the decrease in tool repolishing costs.
Several issues remain. Primarily, the efficacy of this approach has been proven in bench-top experiments, but must be confirmed for the case of strained aluminum that creates new un-oxidized surface during the forming event.

4. Conclusions

1. The tribological performance of anodized AA5083 sheet is significantly better than that of aluminum sheet covered with boron nitride (BN) lubricant alone when sliding against an AISI P20 steel surface at 450°C.
2. Oxide layers of 20 and 10 μm thick on aluminum extended the failure time by 7 to 8 times over that of the "classically" BN-lubricated sheet. For the anodized aluminum, there were no indications of aluminum having been transferred to the steel specimen.
3. Anodized aluminum sheet covered by a thin BN layer performed even better than the oxidized-only sheets, and had failure times extended by 11 to 15 times that of the BN-lubricated aluminum sheet without aluminum becoming welded to the tool.
4. A very thin oxide layer (~3.9μm), covered with a very thin BN layer (5.5μm) showed an endurance time that was 8 times longer than that of bare aluminum with a much thicker BN layer (9.9μm). This result suggests that even lower applied oxide and BN thicknesses may benefit QPF or warm forming processes. The effectiveness of very thin oxide layers suggests an opportunity to implement a relatively low cost commercial process.
5. These results must be verified with QPF production trials to assess the impact on forming behavior and on the quality of formed panels. Cost savings on BN lubricant can also be expected, which can be assessed against the cost of anodizing. In total, the cost of anodization must not exceed that of BN application plus tool repolishing plus panel metalfinishing, all of which are required in the current production process.

REFERENCES

[1] MORALES, A.T.; KRAJEWSKI, P. E.: "Tribological Issues During Quick Plastic Forming", GM R&D Research Report MPL-399, November 11, 2004.

[2] MORALES, A.T.: "Experience with CrC/NiCr Coated QPF Tools During Production Of Malibu Maxx Liftgate Outer Panels, GM R&D Research Report MPL-417, February 2, 2005.

[3] HANNA, M. D.; SCHROTH J.G.: "Optimization of the Nitrocarburizing Process for Surface Treatment of Tools for High-Temperature Aluminum Forming," GM R&D Research Report, MPL–481, December 4, 2005.

[4] HANNA, M. D.: "Friction and Adhesion Characteristics of Nitrocarcurized P20 Tool Steel During High Temperature Aluminum Forming: Tribological Simulation", GM R&D Research Report MPL-487, January 11, 2006.

[5] MORALES, A.T.: "Initial Evaluation of Alternative Lubricants for QPF", GM R&D Research Report MPL-499, March 2, 2006.

[6] HANNA, M. D.; QUINTANA, A.: "A New Test Method for Evaluation of Friction and Adhesion between Aluminum Sheet and Steel Tool at High Temperature", GM R&D Research Report MPL-435, CES-181, January 14, 2004.

[7] FRANETOVIC V.; HANNA, M. D.: "Effect of Boron Nitride Thickness and P20 Tool Steel Surface Condition on Tribological Behavior During Sliding Against Al 5083 Sheet at High Temperature," GM R&D Research Report, MPL-549, January 5, 2007.

[8] MORALES, A.T.; FRANETOVIC, V.: "Adhesion and Friction Behavior of Henkel Lubricants on Al5083/P20 Steel Sliding Surfaces at High Temperature," GM R&D Research Report, to be published.

[9] MORALES, A.T.; FRANETOVIC, V.: "Effect of Humidity on Lubricant Adhesion and Tribological Behavior of Al5083/P20 Steel Sliding Surfaces at High Temperature", to be published.

[10] Aluminum Anodizers Council, www.anodizing.org/faqs.html.

[11] BRACE, A.W.: "The Technology of Anodizing Aluminum."

[12] SHEASBY, P.G.; PINNER, R.: "The Surface Treatment and Finishing of Aluminum and its Alloys," Finishing Publications Ltd., England 1987.

[13] PLINT AND PARTNERS LIMITED – TE 77: High Frequency Friction Machine Operating Instruction, 2001.

[14] BIKERMAN J.J.: "Adhesion in Friction", Wear, 39 (1976) pp.1-13.

[15] BOWDEN, F.P.; TABOR, D.: "The Friction and Lubrication of Solids," Clarendon Press, Oxford, 1950, p. 90.

[16] HUTCHINGS, I.M.: "Friction and Wear of Engineering Materials," CRC Press, London 1992.

Investigating Polymer-Tool Steel Interfaces to Predict the Work of Adhesion for Demoulding Force Optimisation

Kevin D. DELANEY[1)], David KENNEDY[1)], Giuliano BISSACCO[2)]
1) Dublin Institute of Technology
Department of Mechanical Engineering, Dublin Institute of Technology, Bolton St., Dublin1 **Ireland**
2) Technical University of Denmark
Department of Mechanical Engineering, Technical University of Denmark, Kgs. Lyngby, **Denmark**
Kevin.delaney@dit.ie

Keywords
Polymer friction,
Work of adhesion,
Demoulding force prediction.

Ključne riječi
Trenje polimera,
Radnja adhezije,
Predviđanje sile otvaranja.

Original scientific article
Demoulding parts from replication tools is a critical stage of replication processes such as injection moulding and hot embossing. This challenge increases as part size decreases since components and associated replication cores become more fragile and liable to damage. Understanding interfacial characteristics between a polymer and the tool surface is critical to optimise the demoulding of such parts from replication tools. The strength of the polymer-tool interaction is characterised by the adhesion energy and is specific for a particular polymer-tool pair. It's magnitude depends upon the tool material, the chemical structure of the polymer, the processing conditions and the surface roughness.
Interfacial characteristics of a variety of polymer-tool steel surfaces are being studied by measuring contact angles of polymer droplets on the surfaces to predict the work of adhesion. The experimental set-up, selection of test parameters and main challenges faced to date are described and preliminary experimental results presented. In addition a description of how these results may be used to predict the force needed to demould parts from replication tools is discussed.

Istraživanje sučelja polimer - alatni čelika zbog predviđanja adhezijskog rada s svrhom optimiziranja sile otvaranja kalupa
Izvorni znanstveni rad
Odvajanje dijelova iz višekratnih kalupa je kritična radnja procesa kao što su injekcijsko brizganje u kalup i vruće utiskivanje. Ovaj se problem povećava kako se proizvod dimenzionalno smanjuje, te pripadajuće jezgre postaju više lomljive i podložnije nastajanju oštećenja. Razumijevanje interakcija površina polimera i alata je najbitnije za optimiranje vađenja proizvoda iz višekratnih kalupa. Čvrstoća veze između polimera i alata karakterizirana je energijom prijanjanja i specifična je za određeni par polimera-alat. Veličina energije prijanjanja ovisi o materijalu alata, kemijskoj strukturi polimera, proizvodnim uvjetima i površinskoj hrapavosti.
Mjerenjem kutova kontakta polimernih kapljica na površinama alatnog čelika proučavane su karakteristike interakcija površina različitih kombinacija polimer - alatni čelik sa svrhom predviđanja sile prijanjanja.
Opisane su postavke eksperimenta kao i glavna problematika do danas, te su isto tako prikazani i rezultati pokusa. U nastavku provedena je diskusija o mogućnosti korištenja dobivenih rezultata za predviđanje sile odvajanja dijelova iz višekratnih kalupa..

1. Introduction

Demoulding, or ejection, of parts from the tool is a critical stage of replication processes such as injection moulding and hot embossing. As the size of the component being replicated is reduced both the parts themselves and associated tooling becomes more prone to damage due to their reduced strength. Forces preventing demoulding of parts are generally a combination of differential shrinkage of the part and tool, adhesion and/or the possible formation of a suction force.

Friction is generally considered as the result of adhesion and/or deformation. Experimental results have shown that at higher tool surface roughness deformation dominates. This deformation can be elastic, with no permanent damage to the part or it can be plastic where there will be permanent damage to the replicated parts after demoulding, visible in the form of ploughing or scoring of the part surface. At lower tool surface roughness the adhesion component of friction dominates. The most important adhesion mechanisms have been categorized as consisting of thermodynamic/chemical adhesion, electrical / electrostatic adhesion and capillary attraction. However as reported by Ebnesajjad [1] it is difficult to assign adhesive bonding to a specific mechanism.

Understanding interfacial characteristics between the polymer and tool surface is critical to optimise part demoulding. This paper focuses on the adhesion component of friction and how parameters relevant to quantifying it can be determined experimentally using the method of contact angle measurements.

Symbols/Oznake

Θ	- Contact angle, - Kut dodira	γ_{SV}	- Surface tension of the solid in equilibrium with its saturated vapour - Površinska napetost krutnine u ravnoteži s zasićenom parom
γ_{LV}	- Surface tension of the liquid in equilibrium with its saturated vapour - Površinska napetost tekućine u ravnoteži s zasićenom parom	γ_{SL}	- Interfacial tension between the solid and the liquid - Površinska napetost između krute i tekuće faze

2. Using contact angles to quantify adhesion

The objective of this experiment is to quantify the wettability between a solid substrate and a viscous liquid, in this case between simulated tool surfaces and a polymer using the method of contact angles. Quantitatively a contact angle, θ , is the interior angle formed by the substrate being used and a tangent to the drop interface at the apparent intersection of the three interfaces. The tangent line and contact angle are shown schematically in Figure 1.

A static contact angle on a flat surface is commonly defined by Young's equation, which is essentially a force balance. This equation includes the interfacial surface tensions between solid and liquid, solid and vapour and liquid and vapour and is given by:

$$\gamma_{LV}\cos\theta = \gamma_{SV} - \gamma_{SL} \quad (1)$$

where the interfacial tension between the solid and the liquid is given by γ_{SL}, while the surface tension of the liquid and solid in equilibrium with their saturated vapour are given by γ_{LV} and γ_{SV} respectively.

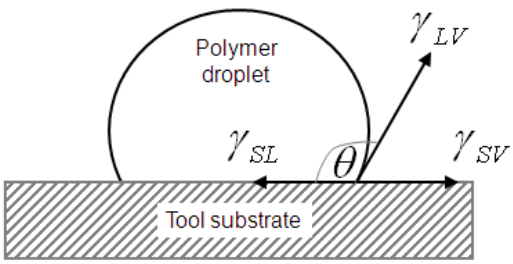

Figure 1. A polymer droplet on a tool substrate at equilibrium

Slika 1. Uravnotežena kapljica polimera na uzorku alata

The two principle methods to measure contact angles are the Wilhelmy plate method which is a specific form of tensiometry and goniometry which uses a profile image of a drop to find contact angles. Associated software analyses the profile image and the contact angle is returned. Profile images can also be recorded for additional analysis.

Anastaiadis and Hatzikirialos [2] measured interfacial characteristics for a series of polymer/wall interfaces using the sessile drop method to calculate the work of adhesion. Part of a broader project relating polymer/wall interface adhesion to the onset of wall slip, the stainless steel substrates tested included both a clean one and others that had been modified though the application of two different fluoropolymers to alter their surface energy. The measured contact angles of polymer droplets and the polymer surface tensions were used to calculate the work of adhesion of the various interfaces. The critical shear stress at which slip was initiated was found to scale linearly with the work of adhesion.

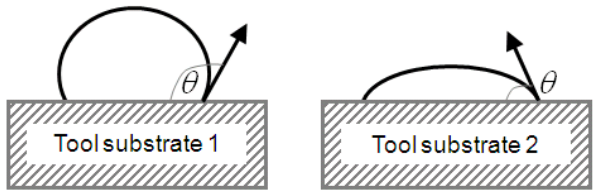

Figure 2. How polymer droplet contact angles vary with replication tool surface

Slika 3. Promjena kontaktnog kuta kapljice na površini alata

Navabpour et al [3] performed experimental work to quantify adhesion between low density polyethylene (LDPE) and various non-stick coatings. Granules of LDPE were placed on the substrate to be evaluated inside the heated oven and positioned in front of a microscope. As the LDPE granules melted drops formed. After reaching steady state the angle between the drop and the surface was recorded as the LDPE contact angle. The images presented in Figure 4 show a clear difference between coated and uncoated substrates.

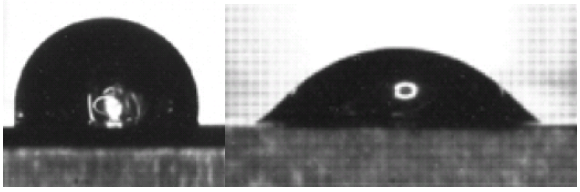

Figure 4. Contact angle variation between coated and uncoated substrates (Navabpour et al)

Slika 5. Promjena kontaktnog kuta kod prekrivene i neprekrivene površine uzorka (Navabpour et al)

3. Experimental set-up

An apparatus manufactured by Dataphysics, [4] and typically used to measure contact angles of liquids on surfaces at room temperature, forms the basis of the experimental set-up. Key elements of the apparatus include a microscope, a backlight, a specimen table and a computer monitor as shown in Figure 6. For this particular application the apparatus was modified with a number of attachments. Specifically a thermal chamber with an integrated Peltier module surrounds the test-piece and the dosing needle is replaced by a heated needle. The heated needle is used to store the polymer prior to dosing onto the test pieces. The surfaces to be tested are inserted into the temperature chamber. Independent temperature control of the heated needle and temperature chambers is possible so that behaviour of the hot polymer as it meets a cooler tool surface can be evaluated.

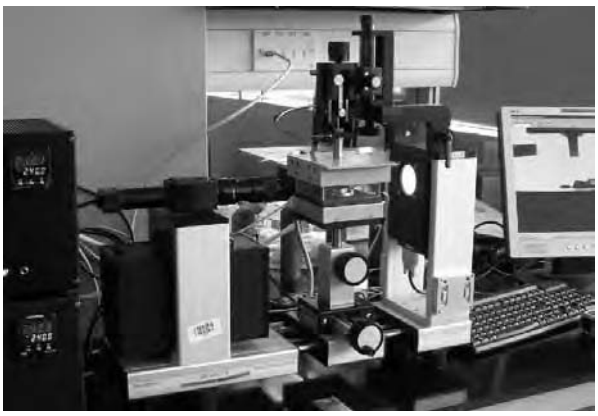

Figure 6. Overview of the complete test apparatus for measuring contact angles

Slika 7. Uređaj za mjerenje kontaktnih kuteva

Figure 8 shows a close-up of the test apparatus. The thermal chamber is in the centre of the image with the microscope and lighting elements of the device on the left and right hand side respectively. The heated needle and dosing system protrude into the thermal chamber from the top of the thermal chamber.

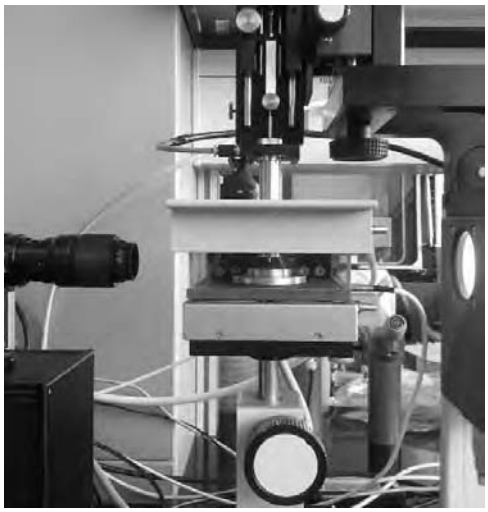

Figure 8. Close-up of the test apparatus

Slika 9. Povećana slika uređaja

4. Test parameters and procedure

4.1. Test parameters

Adhesion between the polymer and substrate depends upon the tool material, the chemical structure of the polymer, the processing conditions and tool surface roughness. The initial experimental studies will focus on a specific polymer; Poly methyl meth acrylate (PMMA). Three different tool surfaces generated from a single supply of steel commonly used for injection moulds are used for initial trials. These surfaces were generated using a polishing process to create a mirror finish. Two of the three surfaces were then "roughened" to produce the target surface roughness levels.

Surface generation through polishing was specifically selected so the resultant surfaces would have an isotropic surface profile and not be influenced by test orientation. After surface generation characterisation of the surfaces was performed to create surface data which can be used in the development of the demoulding force model. Target surface roughness levels were selected based on experimental work reported by Sasaki et al [5] who showed that an optimal surface roughness exists where the demoulding force for an injection moulded part is at a minimum. Surface roughness levels on both sides of this optimum value were selected.

In addition to three different tool surface roughness values relevant processing parameters, specifically the melting temperature of the polymer and the tool surface temperature, are varied during testing to understand how they affect the contact angles. The specific processing

parameters follow the guidelines of the polymer supplier and are summarised in

Table **1**.

Table 1: List of test parameters
Tablica 2: Popis parametara pokusa

Parameter	Units	Low	Mid	High
Tool surface roughness	µm	0.0261	0.0362	0.166
Polymer melt temperature	°C	210	250	290
Tool surface temperature	°C	50	70	90

4.2. Test procedure

An overview of the test procedure is:

1) A quantity of polymer granules should be loaded into a container which is then placed in a temperature control chamber and heated to the required polymer melting temperature.
2) A quantity of the polymer should then be drawn into the heated needle which should be set at the polymer melting temperature.
3) The reservoir of polymer is then removed from the temperature control chamber and the test surfaces inserted instead.
4) The temperature of the thermal control chamber should then be reduced to a suitable temperature so that the tool surface can reach the required test temperature.
5) The polymer is then dosed onto the tool surface for measurement as a sessile drop.

The testing phase of this project is ongoing.

5. Discussion and Conclusions

The rationale for the use of contact angle measurements and selection of the test parameters has been presented together with a description of the test apparatus and procedure.

This investigation constitutes an important element of the development of a model for reliable prediction of demoulding forces. It is planned that the model will be suitable for implementation in Finite Element Modelling (FEM) packages to enable the analysis of complex geometrical configurations. An effort towards the development of such a model is ongoing at the authors' institutions.

Acknowledgements

Support of the SFI-funded National Access Programme (under NAP337), particularly Dr Eric Moore of the Tyndall Institute, and the generation of test surfaces by the Technical University of Denmark's Mechanical Engineering Department is acknowledged.

REFERENCES

[1] EBNESAJJAD C. Surface Treatment of Materials for Adhesion Bonding: William Andrew, 2007.

[2] ANASTASIADIS SH, HATZIKIRIAKOS SG. The work of adhesion of polymer/wall interfaces and its association with the onset of wall slip. Journal of Rheology 1998;42:795-812.

[3] NAVABPOUR P, TEER DG, HITT DJ, GILBERT M. Evaluation of non-stick properties of magnetron-sputtered coatings for moulds used for the processing of polymers. Surface and Coatings Technology 2006;201:3802-9.

[4] Dataphysics. Dataphysics, 2011. p. Company website.

[5] SASAKI T, KOGA N, SHIRAI K, KOBAYASHI Y, TOYOSHIMA A. An experimental study on ejection forces of injection moulding. Precision Engineering 2000;24:270 - 3.

SHOT PEENING PROCESS

Marco Wildhagen

Predavanje - *Presentation*

Cijelo predavanje nalazi se na priloženom CD-u.

The whole presentation is on the attached CD.

Prediction of Mechanical Properties Distribution in Quenched and Tempered Steel Specimen

Božo SMOLJAN, Dario ILJKIĆ and Hrvoje NOVAK
Department of Materials Science and Engineering, Faculty of Engineering, University of Rijeka (Zavod za materijale, Tehnički fakultet, Sveučilište u Rijeci), Vukovarska 58, HR-51000 Rijeka, Croatia
smoljan@riteh.hr

Original scientific paper

Abstract: The mathematical model and method of computer simulation for the prediction of mechanical properties of quenched and tempered steel was developed. Numerical modelling of hardness distribution in as-quenched steel components was performed based on chemical composition of steel as well as based on experimentally results of *Jominy* test. Hardness of quenched and tempered steel was expressed as function of maximal hardness of actual steel and representatives of chemical diffusivity of steel according to the time and temperature of tempering. After that, distribution of other relevant mechanical properties was found out based on predicted as-quenched and tempered hardness of steel. Experimental investigation was performed on high-hardenability steel for tools and dies. The established procedure for estimation of quenched and tempered properties of steel was applied in computer simulation of mechanical properties of quenched and tempered steel workpiece.
The time of cooling at workpiece points was predicted by numerical simulation using the finite volume method. Since the critical cooling rate of martensite transformation of high-hardenability steels is less then maximal cooling rate of *Jominy* specimen the application of the original *Jominy* test in computer simulation is not suitable. Modified *Jominy* test was designed for hardenability prediction of high-hardenability steels. The performances of investigated, modified *Jominy* test have been estimated by comparison of cooling curves of modified *Jominy* specimen and cylindrical one cooled in different quenchants. Yield strength and fracture toughness distributions were estimated using the *Hahn-Rosenfield* approach. Fatigue resistance was estimated based on predicted microstructure and hardness.

Keywords
Quenching
Computer simulation
High-hardenability steels

***Procjena raspodjele mehaničkih svojstava u poboljšanom čeličnom uzorku**

Izvornoznanstveni članak

Sažetak: U radu je razvijen matematički model i metoda računalne simulacije predviđanja mehaničkih svojstava poboljšanog čelika. Numeričko modeliranje raspodjele tvrdoće u kaljenim čeličnim komponentama provedeno je na temelju kemijskog sastava čelika kao i na temelju eksperimentalnih rezultata *Jominy*jevog pokusa. Tvrdoća poboljšanog čelika izražena je kao funkcija maksimalne tvrdoće konkretnog čelika i faktora kemijske difuznosti čelika sukladno vremenu i temperaturi popuštanja. Raspodjela ostalih, relevantnih mehaničkih svojstava dobivena je na temelju predviđene tvrdoće nakon kaljenja, odnosno nakon poboljšanja. Eksperimentalna istraživanja izvedena su na visoko prokaljivom alatnom čeliku. Postavljena procedura procjene svojstava poboljšanog čelika primijenjena je u računalnoj simulaciji mehaničkih svojstava poboljšanog čeličnog izratka.
Vremena ohlađivanja u točkama izratka predviđena su računalnom simulacijom koristeći metodu konačnih volumena. Kako je kritična brzina ohlađivanja za martenzitnu prtvorbu visoko prokaljivih čelika manja od maksimalne brzine ohlađivanja *Jominy*jevog uzorka, primjena originalnog *Jominy*jevog pokusa u računalnoj simulaciji nije podobna. Stoga je za procjenu prokaljivosti visoko prokaljivih čelika konstruiran modificirani *Jominy*jev pokus. Primjenjivost modificiranog *Jominy*jevog pokusa procijenjena je usporedbom krivulja ohlađivanja modificiranog *Jominy*jevog uzorka s krivuljama ohlađivanja cilindričnih uzoraka ohlađivanih u različitim sredstvima za ohlađivanje. Raspodjela granice razvlačenja i lomne žilavosti procijenjena je sukladno *Hahn-Rosenfield*ovom pristupu. Dinamička izdržljivost procijenjena je na temelju procijenjene mikrostrukture i tvrdoće.

Ključne riječi
Kaljenje
Računalna simulacija
Visoko prokaljivi čelici

Primljeno (Received): 20xx-xx-xx
Prihvaćeno (Accepted): 20xx-xx-xx

Symbols/Oznake

A	- material constant - konstanta materijala	t	- time, s - vrijeme
B	- material constant - konstanta materijala	$t_{8/5}$	- cooling time from 800 to 500 °C, s - vrijeme ohlađivanja od 800 do 500 °C
c	- specific heat capacity, $Jkg^{-1}K^{-1}$ - specifični toplinski kapacitet	T	- temperature, K - temperatura
d	- grain size, mm - promjer zrna	T_a	- temperature of austenitization, K - temperatura austenitizacije
F	- boundary area, m^2 - granična površina	T_f	- quenchant temperature, K - temperatura medija za kaljenje
H	- H value - *Grossman*ov intenzitet gašenja	T_s	- surface temperature, K - temperatura površine
$HRC_{quenched}$	- as-quenched hardness HRC - tvrdoća HRC nakon kaljenja	T_{tr}	- reference value of tempering temperature, K - referentna temperature popuštanja
$HRC_{tempered}$	- quenched and tempered hardness HRC - tvrdoća HRC nakon kaljenja i popuštanja	W	- thermal resistances, KW^{-1} - toplinski otpor
HRC_{min}	- material constant - konstanta materijala	ΔV	- volume of the control volume, m^3 - volumen kontrolnog volumena
K	- factor between as-quenched and tempered hardness HRC - faktor odnosa tvrdoće HRC nakon kaljenja i nakon popuštanja		**Greek letters/Grčka slova**
ΔK_{th}	- fatigue crack initiation threshold, $MPam^{1/2}$ - prag propagacije pukotine umaranja,	α	- heat transfer coefficient, $Wm^{-2}K^{-1}$ - koeficijent prijelaza topline
l	- distance, m - udaljenost	α_{Ts}	- heat transfer coefficient at the boundary temperature, $Wm^{-2}K^{-1}$ - koeficijent prijelaza topline granične temperature
n	- parameter depended on ferrite volume - parametar ovisan o volumnom udjelu ferita	λ	- coefficient of heat conductivity, $Wm^{-1}K^{-1}$ - koeficijent vodljivosti topline
n_1	- material constant - konstanta materijala	φ	- angle - kut
R_e	- yield strength, MPa - granica razvlačenja	ρ	- density, kgm^{-3} - gustoća

1. Introduction

Mathematical modelling of hardness distribution in quenched steel specimens is consisted of numerical simulation of specimen cooling, numerical simulation of specimen hardening and respectively prediction of mechanical properties [1].

For the simulation of specimen cooling which is thermodynamical problem, it is necessary to establish the appropriate algorithm which describes cooling process, and it is necessary to accept appropriate input data.

The accuracy of mathematical modelling of quenching directly depends on the correctness of input variables applied in the model. Experimentally acquired heat transfer data have advantages in specific conditions but numerical simulation of quenching with the application of calibrated heat transfer data is a generalized way of simulation and is largely applicable. Calibrated data are not as precise as experimentally acquired data but they are useful for large spectra of specimen dimensions [2].

Structure composition can be defined by kinetic equations of prior structure transformation or can be estimated by using CCT diagrams [3]. Structure

transformation and hardness distribution can be also estimated based on time, relevant to structure transformation [4]. Mechanical properties of quenched steel can be estimated according to prediction of structure composition.

The objective of design of quenching is to estimate the results of quenching, concerning mostly with the estimation of mechanical properties.

Computer simulation of quenching includes several different analyses.

Research of numerical simulation of hardness and microstructure distribution in quenched steel specimen is one of the high priority researches in simulation of phenomenon of steel quenching. The investigation of steel quenching suggests that choosing a proper representative of the cooling phenomenon, which is relevant for structure transformation, is one of the most important factors for a good simulation of hardening.

One of the most common methods of computer prediction of quenching results is based on the chemical composition of steel and on the sample dimensions [5, 6]. Moreover, prediction of microstructure composition usually is based on semiempirical methods derived from kinetic equations of microstructure transformation [7, 8]. Then, the predicted microstructure composition can be used to predict mechanical properties, mostly focused on hardness.

Beside these methods, mathematical model of steel quenching can be based on calculated characteristic time of cooling. Usually, relevant time for quenching results is the cooling time from 800 to 500 °C, $t_{8/5}$ [4, 9, 10].

To accept the assumption that the equal cooling time $t_{8/5}$ of several samples indicates their equal hardness, the history of cooling of these samples must be the same or similar, i.e. their cooling curves must be similar. By involving the cooling time $t_{8/5}$ in the mathematical model of steel hardening, the *Jominy* test results could be involved in the model.

Since the critical cooling rate of martensite transformation of high-hardenability steels is less then minimal cooling rate of *Jominy* specimen the application of the original *Jominy* test is not acceptable. Numerical modelling of the quenched hardness of high-hardenability steel could be performed based on relevant time of cooling by involving the results of modified *Jominy* test [11, 12].

2. Prediction of the cooling time $t_{8/5}$

The temperature field change in an isotropic rigid body with coefficient of heat conductivity, λ/Wm^{-1}K^{-1}, density, ρ/kgm^{-3} and specific heat capacity, c/Jkg^{-1}K^{-1}, without heat sources can be described by Fourier's law of heat conduction:

$$\frac{\delta(c\rho T)}{\delta t} = div\lambda\, gradT \quad . \tag{1}$$

Characteristic initial condition is:

$$-\lambda \left.\frac{\delta T}{\delta n}\right|_s = \alpha\left(T_s - T_f\right) , \tag{2}$$

where T_s/K is surface temperature, T_f/K is quenchant temperature, α/Wm^{-2}K^{-1} is heat transfer coefficient. Solution of Equation (1), i.e., calculation of cooling time at specimen points can be done by using the finite volume method [13, 14].

Transient temperature field in an isotropic rigid body can be defined by 2-D finite volume formulation (Figure 1):

$$T_{ij}^1\left(\sum_{m=1}^{2} b_{\mathrm{I}(i+n)j} + \sum_{m=1}^{2} b_{\mathrm{J}\,i(j+n)} + b_{ij}\right) = \\ = \sum_{m=1}^{2}\left(b_{\mathrm{I}(i+n)j}T_{(i+k)j}^1 + b_{\mathrm{J}\,i(j+n)}T_{i(j+k)}^1\right) + b_{ij}T_{ij}^0 , \tag{3}$$

$$i = 1, 2, ..., i_{\max}, \quad j = 1, 2, ..., j_{\max},$$

$$n = 2 - m, \quad k = 3 - 2m$$

where T_{ij}^0 /K is the temperature in the beginning of time step Δt/s, T_{ij}^1 /K is the temperature in the end of time step Δt/s, $b_{ij} = (\rho_{ij}c_{ij}\Delta V_{ij})/\Delta t$, ΔV_{ij}/m^3 is the volume of the control volume, $b_{\mathrm{I}(i+n)j} = W_{\mathrm{I}(i+n)j}^{-1}$ and $b_{\mathrm{J}i(j+n)} = W_{\mathrm{J}i(j+n)}^{-1}$. Variables $W_{\mathrm{I}(i+n)j}$ and $W_{\mathrm{J}i(j+n)}$ are the thermal resistances between ij and $(i+k)j$ volume and between ij and $i(j+k)$ volume, respectively.

$$W_{\mathrm{I}(i+n)j} = \frac{1}{\Delta F_{\mathrm{I}(i+n)j}}\left(\frac{l_{\mathrm{I}ijm}}{\lambda_{ij}} + \frac{l_{\mathrm{I}(i+n)j(3-m)}}{\lambda_{(i+k)j}}\right) , \tag{4}$$

$$W_{\mathrm{J}\,i(j+n)} = \frac{1}{\Delta F_{Ji(j+n)}}\left(\frac{l_{\mathrm{J}\,ijm}}{\lambda_{ij}} + \frac{l_{\mathrm{J}\,i(j+n)(3-m)}}{\lambda_{i(j+k)}}\right) . \tag{5}$$

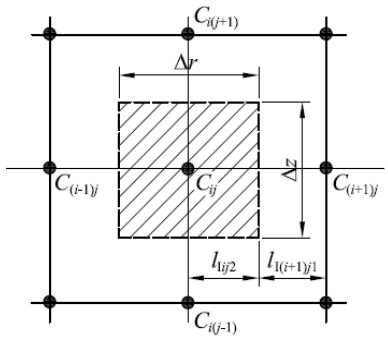

Figure 1. Control volume

Slika 1. Kontrolni volumen

Thermal resistances for boundary volume are:

$$W_{\mathrm{I}(i+n)j} = \frac{1}{\Delta F_{\mathrm{I}(i+n)j}}\left(\frac{l_{\mathrm{I}\,ij}}{\lambda_{ij}} + \frac{1}{\alpha_{\mathrm{Ts\,I}(i+n)j}\cos\varphi_{\mathrm{I}(i+n)j}}\right) , \tag{6}$$

$$W_{\mathrm{J}\,i(j+n)} = \frac{1}{\Delta F_{\mathrm{J}\,i(j+n)}}\left(\frac{l_{\mathrm{J}\,ij}}{\lambda_{ij}} + \frac{1}{\alpha_{\mathrm{TsJ}\,i(j+n)}\cos\varphi_{\mathrm{J}\,i(j+n)}}\right) , \tag{7}$$

where: α_{Ts}/Wm^{-2}K^{-1} is the heat transfer coefficient at the boundary temperature, T_s and cosφ is direction cosines of heat flux.

Discretization system has N linear algebraic equations with N unknown temperatures of control volumes, where N is total number of control volumes. Time of cooling from T_a to specific temperature in particular point is determined as sum of time steps, and in this way, the diagram of cooling curve in every grid-point of a specimen is possible to found out.

$$t_M = \sum_{m=1}^{M} \Delta t_m \quad . \tag{8}$$

3. Simulation of quenched workpiece hardness based on the cooling time $t_{8/5}$

One of the most important factors for efficient simulation of hardening is the proper selection and use of representative cooling phenomena that is relevant for microstructure transformation.

The structure transformations and hardness distribution can be estimated based on time, relevant for structure transformation. Usually, if the cooling time $t_{8/5}$ is equal for two different specimens, i.e. quenched workpiece and *Jominy* specimen, the hardness of these two specimens could be equal to each other. In the developed computer simulation of hardenability of quenched workpiece, the hardness at different workpiece points is estimated by the conversion of the cooling time $t_{8/5}$ to the hardness. This conversion is provided by the relation between the cooling time $t_{8/5}$ and distance from the quenched end of the *Jominy* specimen (Figure 2) [4, 15].

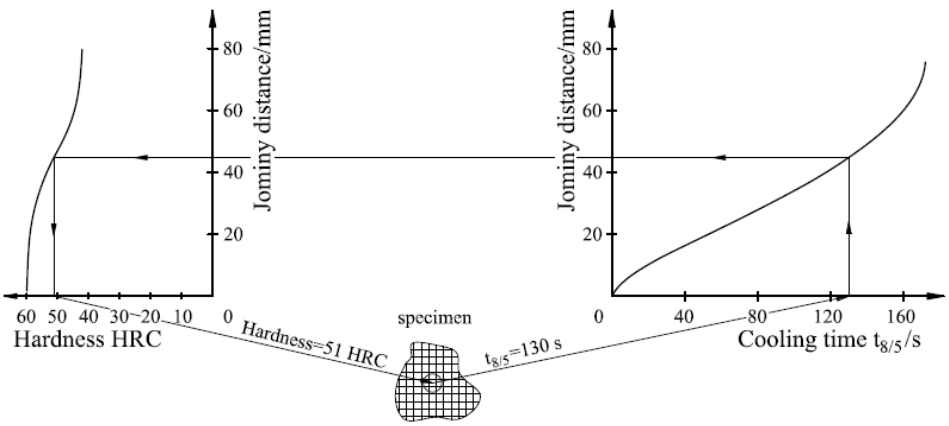

Figure 2. Conversion of the cooling time $t_{8/5}$ to the hardness

Slika 2. Pretvaranje vremena ohlađivanja $t_{8/5}$ u tvrdoću

4. Simulation of quenched workpiece hardness of high-hardenability steel

For prediction of hardness of quenched workpiece, it is necessary that the cooling times $t_{8/5}$ for austenite decomposition in martensite, bainite, pearlite or ferrite of investigated workpiece and the cooling times $t_{8/5}$ of *Jominy* specimen are in the same range. Because of high hardenability, the cooling times $t_{8/5}$ for austenite decomposition of most steels for tools and dies are not comparable with the cooling times $t_{8/5}$ of *Jominy* specimen and there are limits in application of original *Jominy* test in computer simulation of quenching of this kind of steels [16].

Figure 3 qualitatively represents austenite decomposition of some steels for tools and dies i.e. high-hardenability steels and it is visible that the cooling times $t_{8/5}$ of austenite decomposition are ranged from 200 to 1000 s.

The cooling time $t_{8/5}$ for bainite transformation of steels X38CrMoV51 and X45NiCrMo4 is greater than 1400 s. The cooling time $t_{8/5}$ for pearlite transformation of steel X45NiCrMo4 is greater than 45000 s. For other steels start of bainite and pearlite transformation in TTT-diagram matches the cooling times $t_{8/5}$ in interval between 200 and 1000 s.

Original *Jominy* test gives the cooling times $t_{8/5}$ up to a maximum of 200 s (Figure 2), and it is obvious that original *Jominy* test is not suitable for prediction of hardenability of steels for tools and dies.

To achieve times of cooling $t_{8/5}$ longer than 200 s, the modified *Jominy* test was designed for high-hardenability steels, i.e. steels for tools and dies. The assembly of modified *Jominy* test is shown in Figure 4.

JMC® specimen is end-quenched during the test. Other pieces of assembly are slowly cooled. Figure 5 shows the cooling times $t_{8/5}$ at the depth of 0.8 mm from the surface of the JMC® specimen at different distances

from the quenched end of JMC® specimen. Maximal cooling time $t_{8/5}$ of JMC® specimen is nearly ten times longer than the maximal time given by *Jominy* test.

Because of the long time of cooling of JMC® specimen (Figure 5) it is possible by using the JMC® specimen to predict hardenability of high-hardenability tool steels. The JMC® specimen can be used in computer simulation of quenching of high-hardenability steels, in similar manner as *Jominy* specimen in computer simulation of quenching of low alloyed steels.

In Figure 6a are shown hardenabilty curves of steels X40Cr13, X210Cr12, 60WCrV7 and 60WCrV7 made by JMC® test and in Figure 6b are shown hardenabilty curves of some kind of steels made by *Jominy* test.

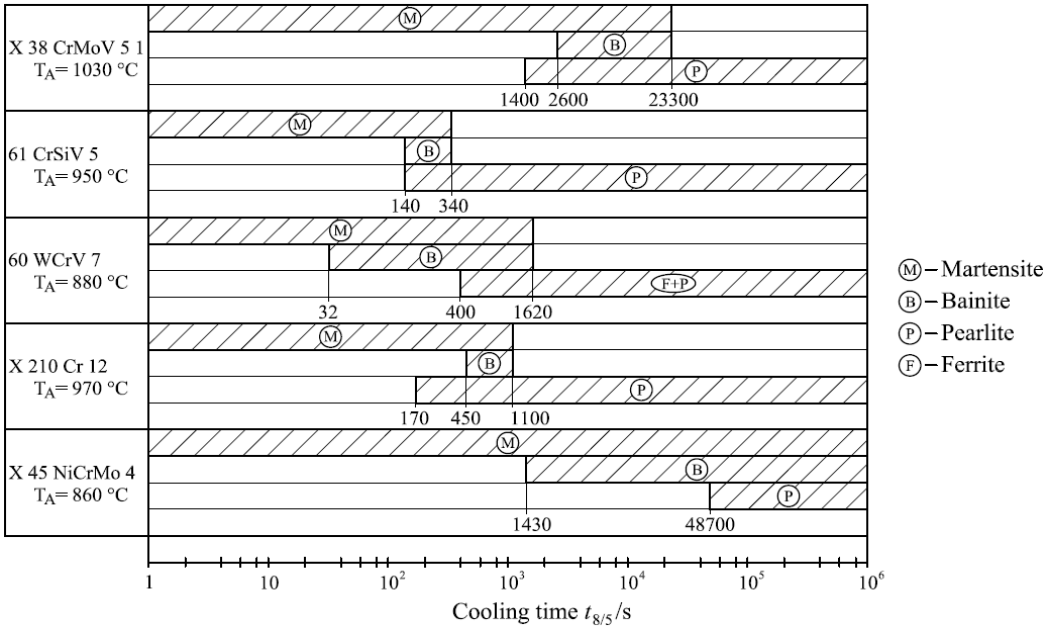

Figure 3. Diagram of cooling times $t_{8/5}$ of several different steels for tools and dies

Slika 3. Dijagram vremena ohlađivanja $t_{8/5}$ za nekoliko alatnih čelika

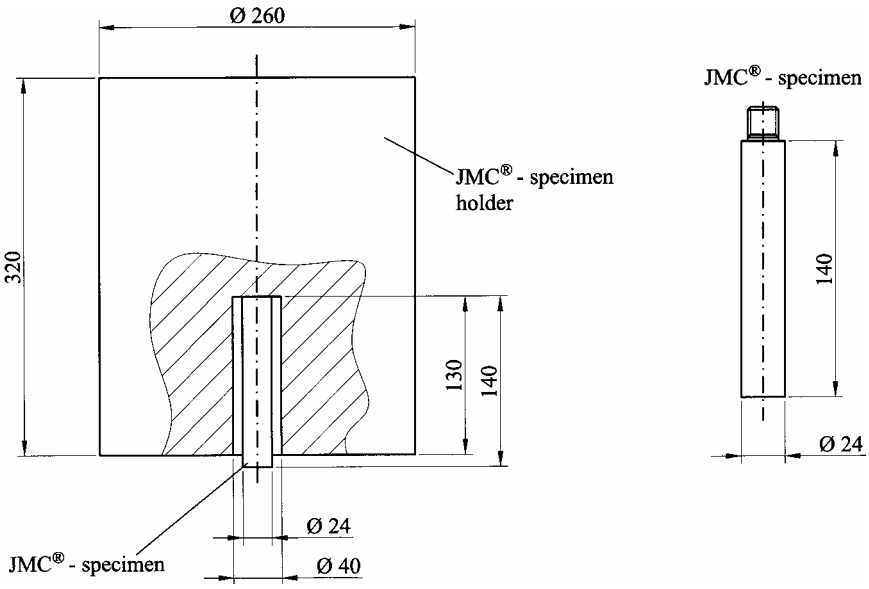

Figure 4. JMC® specimen and JMC® specimen holder

Slika 4. JMC® uzorak i držač JMC® uzorka

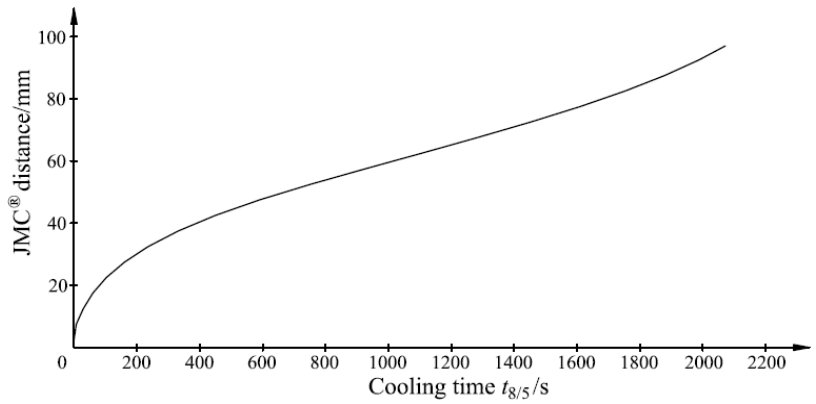

Figure 5. Distance from the quenched end of JMC® specimen vs. cooling time $t_{8/5}$

Slika 5. Udaljenost od gašenog čela JMC® uzoraka naspram vremena ohlađivanja $t_{8/5}$

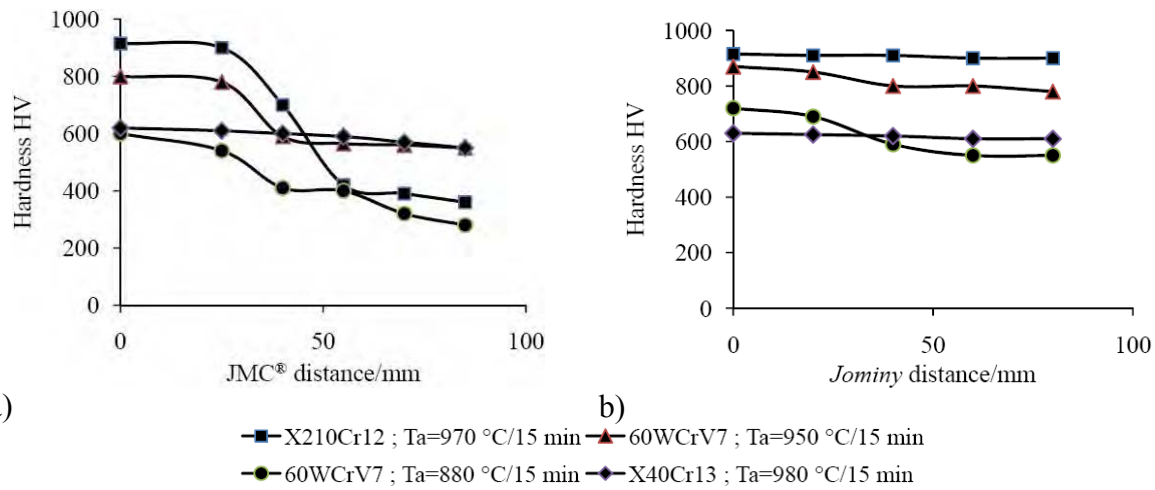

Figure 6. Hardenabilty curves of different steels, a) JMC® test, b) *Jominy* test

Slika 6. Krivulje prokaljivosti različitih čelika, a) JMC® pokus, b) *Jominy*jev pokus

5. Prediction of microstructure and mechanical properties of quenched and tempered steel component

The reference value of hardness of quenched and tempered state can be estimated based on as-quenched hardness, $HRC_{quenched}$, by [17, 18]:

$$HRC_{tempered} = \frac{HRC_{quenched} - HRC_{min}}{K} + HRC_{min}, \quad (9)$$

where HRC_{min} is the material constant. K is the factor between as-quenched and tempered hardness. Factor K can be expressed by:

$$K = \exp\left[AB\left(\frac{T_{tr}}{a}\right)^{n_1} \right], \quad (10)$$

where T_{tr}/K is the reference value of tempering temperature, while A, B, a and n_1 are the material constants, that are established by regression analysis of hardness of quenched and tempered steel. The algorithm for prediction of hardness of tempered and quenched steel given by Equation (9) and Equation (10) was established by regression analysis.

Microstructure composition of as-quenched steel depends on the chemical composition, severity of cooling, austenitizing temperature and steel history.

The austenite decomposition results can be estimated based on time, relevant for structure transformation. The characteristic cooling time relevant for structure transformation for most structural steels, is the time $t_{8/5}$. If other heat treatment parameters are constant, the austenite decomposition results in some location of a cooled specimen will depend only on the time $t_{8/5}$. It could be written for *Jominy* specimen that phase hardness depends on chemical composition and cooling rate parameter that corresponds to actual distance d of *Jominy* specimen quenched end. It was adopted that cooling rate parameter is equal to $\log(t_{8/5})$ [19].

Mechanical properties as are hardness, ultimate tensile stress, yield strength, fracture toughness of quenched

steel or quenched and tempered steel directly depends on degree of quenched steel hardening [20-22].

In comparison with yield strength the fatigue resistance properties additionally depend on microstructure, especially it depend on ferrite phase composition. The effect of tempering and microstructure composition is relatively small for region 2 growth rates, but the effect may be large near the threshold in region 1 growth rates. Continuous ferrite phase reduces fatigue crack growth resistance near the threshold. With segregation of ferrite phase in form of continuous network substantial reducing in fatigue crack growth resistance near the threshold is possible.

It could be find out that microstructure effect of ferrite presence in quenched and tempered microstructure on fatigue crack initiation threshold is equal to [23]:

$$\Delta K_{\mathrm{th}} = f(n, R_{\mathrm{e}}, d^{1/2}) \ , \qquad (11)$$

where n is the parameter which depends on ferrite volume. By experimental work it was found out that fatigue crack initiation threshold is dependent on yield strength and grain size (Figure 7) [24-28].

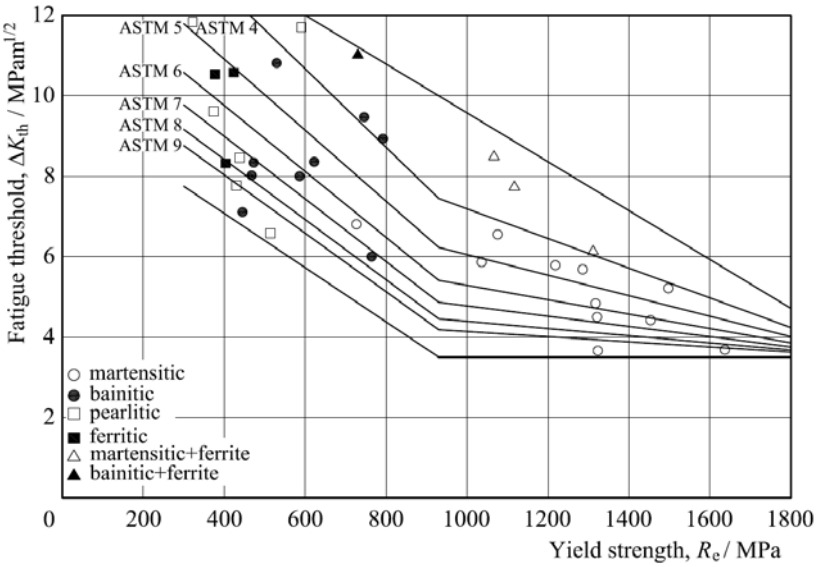

Figure 7. Variation of fatigue crack initiation threshold of steel with yield strength and grain size

Slika 7. Promjena praga propagacije pukotine umaranja čelika u ovisnosti o granici razvlačenja i veličini zrna

6. Application

The established method for prediction of yield strength, fracture toughness and fatigue resistance is applied in design of heat treatment process of the forming die made of steel EN 60WCrV7. Steel EN 60WCrV7 is one of the shock resisting tool steel types with very good toughness and wear resistance in combination with high hardenability. This steel is impact-resistant, tungsten-alloyed cold-work tool steel. In addition, steel EN 60WCrV7 can be used as hot-work tool steel at moderate temperatures.

The chemical composition of investigated steel EN 60WCrV7 is shown in Table 1. Results of the JMC® test of the investigated steel are shown in Table 2.

Table 1. The chemical composition of steel EN 60WCrV7

Tablica 1. Kemijski sastav čelika EN 60WCrV7

Chemical composition/%									
C	Si	Mn	P	S	Cr	Mo	Ni	V	W
0.55	0.94	0.34	0.015	0.012	1.27	0.05	0.12	0.18	2.10

Table 2. JMC® test results of investigated steel EN 60WCrV7

Tablica 2. Rezultati JMC® pokusa istraživanog čelika EN 60WCrV7

JMC® distance/mm	2	4	6	8	10	15	20	25	30	35	40
Hardness HRC	63	63	63	63	62	62	61	60	58	56	55
JMC® distance/mm	45	50	55	60	65	70	75	80	85	90	-
Hardness HRC	53	52	51	51	50	50	50	49	49	49	-

Geometry of the forming die prepared for the heat treating processes is shown in Figure 8.
After heating to 950 °C for 2 hours, forming die was quenched in agitated oil with the severity of quenching H = 0.3. The tempering temperature in process was 500 °C.
Hardness distribution in the quenched and tempered forming die is shown in Figure 9. Critical locations for crack growth are locations 1 and 2 (Figure 8 and Figure 9). The predicted values of microstructure and mechanical properties in critical locations of as-quenched workpiece are given in Table 3. The predicted values of mechanical properties in critical locations of quenched and tempered workpiece are given in Table 4.

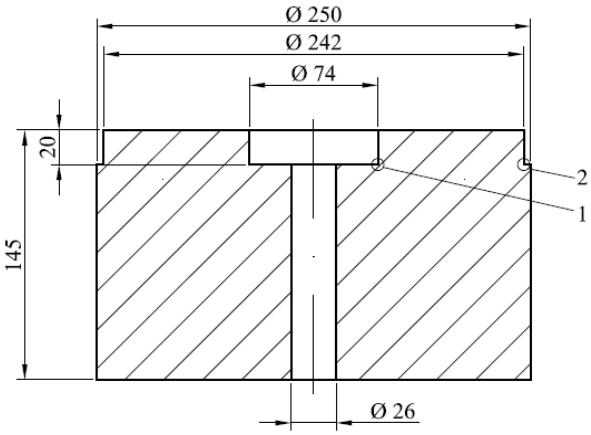

Figure 8. Geometry of the forming die

Slika 8. Geometrija kalupa

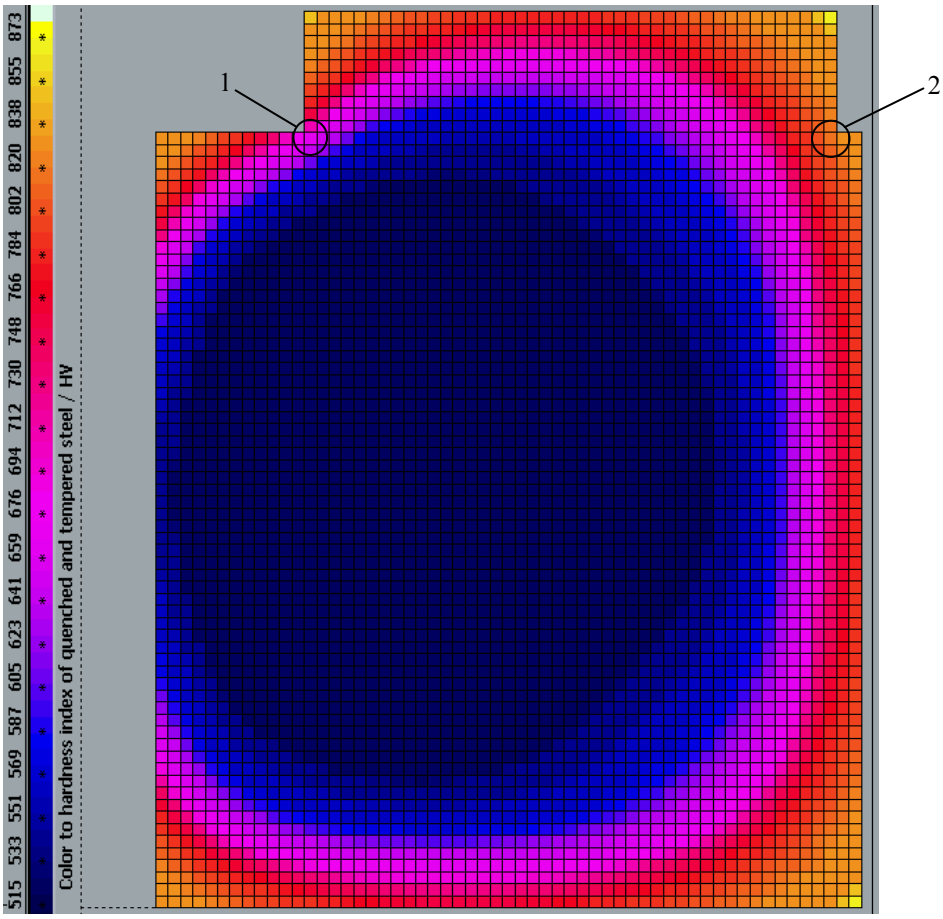

Figure 9. Hardness distribution in quenched and tempered workpiece

Slika 9. Raspodjela tvrdoće u poboljšanom obratku

Table 3. Microstructure and mechanical properties in critical locations of as-quenched workpiece

Tablica 3. Mikrostruktura i mehanička svojstva u kritičnim lokacijama kaljenog obratka

Properties		Critical location in Figure 9	
		1	2
Phase fractions/%	F+P	0	0
	B	1.2	0
	M	98.8	100
Hardness HRC		56	61

Table 4. Mechanical properties in critical locations of quenched and tempered workpiece

Tablica 4. Mehanička svojstva u kritičnim lokacijama poboljšanog obratka

Properties	Critical location in Figure 9	
	1	2
Hardness HV	663	816
Yield strength, R_e/MPa	1897	2382
Fracture toughness, K_{Ic}/MPam$^{1/2}$	40	21
Fatigue threshold, ΔK_{th}/MPam$^{1/2}$	3.8	3.8

7. Conclusion

A mathematical model for prediction of mechanical properties in quenched and tempered steel die was developed. In proposed model material properties and parameters of heat treatment should be taken into account. The computer simulation is based on finite volume method. A developed mathematical model has been applied in computer simulation of a quenched and tempered steel die component.

The as-quenched hardness distribution in the quenched steel die component can be estimated based on calculated time of cooling from 800 to 500 °C, $t_{8/5}$ in workpiece point, and on results of modified *Jominy* test (JMC® test). Hardness of the quenched and tempered workpiece can be predicted based on as-quenched hardness and temperature of tempering. The austenite decomposition results can be estimated based on cooling time $t_{8/5}$, relevant for structure transformation. The prediction of distribution of yield strength, fracture toughness and fatigue crack initiation threshold can be calculated based on steel hardness distribution.

It can be concluded that mechanical properties of quenched and tempered die steel can be successfully calculated by the proposed method.

REFERENCES

[1] SMOLJAN, B.: *Mathematical Modelling of Steel Quenching, 9th International Scientific Conference AMME 2000.* - Proceedings, Gliwice-Sopot-Gdansk, 495 – 498, 2000.

[2] SMOLJAN, B.: *The Calibration of the Mathematical Model of Steel Quenching, 5th World Seminar on Heat Treatment and Surface Engineering* - Proceedings, Isfahan, Eds. M. Salehi, ISSST and IFHT, Vol.1, 709 – 715, 1995.

[3] LIŠČIĆ, B.; TOTTEN, G.: *Controllable Delayed Quenching, International Heat Treating Conference* - Proceedings, Schaumburg, 253 – 262, 1994.

[4] ROSE, A.; WEVER, F.: *Atlas zur Wärmebehandlung der Stähle I*, Verlag Stahleisen, Düsseldorf, 1954.

[5] DOBRZAŃSKI, L. A.; SITEK, W.: *The modelling of hardenability using neural networks*, Journal of Materials Processing Technology (1999), Vol. 92 – 93, 8 – 14

[6] DOBRZANSKI, L. A.; TRZASKA, J.: *Application of Neural Networks to Forecasting the CCT diagrams*, Journal of Materials Processing Technology (2004), Vol. 157-158, 107 – 113

[7] SERAJZADEH, S.: *A Mathematical Model for Prediction of Austenite Phase Transformation*, Materials Letters (2004), Vol. 58, 1597 – 1601

[8] RETI, T.; HORVATH, L.; FELDE, I.: *A Comparative Study of Methods Used for the Prediction of Nonisothermal Austenite Decomposition*, Journal of Materials Engineering and Performance (1997), Vol. 6, 433 – 442

[9] SMOLJAN, B.: *The Calibration of the Heat Conductivity Coefficient in Mathematical Model of Steel Quenching, MicroCAD`99* - Proceedings, Miskolc, 143 – 148, 1999.

[10] MAYNER, P. et al.: *Hardenability Concepts with Application to Steels, Metal. Soc. of AIME*, New York, 1978.

[11] SMOLJAN, B.; ILJKIĆ, D.; SMOKVINA HANZA, S.; TRAVEN, F.: *An analysis of modified Jominy test (JMC® - test)*, Archives of Computational Materials Science and Surface Engineering (2009), Vol. 1, 120 – 124

[12] SMOLJAN, B.; ILJKIĆ, D.; MARETIĆ, M.: *Prediction of Mechanical Properties of Quenched and Tempered Steel Die, 3rd International IFHTSE Conference on Heat Treatment and Surface Engineering of Tools and Dies* - Proceedings, Wels, Austria, 23.-25. March 2011.

[13] SMOLJAN, B.: *Numerical simulation of as-quenched hardness in a steel specimen of complex form* Communications in Numerical Methods in Engineering (1998), Vol. 14, 277 – 285

[14] PATANKAR, S.: *Numerical Heat Transfer and Fluid Flow*, McGraw Hill Book Company, New York, 1980.

[15] SMOLJAN, B.; RUBEŠA, D.; TOMAŠIĆ, N.; SMOKVINA HANZA, S.; ILJKIĆ, D.: *An analysis of application of modified Jominy-test in simulation of cold work tool steels quenching*, Int. J. Microstructure and Materials Properties (2007), Vol. 2, 24 – 34

[16] SMOLJAN, B.; TOMAŠIĆ, N.; ILJKIĆ, D.; FELDE, I.; RETI, T.: *Application of JM®-test in 3D Simulation of Quenching*, Journal of Achievements in Materials and Manufacturing Engineering (2006), Vol. 17, 281 – 284

[17] SMOLJAN, B.; ILJKIĆ, D.; SMOKVINA HANZA, S.: *Computer Simulation of Working Stress of Heat Treated Steel Specimen*, Journal of Achievements in Materials and Manufacturing Engineering (2009), Vol. 34, 152-158

[18] RETI, T.; FELDE, I.; GUERRERO, M.; SARMIENTO, S.: *Using Generalized Time-Temperature Parameters for Predicting the Hardness Change Occurring during Tempering, International Conference on New Challenges in Heat Treatment and Surface Engineering (Conference in honour of Prof. Božidar Liščić), B. Smoljan, B. Matijević, Eds.* - Proceedings, Dubrovnik-Cavtat, Croatia, June 2009.

[19] SMOLJAN, B.: *Computer Simulation of Microstructure Transformation during the Quenching, 1st International Surface Engineering Congress and 13th IFHTSE Congress (ASM International), O. Popoola, N.B. Dahotre, J.O. Iroh, D.H. Herring, S. Midea, H. Kopech, Eds.* - Proceedings, Columbus, OH, USA, October 2002.

[20] SMOLJAN, B.: *Prediction of Mechanical Properties and Microstructure Distribution of Quenched and Tempered Steel Shaft*, Journal of Materials Processing Technology (2006), Vol. 175, 393-397

[21] PAVLINA, E. J.; VAN TYNE, C. J.: *Correlation of Yield Strength and Tensile Strength with Hardness for Steels*, Journal of Materials Engineering and Performance (2008), Vol. 17, 888-893

[22] JUST, E.: *Verguten-Werkstoffbeeinflussung durch Harten und Anlassen*, VDI-Berichte (1976), No. 256, 125–140

[23] WILSON, A. et al.: *Fatigue and Fracture Resistance of ferrous Alloys in ASM Handbook-Volume 19: Fatigue and Fracture*, Material Park, OH: ASM International, 1996.

[24] RITCHIE, R. O.: *Near-Threshold Fatigue-Crack Propagation in Steels*, International Metals Reviews (1979), Vol. 24, 205-230

[25] MASOUNAVE, J.; BAILON, J. P.: *Effect of Grain Size on the Threshold Stress Intensity Factor in Fatigue of Ferritic Steel*, Scripta Metallurgica (1976), Vol. 10, 165-170

[26] CURLE, U. A.: *Near-Threshold Fatigue Crack Growth behaviour of Mild Steel in Steam during Rotating Bending*, M.S. thesis, University of Pretoria, 2006.

[27] ZAMINSKI, G. F.: *Effect of Strength, Load Ratio and Environment on Near-Threshold Fatigue Crack Propagation of 2¼Cr-1Mo Steel*, M.S. thesis, Massachusetts Institute of Technology, 1980.

[28] SURESH, S.; ZAMINSKI, G. F.; RITCHIE, R. O.: *Fatigue Crack Propagation Behavior of 2¼Cr-1Mo Steels for Thick-Wall Pressure Vessels*, Special Technical Publication, *Application of 2¼Cr-1Mo Steel for Thick Wall Pressure Vessels*, ASTM STP 755, G.S. Sangdahl, M. Semchyshen, Eds., American Society for Testing and Materials, 1982, 49-67.

Functional data analysis and its application in production processes

***Branimir LELA*[1)],**
***Igor DUPLANČIĆ*[1)]**
***and Miroslav ŠUPE*[2)]**

1) Fakultet elektrotehnike, strojarstva I brodogradnje, Sveučilišta u Splitu (Faculty of Electrical Engineering, Mechanical Engineering and Naval Architecture, University of Split) Ruđera Boškovića 32, 21000 Split, **Republic of Croatia**
2) TLM-TVP d.o.o (TLM-TVP Inc.) Narodnog preporoda 12, 22000 Šibenik, **Republic of Croatia**

blela@fesb.hr

Keywords
Functional data analysis
Mathematical modelling
Algebraic and differential equation
Production processes

Ključne riječi
Analiza funkcijskih podataka
Matematičko modeliranje
Algebarske i diferencijalne jednadžbe
Proizvodni procesi

Primljeno (Received): 20xx-xx-xx
Prihvaćeno (Accepted): 20xx-xx-xx

Original scientific paper
Modern manufacturing facilities are with no exception equipped with measurement devices that are able to produce high-resolution discrete data for relevant production parameters. Data measured that way can be described by smooth functions having the derivatives of desired order. Each such function is considered as a data in functional data analysis (FDA) method. FDA is an extension of traditional methods for data analysis to data that can be identified as functions. The objective of this work is to describe the possibility of solving inverse problems in production processes by FDA. In this work algebraic and differential equations are introduced through mathematical models describing the behaviour of some production parameters in the hot rolling process of aluminium strip. The results of the computer simulation show that FDA methodology can be successfully applied in modelling of production systems and in solving problems of parameter estimation in dynamic mathematical models.

Analiza funkcijskih podataka i njezina primjena u proizvodnim procesima

Izvornoznanstveni članak
Moderna proizvodna postrojenja su bez iznimke opremljena mjernim uređajima koji mogu stvoriti podatke o proizvodnim parametrima s visokom rezolucijom. Podaci izmjereni na takav način mogu se opisati neprekinutim funkcijama koje su derivabilne do željenog stupnja. Svaka takva funkcija se promatra kao podatak u metodi koja se zove analiza funkcijskih podataka (AFP). AFP je proširenje tradicionalne statističke analize podataka na funkcije kao statističke podatke. Cilj ovog rada je opisati mogućnost rješavanja inverznih problema u proizvodnim procesima pomoću AFP. U ovom radu se preko matematičkim modela u obliku algebarskih i diferencijalnih jednadžbi opisuje ponašanje nekih parametara u procesu toplog valjanja aluminijskih traka. Rezultati računalne simulacije pokazuju da se AFP može uspješno primijeniti za modeliranje proizvodnih sustava i rješavanje problema procjene parametara u dinamičkim matematičkim modelima.

1. Introduction

Parameter estimation in mathematical modelling is very important in many scientific and engineering fields because many physical and technical processes can be described by algebraic or differential equations [1]. There are numerous methods for parameter estimation in mathematical equations and one of them is Functional data analysis (FDA) [2]. The basic idea of the FDA method is that the measured and recorded data on a given technological or physical process is not observed as discrete values but as functions and statistical analysis is performed directly on those functions in functional space. Those functions are called functional data (FD). This way proceeding has numerous advantages over a classical multivariate analysis of high-dimensional data because it allows introducing prior knowledge, dealing with irregularly and missing data and performing mathematical processes of differentiation and integration [3]. Each part of the classical statistics has its counterpart in the FDA and this study deals only with a portion of FDA known as regression analysis and principal differential analysis (PDA). Regression analysis estimates parameters in algebraic equations while PDA estimates parameters in differential equations.

The AFP method can be applied to any technological process where relevant parameters are continuously monitored and recorded. One of such processes is the hot rolling of aluminium strips that this work deals with. One of the main parameters governing the hot rolling process is the rolling force due to its influence on the strip quality [4]. Accurate prediction of the rolling force is rather difficult due to complexity of the rolling process [5]. Understanding the dynamics of the rolling stand is also important for the prediction of strip quality [6]. So this work proposes new mathematical models whose explanation follows.

Symbols/Oznake

FDA	- Functional data analysis - Analiza funkcijskih podataka	x	- Linear basis function expansion - Linearna kombinacija baznih funkcija
FD	- Functional data - Funkcijski podaci	$\mathbf{H}$	- Matrix of radial basis functions - Matrica radijalnih bazni funkcija
PDA	- Principal differential analysis - Analiza glavnih diferencija	$\mathbf{w}$	- Vector of weight parameters - Vektor težinskih parametara
RBF	- Radial basis function - Radijalne bazne funkcije	$\mathbf{Z}$	- Matrix of covariate functions - Matrica nezavisnih funkcijskih podataka
PSSE	- Penalized sum of squared errors - Suma kvadratnih pogrešaka sa kaznom	c	- Rolling stand damping - Prigušenje valjačkog stana
PLS	- Penalized least squares criterion - Kriterij najmanjih kvadrata sa kaznom	z	- Roll gap - Otvor između valjaka
RF	- Rolling force - Sila valjanja	k	- Rolling stand stiffness - Krutost valjačkog stana
BF	- Bending force - Sila savijanja	m	- Mass of work and backup roll - Masa radnog i potpornog valjka
RS	- Rolling speed - Brzina valjanja		**Greek letters/Grčka slova**
OT	- Output tension - Sila natezanja	λ	- Smoothing parameter - Parametar kazne
IT	- Input tension - Sila zatezanja	β	- Regression coefficient function - Regresijski koeficijent u obliku funkcije
$\mathbf{y}$	- Vector of measured data - Vektor izmjerenih podataka	$\boldsymbol{\beta}$	- Vector of regression coefficient functions - Vektor regresijskih koeficijenta u obliku funkcija

2. Mathematical models

In this work a mathematical model for the rolling force prediction and a model for the prediction of rolling stand dynamics are proposed. Both models have been designed and their parameters have been estimated using FDA methodology. The first step in FDA is conversion discretely measured data into functions what is, in this study, carried out by B-spline basis functions and radial basis functions (RBF) approximation. Regarding the modelling of rolling force seventeen B-spline basis functions of order five have been used and the time domain has been divided by fourteen knots. Weight factors in the B-spline linear expansion equation have been determined by using penalized sum of squared errors fitting criterion

$$PSSE = \left[\mathbf{y} - x(\mathbf{t})\right]^{\mathrm{T}} \left[\mathbf{y} - x(\mathbf{t})\right] + \lambda \cdot \int \left[\frac{d^2}{dt^2}\mathrm{x(t)}\right]^2 dt \qquad (1)$$

where $\mathbf{y}$ is a vector of measured data, $x(\mathbf{t})$ is linear basis functions expansion containing weight factors that have to be determined and λ is a smoothing parameter which have been determined for each function by cross-validation.

In the modelling of rolling stand dynamics discrete data were approximated by RBF method i.e. minimizing error function what gives the following matrix equation for weight parameters determination

$$\left(\mathbf{H}^{\mathrm{T}}\mathbf{H}\right)\mathbf{w} + \lambda\mathbf{w} = \mathbf{H}^{\mathrm{T}}\mathbf{y} \qquad (2)$$

where $\mathbf{H}$ is a matrix that contains radial basis functions, $\mathbf{w}$ is a vector of weight parameters that have to be determined, λ and $\mathbf{y}$ have the same meaning as in equation (1). Number of radial basis functions was determined by forward selection method and the value of smoothing parameter for each function was determined using Bayesian criterion.

Functional data have been obtained out of values of parameters measured and recorded in the factory TLM Inc. during the hot rolling of 70 aluminium strips made of alloy AA1050. Each strip was rolled in seventeen passes. Prior to data processing all measured values were scaled within the interval 0 and 1. The parameters

whose values were recorded on the rolling mill are: rolling force, bending force, rolling speed and input and output tension. These parameters have been used in the development of the mathematical models.

2.1. Rolling force model

When all functional data are determined linear regression equation for rolling force prediction can be designed in the form

$$RF(t) = \beta_1(t) + \beta_2(t)\cdot BF(t) + \beta_3(t)\cdot RS(t) + \\ + \beta_4(t)\cdot OT(t) + \beta_5(t)\cdot IT(t) \quad (3)$$

where $\beta_i, i = 1,2,...,5$ are regression coefficient functions that have to be determined, *RF* is the rolling force, *BF* is the bending force, *RS* is the rolling speed, *OT* and *IT* are the output and input tension respectively. Out of the equation (3) regression coefficients β_i can be calculated by fitting penalized least squares criterion extended for FD in the form

$$PLS = \int \left[\mathbf{y}(t) - \mathbf{Z}(t)\cdot\boldsymbol{\beta}(t)\right]^{\mathrm{T}} \left[\mathbf{y}(t) - \mathbf{Z}(t)\cdot\boldsymbol{\beta}(t)\right] dt + \\ + \sum_j \lambda_j \int \left[\frac{d^2}{dt^2}\beta_j(t)\right]^2 dt \quad (4)$$

where $\mathbf{Z}$ is a matrix that contains covariate functions and $\boldsymbol{\beta}$ is a vector of regression coefficient functions.

2.2. Model for dynamics of rolling stand

Dynamical behaviour of the rolling stand is modelled, in this work, as a symmetric linear lumped parameter system where all masses vibrate along the direction perpendicular to the rolled strip. Fig. 1 shows the scheme of that physical model.

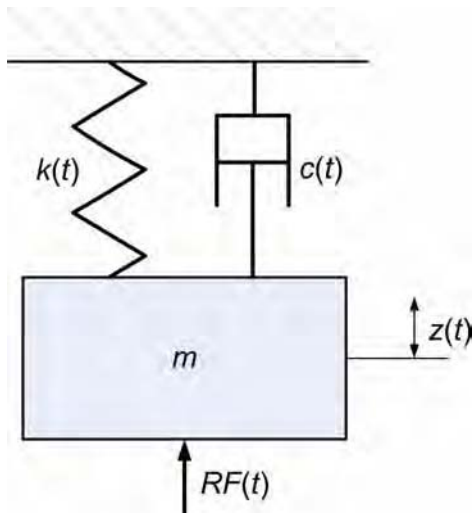

Figure1. Physical model for dynamical behaviour of rolling stand

Slika 1. Fizikalni model za dinamičko ponašanje valjačkog stana

The forces caused by the elastic deformation of the mill housing, screw blocks, work and backup roll bearings, contacts between the work and backup rolls and contacts between the work rolls and strip are taken into account through the stiffness $k(t)$ and damping $c(t)$. Shift of the rolls is represented by the roll gap $z(t)$ and the mass of the work and backup rolls is labelled by m. Observing the condition of dynamic equilibrium a differential equation of the system motion can be obtained in the form

$$RF(t) = m\cdot\ddot{z}(t) + c(t)\cdot\dot{z}(t) + k(t)\cdot z(t), \quad (5)$$

or shown in the standard form as

$$RF(t) = \beta_1\cdot\ddot{z}(t) + \beta_2(t)\cdot\dot{z}(t) + \beta_3(t)\cdot z(t). \quad (6)$$

In the equation (6) unknown parameters are $\beta_2(t)$ representing damping $c(t)$ and $\beta_3(t)$ representing stiffness $k(t)$. Both parameters are determined using PDA. Equation (4) can be used for PDA but with certain modification, specifically, vector $\mathbf{y}$ can contain derivatives of the input or force functions and matrix $\mathbf{Z}$ can contain derivatives of output functions. All functions in the differential equation (6) are represented by RBF linear expansion approximation. All necessary derivatives of the functions were approximated by direct RBF approximation method where derivatives are calculated by direct differentiating of closed form of RBF function approximation.

3. Simulation of mathematical models

When mathematical models have been designed unknown coefficients have to be determined and eventually simulation of the models can be carried out. Coefficient functions β_i in both models were determined using a set of 50 functional data randomly chosen out of the overall data set consisting of 70 FD. The rest of FD was used for the final testing of the models. Due to data extensiveness the results of simulation for both models will be shown only for seventeenth rolling pass although results for other passes are very similar.

3.1. Rolling force model

How regression coefficient functions behave, in the rolling force model, during the seventeenth rolling pass can be seen on Fig. 2. These coefficient functions do not have some specific physical meaning and it can be noticed their variability during the rolling pass.

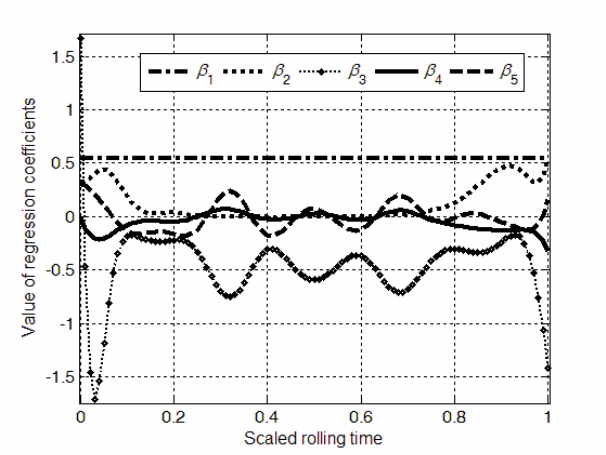

Figure 2. Regression coefficient functions in 17th pass

Slika 2. Funkcije regresijskih koeficijenata u 17 prolazu

Fig. 3 compares rolling force values predicted by FDA method with those measured on the rolling mill during the rolling of the strip made of alloy AA1050 in seventeenth rolling pass

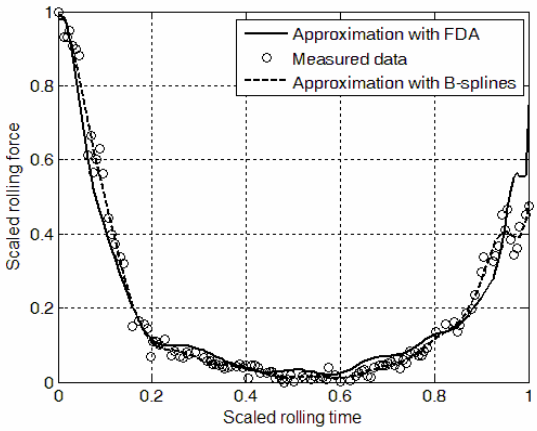

Figure 3. Rolling force prediction with FDA in 17th pass for a randomly chosen FD out of the testing data set

Slika 3. Predviđanje sile valjanja sa AFP u 17 prolazu za jedan slučajno odabrani uzorak iz skupa za testiranje

Prediction of rolling force with FDA was obtained by choosing one FD group out of the testing data set and putting it into the regression equation (3). FD group consists of response function replications and corresponding independent functions replications. Curves form the Fig. 3 show satisfactory agreement, for this particular case, between the prediction with FDA and the measured values. Fig.3 also shows quite good match between approximation of rolling force with B–splines and those values of rolling force predicted with FDA method.

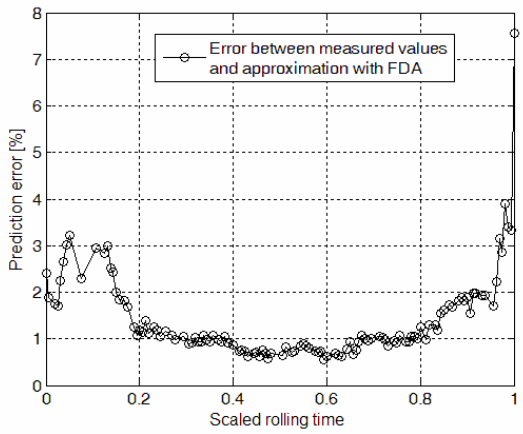

Figure 4. Average prediction error of rolling force for 17th pass calculated over the entire testing data set

Slika 4. Srednja greška predviđanja sile valjanja u 17 prolazu izračunata nad cjelokupnim skupom za testiranje

In order to verify the quality of the regression model average prediction error of the rolling force can be calculated over the entire testing data set. The results of that calculation are shown on Fig. 4. Curve on the Fig. 4 shows that the prediction ability of the model in the starting and ending phases of the rolling pass is worse due to the set-up control in that phases [7]. When the process is stabilized and the on-line control is activated the prediction error can be below 1%.

3.2. Model for rolling stand dynamics

The result of applying FDA method on parameters estimation in differential equation (5), which describes dynamic behaviour of the rolling stand, can be seen on Fig. 5. Coefficient functions in equation (5) were determined out of the training data set for seventeenth rolling pass during the rolling of the strip made of aluminium alloy AA1050. From the Fig. 5 it can be noted that the greatest change experiences coefficient β_2 that represents damping of the rolling stand. This is due to change of rolling conditions primary in the interfaces work-backup rolls and strip-work rolls. Coefficient β_3, which characterizes rigidity of the system, exhibits significantly smaller changes during seventeenth rolling pass and that can be noted on the Fig. 5. Coefficient β_1 characterizes constant mass of the work and backup rolls so it remains constant during the rolling as it can be seen on the Fig. 5.

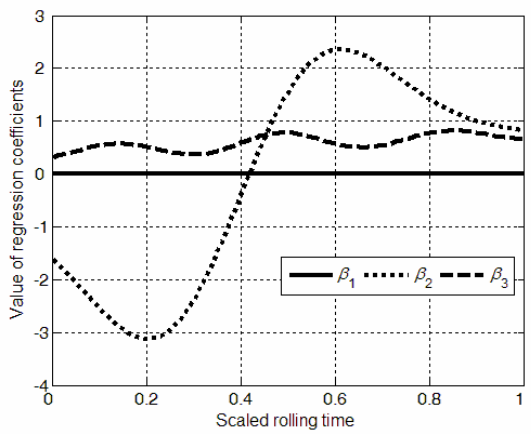

Figure 5. Coefficient functions of differential equation for 17th rolling pass

Slika 5. Funkcije koeficijenata diferencijalne jednadžbe za 17 prolaz

Having determined parameters of the differential equation it can be solved analytically, if it is possible, or numerically. In order to verify the quality of the model differential equation was not solved analytically or numerically but FD was randomly chosen out the testing data set and that group was put into the equation (5). Comparing the right side of the equation (5), obtained in calculation, with the measured values on the rolling mill quality of the model can be tested.

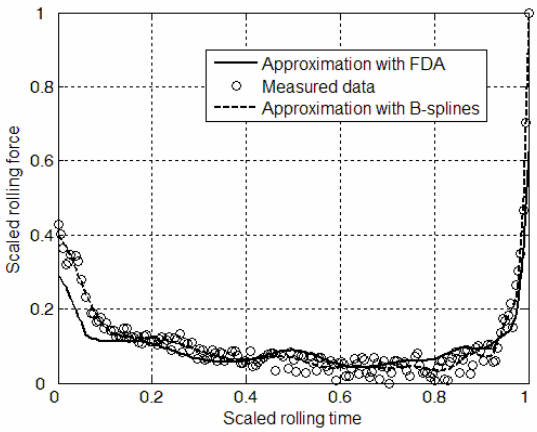

Figure 6. Efficiency validation of parameter estimation in differential equation for 17th pass and one randomly chosen FD out of the testing data set

Slika 6. Provjera uspješnosti procjene parametara diferencijalne jednadžbe za 17 prolaz i jedan slučajno odabrani podatak iz skupa za testiranje

Fig. 6 shows the results of inclusion of one randomly chosen FD out of the testing data set in the equation (5). Fig. 6 also shows discretely measured data on the rolling mill and approximation of that data with B-spline basis functions expansion. It can be noted from the Fig. 6 that all three curves exhibit rather good agreement and can be qualitatively concluded that the mathematical model in the form of differential equation has satisfactory quality.

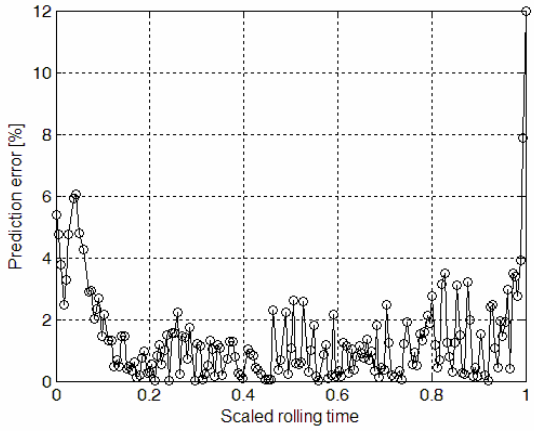

Figure 7. Average prediction error of differential equation for 17th pass over the entire testing data set

Slika 7. Srednja greška predviđanja diferencijalne jednadžbe za 17 prolaz nad cjelokupnim skupom za testiranje

The quantitative quality of the dynamic model can be tested if the average prediction error is calculated over the entire testing data set. Fig. 7 shows the results of the prediction error calculation for seventeenth rolling pass. Analysis of the curve form Fig. 7 reveals that the model exhibits high quality in the middle of the pass when the process is stabilized and controlled on-line. In that case the average prediction error is approximately 1%. At the starting and ending phases of the rolling pass the prediction error amounts, in some cases, to 6% or even higher. The reason for this is set-up control when there is no feedback from measuring devices so the rolling force and the roll gap have to be predicted in advance [7]. That cannot be carried out entirely accurate due to complex influence of control parameters on the rolling process [7].

4. Conclusion

In this study FDA methodology has been presented as a tool for solving inverse problems, i.e. problems of parameter estimation in mathematical models describing the industrial processes of hot aluminium rolling. In order to test the possibilities of FDA method two

mathematical models have been proposed. One in the form of regression equation that is able to predict the rolling force and the other in the form of differential equation that describes dynamics of the rolling stand. All the data that were used in solving mathematical models were measured and recorded in the industrial conditions, in factory TLM-TVP Inc., during the hot rolling of aluminium strip made of alloy AA1050. Results of the simulation of the models shows satisfactory agreement between values predicted with FDA and those measured on the rolling stand. This is especially obvious when the rolling process is stabilized and controlled on-line and in that case prediction error for both models is about 1%. For starting and ending phases of the rolling passes the prediction error is quite higher for both models and amounts from 3% to 6% or even higher in some cases. FDA method can successfully solve parameter estimation problems in static or dynamic models but accurate data with high resolution are very desirable as well as algorithms for reducing numerical effort.

Acknowledgements

The authors acknowledge TLM-TVP Inc. for provision access to rolling facilities and its database for hot rolling of aluminium strips.

REFERENCES

[1] OGUNNAIKE, B.A., RAY, W.H.: *Process Dynamics, Modeling and Control,* Oxford University Press, New York, 1994.

[2] RAMSAY, J.O., SILVERMAN, B.W.: *Functional Data Analysis* (second ed.), Springer, New York, 2005.

[3] HARZELAK, J., COULL, B., LAIRD, N., MAGARI, S., CHRISTIANI, D.: *Penalized solutions to functional regression problems,* Comp. Statist. Data Anal. (2007) 51, 4911–4925.

[4] GINZBURG, V.B., BALLAS, R.: *Flat rolling fundamentals*, Marcel Dekker Inc., New York, 2000.

[5] DUPLANČIĆ, I.: *Obrada deformiranjem,* FESB Split, 2007.

[6] NIZIOL, J., SWIATONIOWSKI, A.: *Numerical analysis of the vertical vibrations of rolling mills and their negative effect on the sheet quality*, Journal of Materials Processing Technology (2005) 162-163, 546-550.

[7] ROY, R.: *A review of rolling system Design Optimisation*, International Journal of Machine Tools and Manufacture (2006) 46, 912-928.

Utjecaj struje i temperature na razvijanje vodika tijekom katodne polarizacije slitina Al-In

***Jagoda RADOŠEVIĆ*[1)], *Ratko MIMICA*[1)], *Sanja SLAVICA-MATEŠIĆ*[2)] *and* *Lea KUKOČ-MODUN*[839]**

1) Fakultet elektrotehnike, strojarstva I brodogradnje, Zavod za strojarsku tehnologiju, Split
2) Pročelnica upravnog odjela za zaštitu okoliša i komunalne poslove Šibensko-Kninske županije, Šibenik, HR
3) Kemijsko-tehnološki fakultet, Zavod za analitičku kemiju, Split, HR.

Ratko.mimica@fesb.hr

Keywords

Hydrogen evolution
Aluminium-indium alloys
Cathodic polarisation

Ključne riječi

Izlučivanje vodika
Slitine aluminija i indija
Katodna polarizacija

Izvorni znanstveni rad

Rezultati predstavljeni u ovom radu odnose se na slitine Al-In pripremljene od super-čistog aluminija (99,999%) kao baze. Iskorištenje na vodiku za vrijeme katodne polarizacije u 2M otopini NaCl mjereno je volumetrijski u funkciji gustoća struja i temperatura. Također je praćena brzina korozije slitina metodom promjene mase u vremenskom periodu od pedeset i jednog dana.

Influence of Current and Temperature on Hydrogen Evolution during Cathodic Polarisation of Al-In Alloys

Original scientific article

Results presented in this article are refering to Al-In alloys prepared using super pure aluminium(99,999%) as a base, yield of hydrogen was measured during cathodic polarisation in 2M NaCl slution as a function of current density and temperature. In addition, corrosion rate was measured using mass change method during time period of fifty one days.

1. Uvod

Aluminij i njegove slitine su zbog svojih fizikalnih, kemijskih, metalurških i tehnoloških svojstava postali materijal koji je prodro u skoro sva tehnička rješenja, a razvoj mnogih grana industrije neraskidivo je vezan za njih. Aluminij je zbog svoje visoke termodinamičke reaktivnosti i visokog energetskog kapaciteta izvrstan aktivni anodni materijal, kako u elektrokemijskim izvorima struje, tako i u protektorskoj zaštiti metala, kao topive anode za katodnu zaštitu konstrukcijskih materijala. Sklonost aluminija da se štiti stvaranjem otpornog oksidnog filma na površini ograničava njegovu upotrebu za navedene svrhe.

Legiranjem aluminija s malim količinama Sn, Ga, Tl, In [1] i drugim elementima pospješuje se njegova anodna aktivnost t.j., izazivaju značajan pomak vrijednosti potencijala otvorenog strujnog kruga (OCP) više od 300
mV u negativnom smjeru u odnosu na čisti aluminij u kloridnim otopinama.

Bilo je ustanovljeno da katodna polarizacija također aktivira slitinu za anodno otapanje [2, 3]. Brzina korozije odabranih slitina ispitana je metodom praćenja volumena oslobođenog vodika i metodom mjerenja promjene mase.

Symbols/Oznake

F	- Faraday constant - Faradayeva konstanta	V_m	- Hydrogen volume(molar), cm^3 - Molarni volumen vodika, cm^3
i	- Applied current, mA - Primjenjena struja, mA		**Greek letters/Grčka slova**
OCP	- open circuit potential, mV - potencijal otvorenog strujnog kruga, mV	η	- yield of hydrogen, - prinos vodika
S	- electrode surface, cm^2 - površina elekrode, cm^2	v	- volume of accumulated hydrogen, cm^3 - volumen izlučenog vodika, cm^3
t	- time, s - vrijeme, s		
v'	- average corrosion rate mg/cm^2day - prosječna brzina korozije mg/cm^2dan		

2. Eksperimentalni dio

Elektrokemijska mjerenja izvedena su u standardnom elektrokemijskom reaktoru sastavljenom od 3 elektrode: radne, protuelektrode i referentne elektrode. Dvostruka staklena stjenka elektrokemijskog reaktora omogućavala je termostatiranje. Za sva mjerenja upotrebljena je grafitna protuelektroda u obliku štapa, površine 10 puta veće od radne elektrode. Kao referentna elektroda korištena je Ag/AgCl 3M elektroda. Radna elektroda izrađena je od Al – 0,10% In slitine u obliku kocke a elektrodni kontakt je ostvaren pomoću izolirane bakrene žice. Uzorak je sa svih strana, osim s jedne, zaštićen epoksi smolom. Slobodna površina iznosila je približno 0,5 cm^2. Prije svakog mjerenja površina elektrode je mehanički i kemijski obrađena. Elektroda je brušena brusnim papirima finoće: 360, 600, 800. Da bi se odstranio površinski oksidni sloj i eventualno unesene nečistoće, elektroda je držana 1 minutu u alkalnoj otopini 0,1M NaOH, zagrijanoj na 40 $^oC \pm 0,1^oC$. Potom je elektroda ispirana redestiliranom vodom, i postavljena u elektrokemijski reaktor na način da je smještena pod biretom, čiji je otvoreni završetak proširen, tako da se mogao hvatati ukupni oslobođeni plin (vodik). Elektrolit je bio deareriran, upuhivanjem pročišćenog dušika u reaktor. Elektrokemijska mjerenja provedena su pomoću potenciostata/galvanostata BioLogic Science Instruments SP-150, upravljanog s odgovarajućim softverom „EC.Lab" (v.9,55).

Ispitivanja su se provodila na temperaturama: 25 ^oC, 50 ^oC i 75 ^oC pri primjenjenim strujama od 0,06 do 2,30 mA. Nakon postizanja stabilne vrijednosti OCP, provodio se eksperiment pri određenoj jakosti struje te pratila promjena potencijala u vremenskom periodu od 60 minuta. U bireti se kontrolirao volumen reakcijom oslobođenog vodika. Elektrolit je prije početka eksperimenta usisavan, da bi ispunio biretu, a razvijeni vodik ga je istiskivao nazad u ćeliju.

Katodnom polarizacijom slitine Al–0,10%In pri određenoj gustoći struje i temperature , eksperimentalno su određeni parametri i konačni potencijal, te volumen oslobođenog vodika. Na osnovu dobivenih podataka izračunato je iskorištenje vodika, polazeći od relacije:

$$\eta = \frac{2F\left(\frac{v}{V_m}\right)}{i \cdot t} = \frac{7{,}89v}{i \cdot t} \qquad (1)$$

Gdje je V_m molarni volumen i iznosi 24,466 cm^3 i uzet je kao molarni volumen vodika, budući da je plin u bireti bio izvan termostata i na temperaturi okoline.

Da bi se pratila promjena mase slitina Al-In uzorci su pripremljeni i obrađeni kao i za prethodna ispitivanja. Uzorci su bili uronjeni u elektrolit pedeset i jedan dan, pri uvjetima sobne temperature i atmosferskog tlaka zraka. Mjerenja promjene masa provodila su se u određenim vremenskim razmacima. Pri svakom mjerenju slijedio se isti postupak: uzorci izvađeni iz elektrolita isprani su u destiliranoj vodi da bi se uklonili kristali NaCl, sušeni na zraku i vagani. Nakon vaganja uzorci su vraćeni u elektrolit. Prilikom svakog mjerenja promatrane su i bilježene promjene na površinama uzoraka i elektrolitima.

Prosječnu brzinu korozije v' određujemo po relaciji:

$$v' = \frac{\Delta m}{S \cdot \Delta t}; \qquad (2)$$

U kojoj je $\Delta m = m_2 - m_1$; $\Delta t = t_2 - t_1$; S = površina elektrode.

Površinsku promjenu mase izražavamo kao: $\frac{\Delta m}{S}$, a prirast mase (%) kao: $\frac{\Delta m}{M} \cdot 100$ gdje M predstavlja početnu masu.

Morfologija površine je promatrana optičkim mikroskopom (OPTON Axioscop povećanja 20x10, s izmjenjivim lećama) a snimke su dobivene s kamerom (JVC KY – F1030; KY – Link Softver) uzoraka prije izlaganja agressivnom elektrolitu i nakon praćenja promjene mase tijekom 51 dana.

3. Rezultati i rasprava

Primjenjene struje od 0,06 do 2,30 mA proizvele su mjerljive volumene plina, unutar zadanog vremenskog razmaka od jednog sata. Promjena potencijala za vrijeme elektrolize prikazana je na slici 1.

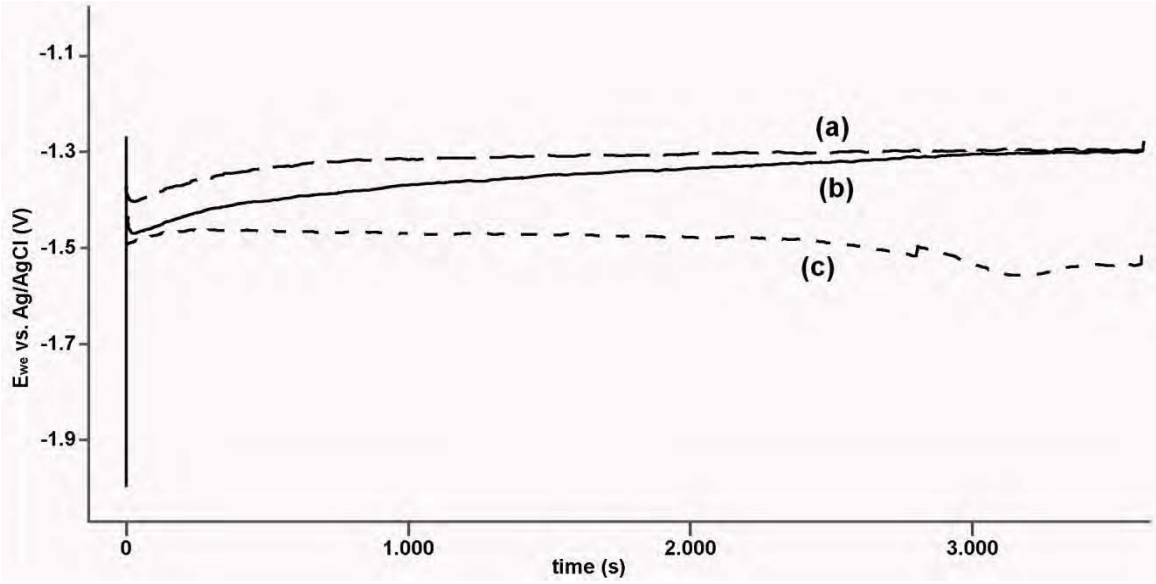

Figure 1. Changes of potential in time for Al-0.10%In in 2M NaCl with temperatures (a) 25 °C, (b) 50 °C i (c) 75 °C and cathodic current density of 3.5 mAcm^{-2}

Slika 1. Grafički prikaz promjene potencijala s vremenom za Al-0.10%In u 2M NaCl pri temperaturama (a) 25 °C, (b) 50 °C i (c) 75 °C i katodnoj gustoći struje od 3.5 mAcm^{-2}

Na slici 2 vidljivo je da Tafelovi pravci pokazuju jasnu linearnu ovisnost *E* o *log i* u cijelom temperaturnom području u kojem su se pratila istraživanja (od 25 °C do 75 °C) (točke se odnose na potencijale zabilježene na početku mjerenja). Ustaljeno pomicanje potencijala s vremenom ustanovljeno je u ranijim istraživanjima [4]. Pri višim temperaturama polarizacija je manja.

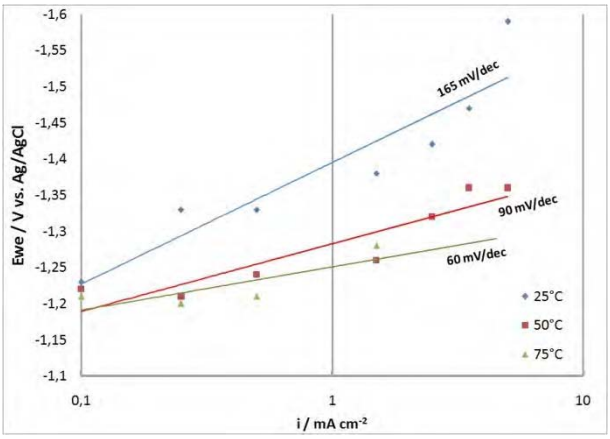

Figure 2. Tafel plots for cathodic polarization of Al-0.10%In alloy at different temperatures.

Slika 2. Tafelovi dijagrami za katodnu polarizaciju Al-0.10%In slitine na različitim temperaturama.

Postignuti prinosi vodika mogu se vidjeti na slici 3.

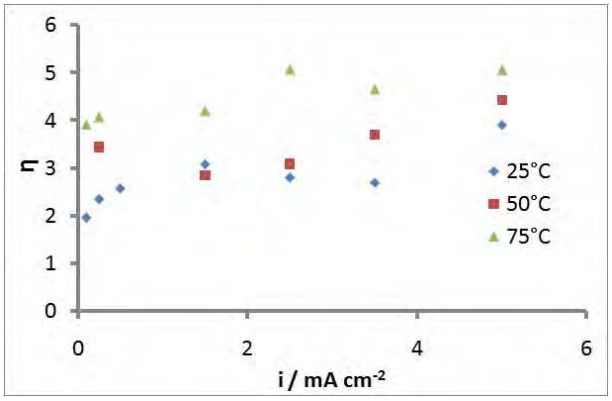

Figure 3. The yield of hydrogen as a function of cathodic current density for Al-0.10% In at different temperatures.

Slika 3. Iskorištenje na vodiku kao funkcija katodne gustoće struje pri različitim temperaturama za Al-0.10%In.

Pri svim primjenjenim gustoćama struje i temperaturama, prinos je bio praktički uvijek iznad vrijednosti 2. Nadalje, pri danim temperaturama praktički nije bilo ovisnosti prinosa o gustoći struje. Porastom temperature do vrijednosti 50 °C prinos

postiže vrijednost 3 i na 75 °C vrijednost 4.
Uspoređujući ostvarene rezultate s podacima iz literature [5] za čisti aluminij, vidljivo je da je iskorištenje vodika promatrane Al-In slitine nešto veće, uslijed aktivacije aluminija indijem. Rezultati su u skladu s teorijom Van de Vena i Koelmansa [6] o kombiniranom djelovanju kemijskog i elektrokemijskog procesa.
U prvom elektrokemijskom stupnju (Volmerova reakcija) prijelazom elektrona nastaje vodikov atom iz molekule vode, ostavljajući za sobom OH^- ion na samoj površini. Predaja elektrona iz aluminijevog atoma protonu u molekuli vode može biti stimulirana prisustvom triju vrsta: H_2, aluminijevog atoma sa slabo vezanim 3p elektonom u vanjskoj ljusci, te vrlo polarne molekule vode. Uslijed njihovog međusobnog kontakta može doći do otpuštanja elektrona iz aluminijevog atoma s posljedicom formiranja dviju kovaletnih veza, jedna u molekuli vodika, a druge u novim vrstama formiranim na površini. Mehanizam reakcije može se prikazati:

$$H_2O + e^- \longrightarrow H + OH^- \quad (3)$$
$$H + Al + H_2O \longrightarrow AlOH + H_2 \quad (4)$$

Formiranje molekule vodika je reakcija tipa elektrokemijske desorpcije (Heyrovskijeva reakcija), ali dodatno stimulirana afinitetom za stvaranje Al-OH veze otpuštanjem unutarnjeg elektrona, umjesto iz vanjskog izvora struje. S ovim mehanizmom, za svaki elektron iz vanjskog izvora, stvara se jedna molekula H_2. Zbog toga iskorištenje (prinos) ima vrijednost 2. Ako se ova reakcija i odvije, AlOH vrste će ipak još uvijek imati značajan oksidacijski potencijal (zbog tendencije Al^+ iona da konvertira u Al^{3+}).
Stoga se mogu odvijati tri različite reakcije:

a) s drugom molekulom vode:

$$AlOH + H_2O \longrightarrow AlOOH + H_2 \quad (5)$$

b) s OH^- ionom, koji nije uspio „pobjeći" difuzijom:

$$AlOH + OH^- \longrightarrow AlO_2^- + H_2 \quad (6)$$

c) disorpcioniranje na površinu:

$$3AlOH \longrightarrow 2Al + AlOOH + H_2O \quad (7)$$

Reakcije (a) i (b) dovode do stvaranja dviju molekula vodika i time je iskorištenje 4. Činjenica da je ovo nađeno samo kod visokih temperatura pokazuje da su kemijske reakcije (5) i (6) spore i da ipak trebaju termičku aktivaciju.

Odsupanje rezultata od vrijednosti 4, pri najvišim temperaturama, može se pripisati ponekom OH^- ionu koji s površine pobjegne difuzijom.
Dijagram promjene mase slitina u ovisnosti o vremenu prikazan je na slici 4.

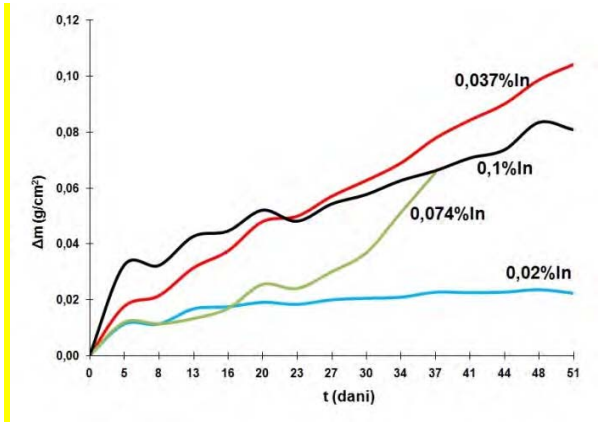

Figure 4. Variation of mass as a function of time
Slika 4. Dijagram promjene mase slitina s vremenom

Kao što se vidi na slici 4. slitina Al-0,02%In pokazuje prvih devetnaest dana rast mase. Nakon toga razdoblja, pa do kraja mjerenja, masa se uglavnom ustalila. Slitina se ponašala vrlo slično superčistom aluminiju zbog malog udjela In. Prosječna brzina korozije za superčisti aluminij iznosila je v' = 0,0306 $mgcm^{-2}dan^{-1}$ a slitina Al-0,02%In imala je vrijednost v' = 0,0439 $mgcm^{-2}dan^{-1}$.
Tijekom eksperimenta u elektrolitu su zapaženi istaloženi korozijski produkti.
U tablici 1 prikazane su vrijednosti prosječnih brzina korozije, površinske promjene masa i prirast mase ispitivanih slitina Al-In.

Table 1: Average corrosion rate, surface mass change and mass increase for examined alloys.
Tablica 1: Prosječne brzine korozije, površinska promjena mase i prirast mase za ispitivane slitine.

Slitina / Veličina	0,02% In	0,037% In	0,074% In	0,10% In
Prosječna brzina korozije (v') [$mgcm^{-2}dan^{-1}$]	0,439	2,046	1,284	1,586
Površinska promjena mase (Δm/s) [$mgcm^{-2}$]	22,4	104,3	65,5	80,9
Prirast mase [%]	0,192	0,381	0,409	0,382

Izlučivanje vodika vjerojatno prati taloženje In. Brzo stvaranje vodikovih džepova ima za posljedicu pucanje oksidnog filma, nukleaciju i povećanje pukotina. Kombinirani efekt površine obogaćene In, i njegova akumulacija na zrnatim međugraničnim površinama pridonosi aktivaciji površine. Taloženje In na površini elektrode potiče povećanu adsorpciju Cl^- iona što također pridonosi efektu aktivacije [7].
Napredovanje korozije praćeno je optičkim mikroskopom uzoraka prije i poslije izlaganja agresivnom mediju u trajanju od pedeset i jednog dana.

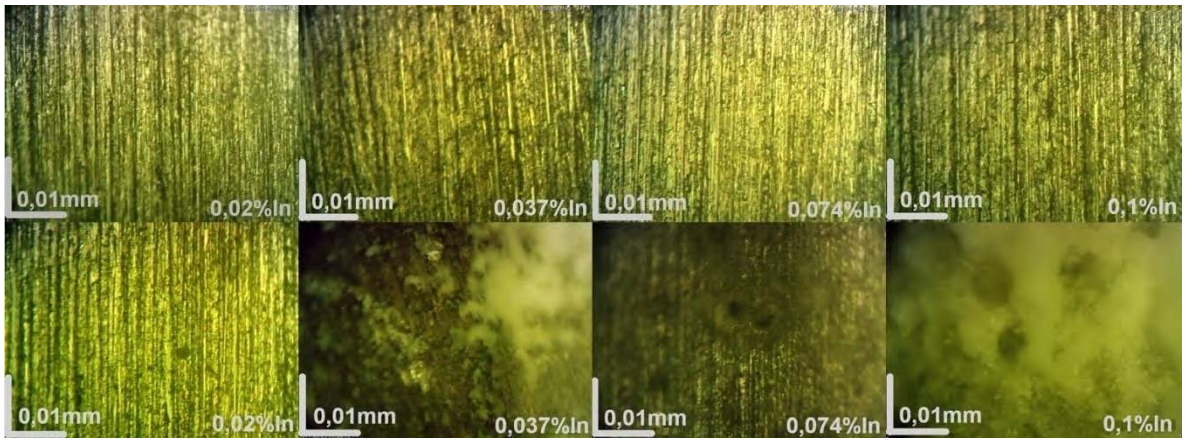

(a)

(b)

Figure 5. Metallographic image of tested samples before exposure in 2MNaCl (a) and after exposure (b). Magnification 200X

Slika 5. Metalografski snimak uzoraka slitina Al-In prije izlaganja 2M NaCl (a) i nakon izlaganja (b). Povećanje 200X

Na slici 5 uočljivo je da je napredovanje korozije najviše izraženo na slitinama Al-0,037%In i Al-0,1%In, što je sukladno s dobivenim rezultatima praćenja promjene mase ispitivanih uzoraka.

4. Zaključak

Rezultati prezentirani u ovom radu pokazuju da kod svih primjenjivanih gustoća struje i temperature od 25 ^oC iskorištenje na vodiku, prilikom katodne polarizacije ima vrijednost 2. Pri višim temperaturama prinos raste i doseže vrijednost 3 za 50 ^oC odnosno vrijednost 4 za temperaturu od 75 ^oC.
Nadalje, prosječna brzina korozije najveća je kod slitine Al-0,037%In i iznosi v' = 2,046 $mgcm^{-2}dan^{-1}$.

Zahvale

Ovaj rad je izrađen u okviru projekta „ELGRAFA III" uz potporu Ministarstva znanosti, obrazovanja i športa Republike Hrvatske.

REFERENCE

[1] T. READING, J.J.NEWPORT, Materials Protection, 5 (1966) 15.

[2] M.KLIŠKIĆ, J. RADOŠEVIĆ, S.GUDIĆ, Electrochimica Acta. 48(2003) 4167.

[3] A. VIŠEKRUNA, J. RADOŠEVIĆ, S.SLAVICA-MATEŠIĆ, N.KRNIĆ, J. Appl. Electrochemistry 40(2010) 621.

[4] J.RADOŠEVIĆ, M.KLIŠKIĆ, P.DUBIĆ, R.STEVANOVIĆ, A.DESPIĆ, J. Electroanal. Chem. 277(1990) 105.

[5] A.R.DESPIĆ, J.RADOŠEVIĆ, P.DABIĆ, M.KLIŠKIĆ, Electrochimica Acta. 35 (1990) 1743.

[6] E.P.G.T.VAN DER VEN, H.KOELMANS, J. Electrochemical Soc. 123(1976).

[7] H.A EL SHAYEB, F.M. ABD EL WAHAL, S. ZEIN EL ABDIN, Corrosion Sci. 43(2001) 643.

Optimization of cutting parameters for surface roughness in abrasive water jet machining

Veselko MUTAVGJIĆ[1], Zoran JURKOVIĆ[2], Mladen PERINIĆ[2] and Vesna MANDIĆ[3]

1) Municipality of Crikvenica
Kralja Tomislava 85
HR-51260 Crikvenica, **Republic of Croatia**
2) Faculty of Engineering, University of Rijeka
Vukovarska 58
HR-51000 Rijeka, **Republic of Croatia**
3) Faculty of Mechanical Engineering, University of Kragujevac
Sestre Janjic 6
RS-34000 Kragujevac, **Republic of Serbia**

zoran.jurkovic@riteh.hr

Keywords

abrasive water jet machinig
surface roughness
Taguchi method
cutting parameters optimization

Ključne riječi

obrada abrazivnim vodenim mlazom
površinska hrapavost
Taguchi metoda
optimizacija parametara procesa

Originaly scientific article

Abrasive water jet machining belongs to the non-conventional machining processes. Abrasive water jet machining as a tool used by water jet under high pressure with the addition of abrasive particles. The most important characteristic of this technology is a cold cut that heat does not affect the material and a wide range of materials and thicknesses can be machined. The aim of this paper is to conduct the experimental research of process parameters influence on surface roughness of the machined parts, and obtained data on how the process parameters affecting the surface roughness. The research was carried out for two different materials (stainless steel and aluminium alloy) using orthogonal experiment plan. Based on the obtained experimental results are defined by the optimal values of process parameters, verified through confirmation tests, to minimize surface roughness by using Taguchi method.

Optimizacija parametara procesa za površinsku hrapavost pri obradi abrazivnim vodenim mlazom

Izvorni znanstveni rad

Obrada abrazivnim vodenim mlazom spada u nekonvencionalne postupke obrade. Obrada abrazivnim vodenim mlazom kao alat koristi mlaz vode pod visokim tlakom sa dodatkom čestica abrazivnog sredstva. Najznačajnija karakteristika tehnologije rezanja abrazivnim vodenim mlazom je hladno rezanje koje termički ne utječe na materijal i širok spektar materijala koji se mogu obrađivati. Cilj rada je provesti istraživanje utjecaja parametara obrade na površinsku hrapavost obrađenih dijelova, te doći do podatka na koji način određeni parametri obrade utječu na hrapavost površine. Eksperimentalno istraživanje je izvedeno za dva različita materijala (nehrđajući čelik i aluminijska slitina) primjenom ortogonalnog plana eksperimenta. Temeljem dobivenih eksperimentalnih rezultata definirane su optimalne vrijednosti parametara obrade, verificirani kroz nove pokuse, s ciljem minimalizacije hrapavosti obrađene površine primjenom Taguchijeve metode.

1. Introduction

Water jet machining is suitable for cutting plastics, foods, rubber insulation, automotive carpeting and headliners, and most textiles. Harder materials such as glass, ceramics, concrete and tough composites can be cut by adding abrasives to the water jet during abrasive water jet machining (AWJM), which was first developed in 1974 to clean metals prior to their surface treatment. The addition of abrasives to the water jet enhanced the material-removal rate and produced cutting speeds between 51 and 460 mm/min. Generally, AWJM cuts 10 times faster than the conventional machining methods used for composite materials [1]. Advantages of abrasive water jet machining technology:

- There is no thermic effect on the material, and there are no changes in its structure.
- Minimum influence of jet power on the material being cut, there are no micro-cracks.
- In the regular working process, cutting of materials, minimum quantity of dust is created.
- Cutting without smoke and gas emission, which can occur in the process of piercing.
- There are no chemical effects on the material.
- High-quality cut without burr, cutting edge and the surface do not require additional machining.
- Precision of the cut is relatively high and very similar to classic machining.
- Material thickness ranges from foils to very thick half-manufactured products.
- Possibility of cutting complex and complicated forms.
- It is also possible to cut materials which are otherwise hard to separate.
- It is possible to cut layered materials with very complex characteristics of individual layers and composites.

Symbols/Oznake

Ra	- arithmetical mean roughness, µm - srednje aritmetičko odstupanje profila	*n*	- number of repetitions of the experiment - broj ponavljanja eksperimenata
Rz	- maximum peak-to-valley roughness height, µm - najveća visina profila		**Greek letters/Grčka slova**
y_i	- measured value of quality characteristic - izmjerena vrijednost karakteristike kvalitete	η	- signal-to-noise ratio (S/N) - omjer signala i šuma

Disadvantages of abrasive water jet machining technology:

- In the linear high speed cutting, the cut obtains V profile.
- In the process of high-speed cutting of inner angles, water jet may cause indents in the material.
- In the process of high-speed cutting of circles and arches, a deviation of the water jet may occur.
- Materials affected by corosion must be protected from corosion after cutting.
- Machining of very hard materials is difficult or impossible.

2. Experimental procedure

The objective of the experiment is to derive conclusions based on the measured surface roughness, in which manner certain machining parameters affect surface roughness of the workpiece, examined for various materials of different thickness. In order to derive optimal machining parameters for certain materials, it was necessary to conduct the experiment, and obtain the most favourable machining parameters in real conditions, which will result in minimum surface roughness.

2.1. Experimental conditions

Experimental investigation was conducted on the NC3015 machine, Water Jet Sweden (Figure 1). The machine is triaxial, its dimensions are 3 m × 1,5 m. High pressure pump Streamline SL-IV 50 is a product of Ingersoll Rand, 37 kW, of maximum pressure of 410 MPa. Measuring of surface roughness was conducted on the machine type T1000 basic, by manufacturer Hommel-Tech. Measuring of surface roughness of the workpiece shall be conducted for two surface roughness parameters; *Rz* maximum height of roughness profile, *Ra* arithmetical mean deviation of roughness profile. Sample materials are the following: stainless steel (EN 10088-3), Aluminium (EN AW-5083). The abrasive used in the experiment is Garnet 80. Mesh grain size equals from 300 to 150 µm. In the experimenting process, specific conditions were set on the machine and shall not be changed during the experiment. The water nozzle (orifice) is sapphire, and the diameter of the nozzle equals 0,254 mm. The abrasive water nozzle is made of carbide, 0,76 mm in diameter. The cutting angle of 90°, i.e. abrasive water nozzle is perpendicular to the machining surface [2].

Figure 1. Cutting of the sample, machine NC3015 and measuring of surface roughness parameters on the mobile measuring station T1000 basic

Slika 1. Prikaz rezanja uzoraka na stroju NC3015 i mobilni mjerni uređaj T1000 za mjerenje parametara površinske hrapavosti

Table 1. Levels of independent AWJM process parameters

Tablica 1. Razine neovisnih parametara procesa abrazivnim vodenim mlazom

Symbol	Parameters/Levels	1	2
A	type of material	stainless steel	aluminum
B	abrasive flow rate (g/min)	220	350
C	stand-of distance (mm)	2	4
D	water pressure (MPa)	220	330
E	traverse rate (mm/min)	100	300
F	sample thickness (mm)	2	4

2.2. Experimental plan

Samples of dimensions 100 x 20 mm were cut out of the boards of greater dimensions, which were used for measuring of surface roughness. After the machining of samples, surface roughness of each sample was measured. Measuring was conducted in three places per each sample, at the beginning, in the middle and at the end of the cut. Finally, average value of surface roughness parameters was calculated from the obtained results. Figures for various parameters in relation to the measured surface roughness values were designed based on data obtained in this way. Changeable machining parameters which will be set on the machine in order to derive conclusions referring to how they affect quality of the machined surface are the following. Material type is a parameter of the experiment which shows the quality of the machined surface for various materials. The following changeable parameter is abrasive flow rate, i.e. its impact on the surface quality for two materials. An important changeable parameter is also stand-of distance. Water pressure will change on two levels, and water flow rate will also be changed for each change of the pressure. Traverse rate, i.e. cutting speed is a parameter which varies on three levels. It may be considered a crucial parameter for machining productivity. The desired machining quality and optimally set parameters will provide the greatest cutting speed for certain surface quality, which will achieve maximum possible productivity. The experiment is conducted by specific methodology, i.e. by using the Taguchi's experiment plan (Table 1 and 2) [3] and [4].

3. Analysis of obtained experimental results

Analysis of figures obtained on the basis of results of experimental investigation, conclusions are derived on the way a certain machining parameter affects surface roughness. Figure 2 shows the impact of abrasive flow rate on the *Rz* parameter for different materials. Abrasive water jet machining was conducted by three different water flow rates, i.e. 220 g/min, 285 g/min, and 350 g/min. The results of surface roughness measuring were entered in the figure. The other parameters are the same for all measurements; thus, stand-of distance equals 2 mm. Water pressure equals 220 MPa, traverse rate 200 mm/min, and sample thickness 2 mm for all materials. Taking into consideration that water pressure equals 220 MPa, abrasive water flow equals 1,41 l/min.

Table 2. Two-level orthogonal array, L_8 (2^7), with experimenatal results (average) and calculated signal-to-noise (S/N) ratios according to Taguchi method

Tablica 2. Ortogonalni plan na dvije razine, L_8 (2^7), s eksperimentalnim rezultatima i izračunatim vrijednostima omjera signala i šuma (S/N) prema Taguchijevom planu ekperimenta

No.	Parameters						Surface roughness parameters (μm)		S/N ratio	
	A	B	C	D	E	F	*Ra*	*Rz*	*Ra*	*Rz*
1	stainless steel	220	2	220	100	2	3,968	25,197	-11,984	-28,046
2	stainless steel	220	2	330	300	4	4,886	30,133	-13,826	-29,633
3	stainless steel	350	4	220	100	4	3,521	21,050	-10,938	-26,475
4	stainless steel	350	4	330	300	2	4,119	24,620	-12,295	-27,85
5	aluminium	220	4	220	300	2	7,015	40,713	-16,944	-32,264
6	aluminium	220	4	330	100	4	5,142	33,130	-14,239	-30,444
7	aluminium	350	2	220	300	4	5,272	30,310	-14,447	-29,639
8	aluminum	350	2	330	100	2	4,268	26,523	-12,646	-28,501

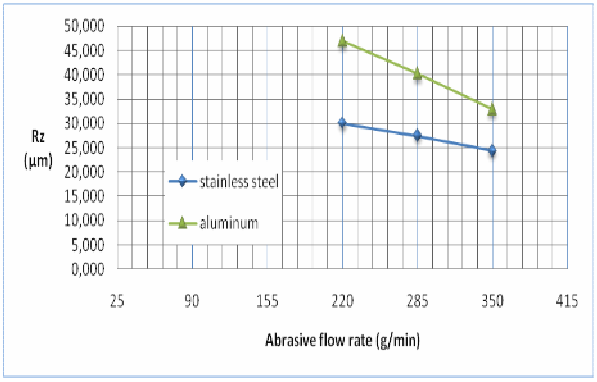

Figure 2. Graph of *Rz* dependence on material type and abrasive flow rate

Slika 2. Prikaz utjecaja materijala i masenog protoka abraziva na *Rz*

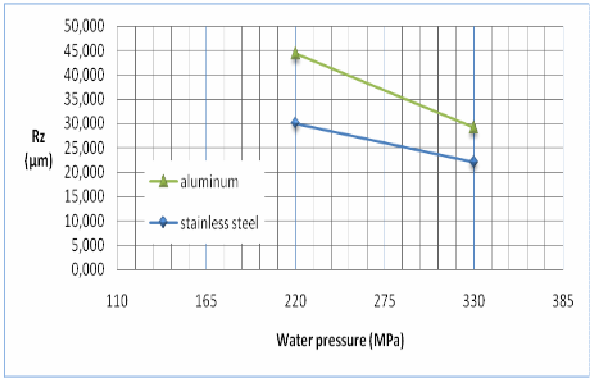

Figure 3. Graph of *Rz* dependence on material type and water pressure

Slika 3. Prikaz utjecaja materijala i tlaka vode na *Rz*

The parameter of roughness of the machined stainless steel surface continuously declines when abrasive flow rate increases. Aluminum shows more unfavorable results of the roughness parameter *Rz* of the machined surface. Surface roughness of aluminum is up to 25% higher, compared to stainless steel. It is important to note that roughness parameter *Rz* declines much faster (the steepest) when abrasive flow rate for aluminum is increased. Figure 3 shows the impact of water pressure parameter on the two examined materials. The other parameter remained unchained; thus, abrasive flow rate equals 220 g/min, stand-of distance 2 mm, traverse speed 200 mm/min, sample thickness 2 mm. Water pressure level was 220 MPa and 330 MPa for both materials. The figure shows that water pressure affects the *Rz* parameter, as well as abrasive flow rate. Stainless steel shows the best surface machining quality, when water pressure increases surface roughness quality also increases, taking into consideration the *Rz* parameter. When water pressure increases the aluminum shows an increase of surface roughness quality and a somewhat lesser quality of surface roughness than stainless steel. But when water pressure increases, it shows the greatest increase in the machined surface quality. Figure 4 shows that stand-of distance affects the *Ra* parameter. All machining parameters are constant, and the experiment was conducted on an aluminum workpiece. Abrasive flow rate equals 220 g/min, water pressure 220 MPa, traverse speed 200 mm/min, material thickness 2 mm, and stand-of distance 2 mm, 3mm, 4 mm. Great nozzle speed does not provide the best surface roughness results. The figure shows that the greatest surface roughness is realized on the stand-of distance of 2 mm, and it grows as the distance between the workpiece and the nozzle increases to the distance of 3,2 mm. The least surface roughness *Ra* is realized at this distance for the set machining parameters. Further increase of the stand-of distance declines the quality of the machined surface.

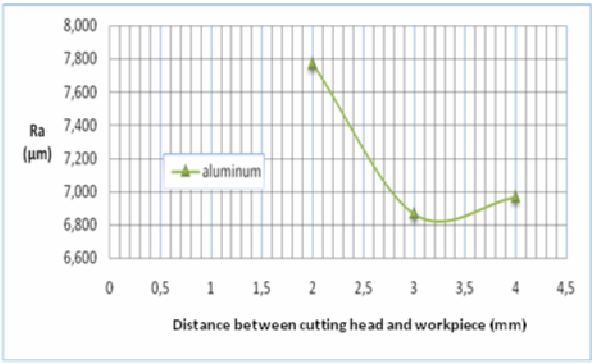

Figure 4. Graph of *Ra* dependence on the stand-off distance for aluminum

Slika 4. Prikaz ovisnosti *Ra* o udaljenosti mlaznice od obratka za aluminijum

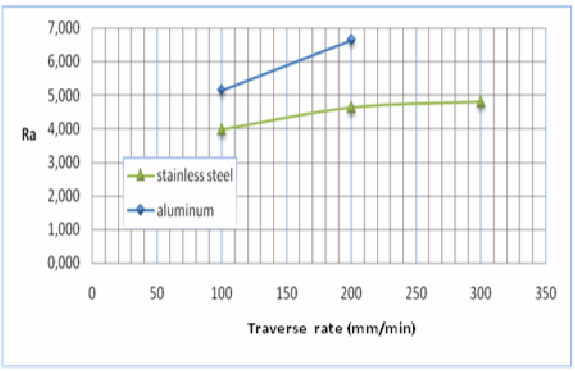

Figure 5. Graph of *Ra* dependence on the type of material and traverse rate

Slika 5. Prikaz ovisnosti *Ra* o vrsti materijala i posmaku

Table 3. The comparision of the obtained optimal results for *Ra* and *Rz* with carried out confirmation tests

Tablica 3. Usporedba optimalnih rezultata za *Ra* i *Rz* sa provedenim verifikacijskim pokusima

	Taguchi method – optimal results	Confirmation tests
Parameters levels	A1B2C1D2E1F2	
Ra (μm)	3,185	3,295
Parameters levels	A1B2C1D1E1F2	
Rz (μm)	20,098	21,603

Figure 5 shows the impact of traverse cutting speed on the *Ra* parameter for the two materials. The other machining parameters are constant for each material. Stainless steel has abrasive flow rate of 220 g/min, stand-of distance of 2 mm, water pressure 220 MPa, sample thickness of 2 mm. For aluminum: abrasive flow rate equals 220 g/min, stand-of distance 4 mm, water pressure 220 MPa, sample thickness 4 mm. Aluminum shows a greater decline in the quality of the machined surface than stainless steel when traverse speed is increased [2].

4. Taguchi method

Optimization based on Taguchi method [4], [5], [6] and [7] is used to achieve more efficient cutting parameters. Parameter design is the key step in the Taguchi method to achieve high quality without increasing cost. To solve this problem Taguchi method uses a special design of orthogonal arrays where the experimental results are transformed into the S/N ratio as the measure of the quality characteristic deviating from the desired value. Table 1 shows that the experimental plan has two levels and an appropriate Taguchi orthogonal array with notation L_8 (2^7) was chosen (Table 2.). The right side of the Table 2 includes the average results (each trial has 3 samples), of the measured arithmetic average surface roughness (*Ra*) and maximum peak-to-valley roughness height (*Rz*), as well as the calculated signal-to-noise (S/N) ratio, respectively. The S/N ratio, as the yardstick for analysis of experimental results, is calculated according to the following equation:

$$\mathrm{S/N} = \eta = -10\log_{10}\left(\frac{1}{n}\sum_{i=1}^{n} y_i^2\right) \quad (1)$$

where: η – signal-to-noise ratio (S/N); n – number of repetitions of the experiment; y_i – measured value of quality characteristic.

The above equation (1), which is used to calculate the S/N ratio, is in relation to the *smaller-is-better* quality characteristics, what means minimization of output parameter to achieve the desired optimal or near optimal solution, what in the particular case means minimization of arithmetic average roughness to achieve the desired surface roughness. On the same way *bigger-is-better* or *nominal-is-best* quality characteristics means maximization or target value of output parameter, respectively. Finally, three objectives can be achieved through the parameter design of Taguchi method: (i) determination of the optimal design parameters for a process, (ii) estimation of each design parameter to the contribution of the quality characteristics, and (iii) prediction of the quality characteristics based on the optimal design parameters.

4.1. Optimal cutting parameters by Taguchi method

Optimal cutting parameters and their influences on the surface roughness were analyzed. According to the analysis of variance the most influence on the surface roughness has the type of material with 42,7% and 43,37% of contribution for *Ra* and *Rz,* respectively. Influence of abrasive flow rate and traverse rate are also considerable between 34% and 19% of contribution for *Ra* and *Rz*. In this case study there are no significant influences of the stand-of distance, water pressure and thickness (small variation) on *Ra* and *Rz*. The optimal parameters levels of AWJM process and optimal values of the surface roughness parameters obtained with Taguchi method were verified with the confirmation tests, shown in Table 3.

5. Conclusions

Abrasive water jet machining is machining which has much more advantages than disadvantages. The objective of the paper was to analyze the impact of several machining parameters on surface roughness. Maximum height of the roughness profile *Rz* was controlled in the process, as well as mean arithmetic deviation of the roughness profile *Ra*. Analysis of the obtained figures has indicated the following changes. Increased abrasive flow rate and likewise increased water pressure provide improved results of surface roughness. The impact of the distance of the abrasive nozzle on the example of aluminum workpiece produced optimal value which, according to experimental investigation, amounts 3,2 mm. Surface roughness of machining increases when traverse speed increases. The following step in further experimental research is optimization of machining parameters with the objective to minimize the roughness of the machined surface.

In this paper application of Taguchi method to find optimal parameters of AWJM process is shown The presented optimization technique has its features, merits and limitations. Finally, presented optimization technique have potentiality to improve initial process parameters or in study case the achievement of the

desired surface roughness at AWJM process, with high accuracy which was clearly verified by confirmation experiment.

Acknowledgements

The authors wish to thank the management of the company *Scam Marine d.o.o.* for the AWJ machine and materials supplied for the experiments and also for technician support during execution of the tests.

REFERENCES

[1] EL–HOFY H.: *Fundamentals of Machining Processes: Conventional and Nonconventional Processes*, *Taylor & Francis Group*, Boca Raton, 2007.

[2] MUTAVGJIĆ, V.: *Istraživanje površinske hrapavosti dijelova dobivenih abrazivnim vodenim mlazom*, *Faculty of Engineering, University of Rijeka,* Rijeka, 2010.

[3] JURKOVIĆ, M., CUKOR, G., JURKOVIĆ, Z.: *Stohastičko modeliranje i optimalizacija rezne geometrije alata za tokarenje*, Strojarstvo 40(1998)1-2, 17-29.

[4] ROY, R.K.: *Design of experiments using the Taguchi approach: 16 steps to product and process improvement*, *Wiley-Interscience,* New York, 2001.

[5] JURKOVIĆ, Z., BREZOČNIK, M., GRIZELJ, B., MANDIĆ, V.: *Optimization of Extrusion Process by Genetic Algorithms and Conventional Techniques*, Tehnički vjesnik/Technical Gazette 16(2009)4, 27-33.

[6] JURKOVIĆ, Z., CUKOR, G., ANDREJČAK, I.: *Improving the Surface Roughness at Longitudinal Turning Using the Different Optimization Methods*, Tehnički vjesnik/Technical Gazette 17(2010)4, 397-402.

[7] CUKOR, G., JURKOVIĆ, Z., SEKULIĆ, M.: *Rotatable Central Composite Design of Experiments versus Taguchi Method in the Optimization of Turning*, Metalurgija/Metallurgy, 50(2011)1, 17-20.

Konstruiranje kalupa za injekcijsko prešanje primjenom reverzibilmog inženjerstva

Tedi MENDIKOVIĆ[1)], Zoran JURKOVIĆ[1)], Mladen PERINIĆ[1)] and Vesna MANDIĆ[2)]

1) Tehnički fakultet Sveučilišta u Rijeci
Faculty of Engineering, University of Rijeka
Vukovarska 58
HR-51000 Rijeka, **Republic of Croatia**
2) Faculty of Mechanical Engineering ,
University of Kragujevac
Sestre Janjic 6,
RS-34000 Kragujevac, **Republic of Serbia**

tedi.mendikovic@gmail.com

Keywords

mould design
injection moulding
reverse engineering

Ključne riječi

konstruiranje kalupa
injekcijsko prešanje
reverzibilno inženjerstvo

Izlaganje sa znanstvenog skupa

Rad ima za cilju dati u uvodu osnovna svojstva polimernih materijala, te opisati plastomere kao jednu od skupina polimernih materijala. Postupak i proces injekcijskog prešanja, parametre koji utječu na injekcijsko prešanje, te sustav za injekcijsko prešanje. Temeljem konkretnog proizvoda potrebno je konstruirati alat (sifonski luk) primjenjujući tehnike reverzibilnog inženjerstva u cilju dobivanja digitalnog zapisa proizvoda, kao osnov za daljnji razvoj i konstrukciju alata za injekcijsko prešanje.

Mould design for injection moulding using reverse engineering

Conference paper

The paper aims to provide an introduction to the basic properties of polymers, described thermoplastics as one of the group of polymeric materials. The procedure of the injection molding process, the parameters that influence on the injection molding and injection molding system also have been presented. Based on a specific product (spigot bend) is necessary to mould design applying reverse engineering techniques in order to receive digital products, as a basis for further development and mould design for injection molding.

1. Uvodna razmatranja

U posljednjem desetljeću sve više se javlja potreba za izradom dijelova od polimernih materijala, zbog napretka u istraživanju i primjeni plastičnih masa ali i zbog napretka u razvoju procesa prerade polimera. Upotreba polimernih materijala je u stalnom porastu u odnosu na metale. Razlog stalno rastućoj primjeni polimernih materijala i istiskivanje metala iz mnogobrojne primjene leži u mnogim povoljnim svojstvima polimera. Polimeri su niske gustoće, imaju visoku čvrstoću, postojani su u nekim vidovima korozije, jeftiniji su od metala i lako se proizvode. Pojedini polimerni materijali su pogodni za masovnu proizvodnju zbog jednostavnosti postupaka prerade polimera ali i zbog ekonomske opravdanosti pojedinih proizvodnih postupaka. Polimeri su zbog svojih svojstava vrlo zanimljivi i kao alternativni konstrukcijski materijali u sve više područja, iako prilikom njihove primjene treba biti svjestan i njihovih ograničenja, mana i razlika u odnosu na klasične konstrukcijske materijale, prvenstveno na metale. Zbog svih ovih svojstava polimerni materijali su pronašli masovnu primjenu u različitim područjima kao što su: automobilska industrija, brodograđevna industrija, informatička industrija, industrija pakiranja i zaštite (posebice prehrambenih proizvoda) kućna i uredska primjena, robe za široku potrošnju. Samo u SAD-u je poznato preko 18000 različitih vrsta polimernih materijala, u Europi je poznato preko 6000 različitih vrsta dok je u Japanu poznato preko 10000 različitih vrsta polimernih materijala. Tako veliki broj poznatih polimera i brzi razvoj omogućen je miješanjem dvaju ili više vrsta polimera, kopolimerizacijom i upotrebom različitih dodataka čime nastaju potpuno nove vrste polimernih materijala. Plastomeri su jedna od podvrsti polimera koji pri rastu temperature omekšavaju (formiran komad se može zagrijati i preoblikovati) te se potom, pri opadanju temperature skrućuju i na taj način dobivamo konačni oblik gotovog izratka. Količinski najviše polimera se proizvodi kao polietilen - PE, polipropilen - PP, poli(vinil-klorid) - PVC, polistiren - PS i poli(etilen-tereftalat) - PET (75% ukupne

proizvodnje). Plastomeri su danas prema preradi najproširenija skupina polimernih materijala. Proizvodnja, prerada i potrošnja polimernih materijala pokazatelj je gospodarske razvijenosti pojedinih zemalja, kao i gospodarskog rasta. U većini razvijenijih zemlja preko polovine diplomiranih kemičara i kemijskih inženjera izravno ili neizravno bavi polimerima i polimernim materijalima [1].

2. Injekcijsko prešanje

Prerada plastomera injekcijskim prešanjem najstariji je i najrazvijeniji postupak prerade plastike. Injekcijsko prešanje ima svoje početke još u 19. stoljeću kada se susrećemo sa rješenjima strojeva koji omogućuju injekcijsko prešanje prirodnih, modificiranih plastomera. Injekcijskim se prešanjem prerađuju sve vrste polimera, danas injekcijskim prešanjem se prerađuju i keramičke smjese, kombinacije različitih materijala (npr. plastika, metal i keramika), pa i žive stanice. Istodobno se i tlačno lijevanje metala isto može smatrati inačicom injekcijskog prešanja. Stoga je do sada zabilježeno najmanje 240 inačica toga postupka [2].

2.1. Postupak injekcijskog prešanja

Injekcijsko prešanje je najvažniji ciklički postupak preradbe polimera. Injekcijsko prešanje izvodi se na način da se polimerne tvari potrebne smične viskoznosti iz jedinice za pripremu i ubrizgavanje ubrizgavaju pod tlakom u temperiranu kalupnu šupljinu. Nakon polireakcije i umreživanja, geliranja ili hlađenja otpresak se skruti i postaje pogodan za vađenje iz kalupne šupljine. Produkt injekcijskog prešanje naziva se otpresak. Otpresci mogu biti različitih veličina, mase manje od miligrama do približno 180 kg [2].

2.2. Sustav za injekcijsko prešanje

Za postupak injekcijskog prešanja potrebna je preradbena linija koju čine sustav za injekcijsko prešanje (Slika 1) i dopunska oprema. Dopunska oprema povisuje djelotvornost procesa, a sastoji se od elemenata rukovanja tvarima, materijalom i proizvodom (oprema za transport). Osnovno obilježje suvremene opreme za injekcijsko prešanje je visok stupanj automatiziranosti, posebno ubrizgavalica, te najsuvremenije vođenje procesa, najčešće temeljeno na mikroprocesorima i primjeni računala. U Hrvatskoj je tijekom druge polovice 20. stoljeća postojao proizvođač ubrizgavalica, a proizvodile su se i obrtnički, dok se danas ubrizgavalice isključivo uvoze. Dio potrebnih kalupa za injekcijsko prešanje izrađuje se u Hrvatskoj. Sustav za injekcijsko prešanje moguće je okarakterizirati kao dinamički, kontinuirani i nelinearan, stohastički, stabilan s povratnim vezama. Istodobno je riječ o fleksibilnom, kompliciranom i kompleksnom sustavu [2].

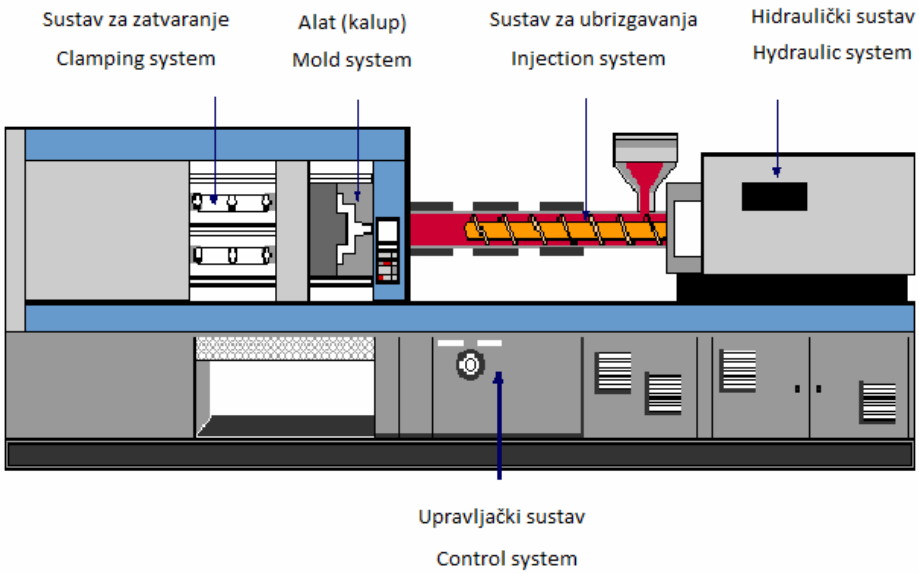

Figure 1. System for injection molding [3]

Slika 1. Sustav za injekcijsko prešanje [3]

3. Kalup za injekcijsko prešanje

Kalup za injekcijsko prešanje polimera je dio o kojemu ovisi cijeli postupak prerade polimera. Ako je kalup kvalitetno konstrukcijski napravljen onda se skraćuje vrijeme ohlađivanja taljevine, samim time i vrijeme ciklusa izrade jednog otpreska, a to samo po sebi znači i jeftiniji otpresak. Kalup se može upotrijebiti samo za jedan konstrukcijski oblik izratka neovisno o broju otpresaka. Kalup, zbog velikog broja faktora koji moraju biti zadovoljeni kako bi otpresak bio tehnički iskoristiv, mora biti kvalitetno konstruiran i izrađen.

3.1. Kalup

Alat predstavlja središnji dio sustava za injekcijsko prešanje (Slika 2). U kalupu se taljevina plastomera skrućuje i pretvara u upotebljivi otpresak. O kalupu ovisi konačni oblik otpreska, kako geometrijski oblik tako i struktura otpreska. Tako da je kalup kao najutjecajniji dio u procesu izrade otpreska veoma zahtjevan kako tehnološki tako i konstrukcijski. Kako su otpresci sve kompleksniji i kompliciraniji, to zahtijeva sve kompleksnija konstrukcijska rješenja za ostvarivanje ukupne funkcije kalupa. S druge strane, postupak injekcijskog prešanja nastoji se maksimalno automatizirati, što podrazumijeva i potpuno automatsko djelovanje kalup. Neke se stvari u samoj izradi kalupa ne mogu pretpostaviti ili izračunati tako da i utjecaj iskustva ima značaj faktor pri projektiranju kalupa za injekcijsko prešanje. Danas postoje softveri koji omogućavaju simulaciju tečenje materijala u kalupu, ali ne mogu ni softver uzeti u obzir sve moguće parametre, npr. znamo da temperatura zraka noću i danju nije ista što također jednim djelom utječe na proces hlađenja otpreska.

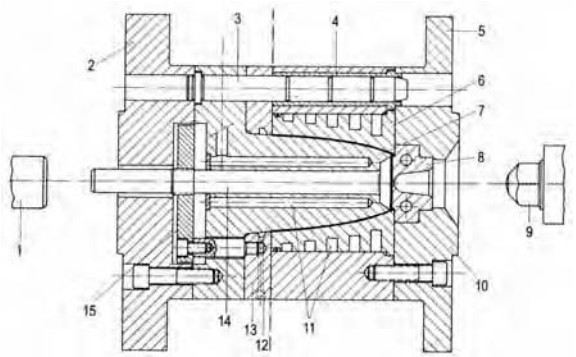

Figure 2. Mould for injection molding [2]

Slika 2. Kalup za injekcijsko prešanje [2]

4. Reverzibilni inženjering

Pojam reverzibilno inženjerstvo (engl. reverse engineering) možemo definirati kao proces kopiranja (Slika 3) neke postojeće komponente, sklopa ili proizvoda, bez pomoći crteža, tehničke dokumentcije ili računalnog modela. Reverzibilno inženjerstvo se sve više primjenjuje danas u pogledu aktualnih dizajnerskih trendova gdje se sve više zahtijevaju vrlo složeni geometrijski oblici, pa tako i CAD izrada modela postaje sve veći izazov. Značaj reverzibilnog inženjerstva je danas i u skraćenju vremena potrebnog za razvoj novog proizvoda. Proces reverzibilnog inženjeringa možemo podjeliti u tri osnovne faze: 3D digitalizacija, preprocesiranje podataka, generiranje CAD modela.

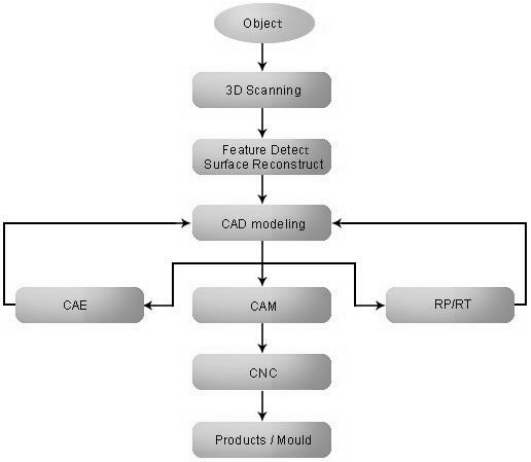

Figure 3. Diagram of reverse engineering process [4]

Slika 3. Dijagram procesa reverzibilnog inženjeringa [4]

4.1. 3D laserska digitalizacija izratka

3D laserska digitalizacija je metoda prikupljanja točaka prostornog oblika nekog realnog objekta u format pogodan za obradu na računalu. Rezultat 3D digitalizacije (Slika 4) je ogroman broj korisnih podataka (oblak točaka) o objektu, uz prisutnost odgovarajućih pogrešaka (šumova), te ih je stoga potrebno preprocesirati. Podaci koji su dobiveni 3D digitalizacijom predstavljeni su u stl. obliku. Nakon toga potrebno je izvršiti rekonstrukciju fizičkog izratka kreiranjem plošnih oblika u cilju dobivanja 3D modela izratka, koji se dalje koristi za modeliranje izratka (solid modela) primjenom nekog od CAD softvera (Solid Works, Catia i sl.) [5].

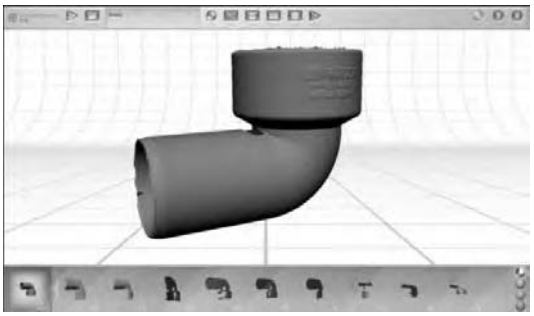

Figure 4. Processing of digitized data

Slika 4. Obrada digitaliziranih podataka

4.2. Izrada 3D modela kalupa

Izradom kalupa za injekcijsko prešanje kao 3D modela (Slika 5) dobivamo bolji uvid u funkcioniranje kalupa, što nam omogućava znatno smanjenje pogrešaka u fazi konstrukcije izrade kalupa. Primjenom naprednih softverskih rješenja, u ovom primjeru korišten Solid Works, omogućen je cjelovit pristup konstrukciji i simulaciji gibanja kalupa, te izradi kalupa i kalupnih šupljina generiranjem NC koda za strojnu obradu.

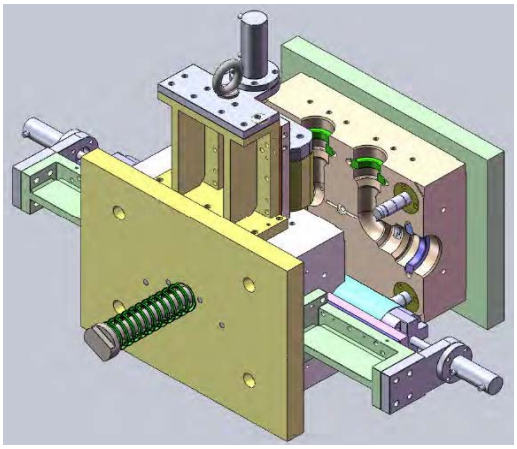

Figure 5. 3D mould for injection molding spigot bend

Slika 5. 3D kalup za injekcijsko brizganje sifonskog luka

5. Konstrukcija kalupa sifonskog luka

Kalup je konstruiran na način da istodobno dva otpreska se izrađuju u jednom ciklusu izrade. Potrebno je bilo izvesti sustav hlađenja alata vodom koja cirkulira kanalima u matrici i u jezgrama, zbog smanjenja ciklusa izrade otpreska. Alat mora imati prekidač sa mehaničkim ticalom koji u slučaju da se izbacivači ne vrate u početnu poziciju ima za funkciju zaustaviti zatvaranje kalupa, s ciljem zaštite kalupa kako ne bi došlo do loma vitalnih djelova kalupa (Slika 6). U kalupu je smještena i USB memorija (engl. Moldstick) na kojoj se nalaze svi parametri za namještanje stroja za brizganje, a cilju smanjenja vremena potrebnog za namještanje stroja i njegovo puštanje u rad.

5.1. Tehnologija izrade kalupa

Tehnologija izrade kalupa je dugotrajan i skup proces koji čini najveću troškovnu stavku u procesu konstrukcije novoga kalupa. Za izradu nestandardnih dijelova korištene su tehnologije obrade odvajanjem čestica od grubog i finog glodanja, tokarenja i brušenja. Tako obrađeni dijelovi kalupa se dalje toplinski obrade, a nakon toplinske obrade izvodi se elektroerozijska obrada (EDM), te završna obrada poliranja kalupne šupljine. Ovakav način izrade kalupa predstavlja konvencionalni pristup koji se danas sve više mijenja primjenom novih tehnologija, kao što su: visokobrzinska obrada (HSM) i obrada otvrdnutih materijala (HM).

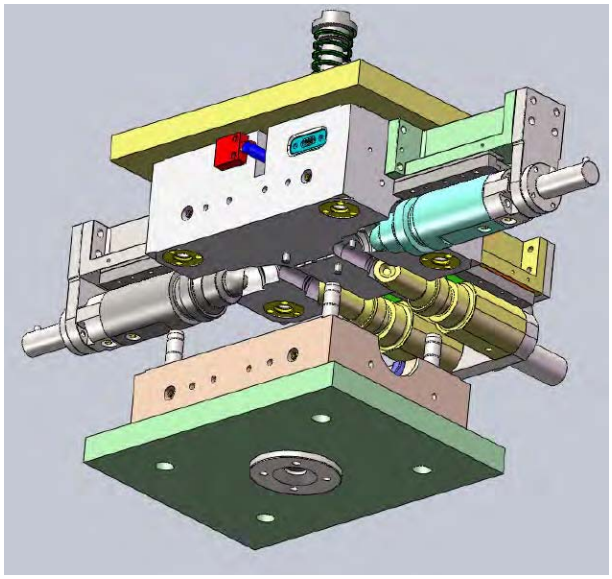

Figure 6. Bottom view 3D mould for injection molding spigot bend

Slika 6. Donji pogled 3D kalupa za injekcijsko brizganje sifonskog luka

6. Zaključak

Ovaj rad imao je za cilj iz postojećeg fizičkog objekta (otpresak sifonskog luka ∅40) izraditi kalup za injekcijsko brizganje, primjenom reverzibilnog inženjeringa. Otpresak (gotov izradak) je bez tehničke dokumentacije, te je u početnoj fazi bilo potrebno digitalizirati fizički objekt i na taj način dobiti 3D digitalni model izratka za koji je konstruiran kalup za injekcijsko brizganje dva izratka u jednom ciklusu.

Zahvala

Autori se zahvaljuju poduzećima *Vargon d.o.o.* za pružene savjete pri konstrukciji alata, te *Noven d.o.o.* za pruženu uslugu korištenja potrebne opreme za skeniranje.

REFERENCES:

[1] ERCEG, M.: *Oporaba plastike, skripta Kemijsko – tehnološkog fakulteta u Splitu*, Split 2010.

[2] ČATIĆ, I.: *Proizvodnja polimernih tvorevina, Društvo za plastiku i gumu,* Zagreb 2006.

[3] http://www.dc.engr.scu.edu/cmdoc/dg_doc/images/process/control/b1000001/inj_mach.gif

[4] http://autopoiesis.foi.hr/wiki.php?edit=yes&name=KM+-+Tim+12&page=reverzni+in%C5%BEenjering

[5] MARIČIĆ, S., PERINIĆ, M., ZAMARIN, A.: *An Economic and Visual System for Position Check,* Strojarstvo, 50(2008)3, 161-168.

Split

ISSN 1847-7917